Journal of Photochemistry and Photobiology B: Biology xxx (2011) xxx–xxx

Contents lists available at ScienceDirect

Journal of Photochemistry and Photobiology B: Biology

journal homepage: www.elsevier.com/locate/jphotobiol

On the relation between the Kautsky effect (chlorophyll *a* fluorescence induction) and Photosystem II: Basics and applications of the OJIP fluorescence transient ☆

Alexandrina Stirbet [a], Govindjee [b,*]

[a] 204 Anne Burras Lane, Newport News, VA 23606, USA
[b] Department of Plant Biology, Department of Biochemistry and Center of Biophysics, 265 Morrill Hall, 505 South Goodwin Avenue, Urbana, IL 61801, USA

ARTICLE INFO

Article history:
Available online xxxx

Keywords:
Bioenergetics
Chlorophyll *a* fluorescence
Fluorescence induction
OJIPS transient
Photosynthesis
Photosystem II

ABSTRACT

Chlorophyll *a* fluorescence is a highly sensitive, non-destructive, and reliable tool for measuring, rather quickly, photosynthetic efficiency, particularly of Photosystem II (PSII), the water-plastoquinone oxidoreductase. We briefly review here the connection between the fast (up to 2 s) chlorophyll fluorescence rise and PSII, as well as the empirical use of the fluorescence rise kinetics in understanding photosynthetic reactions, particularly of PSII. When dark-adapted photosynthetic samples are exposed to light, a fluorescence induction is observed, known as the Kautsky effect, after Hans Kautsky, the discoverer of the phenomenon showing the existence of variable fluorescence. The chlorophyll fluorescence intensity rises from a minimum level (the O level), in less than 1 s, to a maximum level (the P-level) via two intermediate steps labeled J and I. This is followed by a decline to a lower semi-steady state level, the S level, which is reached in about one minute. We provide here an *educational review* on how this phenomenon has been exploited through analysis of the fast OJIP fluorescence transient, by discussing basic assumptions, derivation of equations, as well as application to PSII-related questions.

1. Introduction

1.1. Background

The tiny (2–10% of the absorbed light [1]) Chlorophyll (Chl) *a* fluorescence has proven to be an open window in the heart of the photosynthesis process, due to its intricate connection with the numerous processes taking place during the energy conversion of light into a stable chemical form (reviewed in [2] and in Papageorgiou and Govindjee [3]). The analysis of the kinetics of Chl *a* fluorescence has been a widespread non-invasive technique used extensively for the study of oxygenic photosynthetic organisms (higher plants, algae and cyanobacteria), both in basic and applied research. It has provided both qualitative as well as quantitative information on a large variety of photosynthetic events (see e.g., many reviews [4–24] published during 1966–2009).

The fluorometers, that are currently in use for kinetic fluorescence studies, are based on different approaches to measure the variable Chl *a* fluorescence [25], differing in the manner by which the photochemistry is saturated (e.g., shutterless and LED-based instruments for direct fluorometry, as plant efficiency analyser (PEA) [26,27], pulse amplitude modulation, PAM, fluorometry [28], the pump and probe (P & P) fluorometry [29,30], the fast repetition rate (FRR) fluorometry [31], the pump during probe (PDP) fluorometry [32], and several others that are functionally similar, such as the fluorescence induction and relaxation (FIRe) technique [33], the background irradiance gradient single turnover (BIG-STf) fluorometry [34], and advanced laser fluorometry (ALF) [35]). However, the main phenomenon under analysis, in all these instruments, is the same. When photosynthetic samples, kept in darkness (e.g., for 10 min) are illuminated, Chl *a* fluorescence intensity shows characteristic changes called fluorescence

☆ This educational review honors Reto Jörg Strasser, of the Bioenergetics Laboratory, University of Geneva, Switzerland. Reto is one of the most influential leaders in the deep understanding and incisive application of chlorophyll a fluorescence to studies on plants. We have admired his pioneering and excellent work that includes the so-called Tripartite Model (with Warren Butler), the development and formulation of the energy flux theory in relation to photosynthetic energy conversion, and the presentation, on a logarithmic time scale, of the polyphasic OJIP chlorophyll *a* fluorescence induction curve in the 1990s, in which one of us (G) was involved. A model in which both of us (AS and G) were involved followed this. Then came Reto's so-called JIP test-model. His research has been inspiring to many. He continues to teach selflessly with great enthusiasm around the World (e.g., in South Africa, Mexico, Bulgaria, China, Korea and India), carrying with him the complete fluorescence instrument, all the necessary accessories, the software, and even the printer!

* Corresponding author.
E-mail addresses: stirbet@verizon.net (A. Stirbet), gov@illinois.edu (Govindjee).

1011-1344/$ - see front matter © 2011 Elsevier B.V. All rights reserved.
doi:10.1016/j.jphotobiol.2010.12.010

Please cite this article in press as: A. Stirbet, Govindjee, On the relation between the Kautsky effect (chlorophyll *a* fluorescence induction) and Photosystem II: Basics and applications of the OJIP fluorescence transient, J. Photochem. Photobiol. B: Biol. (2011), doi:10.1016/j.jphotobiol.2010.12.010

induction, fluorescence transient, or simply the Kautsky effect, named after Hans Kautsky (1891–1966). (See the brief 1931 paper by Kautsky and Hirsh [36]; also see http://www.fluoromatics.com/kautsky_effect.php.) For higher plants and algae, Chl *a* fluorescence induction curve measured under continuous light has a fast (within a second) increasing phase, and a slow (within a few minutes) decreasing phase (see Fig. 1). Further, light-exposed samples also exhibit fluorescence changes, upon change of wavelength [37], or intensity of light (see e.g., Strasser [38]; and Srivastava et al. [39]) (and reviews in [2,3]). After the light is turned off, and a sufficiently long dark period is given (e.g., 15–30 min to an hour), the original fluorescence induction kinetics are observed again when the same light is turned back on. This transient has inflection points (see [14] for a history of the nomenclature used for fluorescence transient curves): the fast phase is labeled as OJIP, where O is for origin, the first measured minimal level, J and I are intermediate levels, and P is the peak. The slow phase is called PSMT [40,41], where S stands for semi-steady state, M for a maximum, and T for a terminal steady state level; sometimes the maximum M is missing, or several steady states and maxima labeled S_1M_1, S_2M_2 are observed [42]. For the fast phase we will use in this review the OJIP label introduced, in 1991 and 1992, by Strasser and Govindjee [26,27]. Tsimilli et al. [43] showed that in some photosynthetic samples (foraminifers, zooxanthellae, lichens and some algae), the P-level splits into two steps, called G (a peak that does not exist in angiosperms, as a consequence of an early activation of the ferredoxin-$NADP^+$-reductase, FNR, [44]), and H (equivalent to P). In some heat-stressed samples, another step called K [45–47] appears between O and J levels, at about 300 μs.

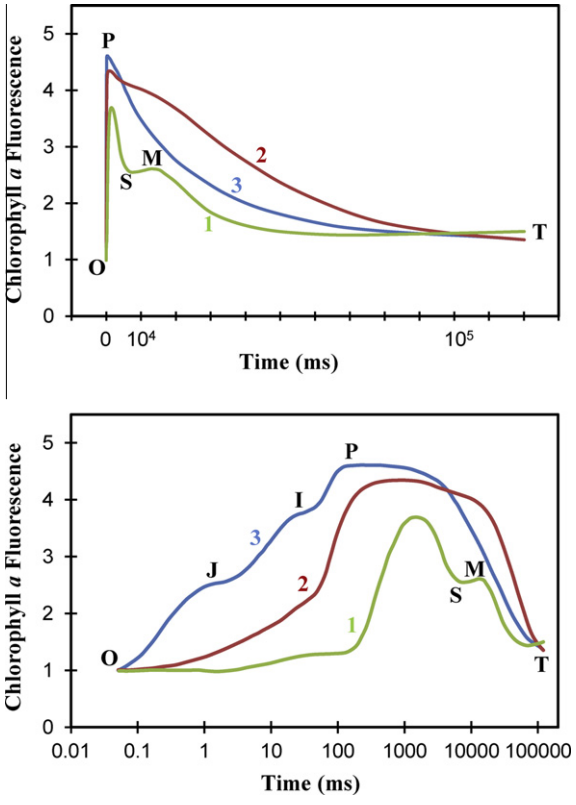

Fig. 1. Chlorophyll *a* fluorescence induction transients of a pea leaf (kept in darkness for ~20 min before the measurement). *Top graph*: on a linear time scale; *Bottom graph*: on a logarithmic time scale. Wavelength of excitation: 650 nm. Excitation light intensity for curves labeled 1, 2 and 3 was, respectively, 32, 320, and 3200 μmol photons m^{-2} s^{-1} at the leaf surface. For definition of OJIPSMT symbols, see text. Fluorescence is given in arbitrary units. Source of the original figure: Strasser et al. [50]; modified by Alaka Srivastava.

Fluorescence changes during the fast part of the transient (i.e., until the fluorescence yield reaches its maximum value at P) can be primarily correlated with the events taking place in the course of successive reduction of the electron acceptors of the entire photosynthetic electron transport chain (see e.g., reviews in reference [3]). The slow part is more difficult to interpret, as an increasing number of different processes begin to be involved during this phase (e.g., non-photochemical Chl *a* fluorescence quenching, ATP synthesis, Calvin–Benson cycle, State 2 to State 1 transition, among others); this will not be discussed in this review. For a history of the development of the State transitions, see Papageorgiou and Govindjee (this special issue).

1.2. The connection of Chlorophyll a fluorescence induction with the Photosystem II

Several experimental and theoretical studies have been dedicated to the fast phase of the fluorescence induction since it is easier to be analyzed than the slow phase (see [48–50] for experimental work; [18,51–57] for modeling; and [24,58,59] for reviews). The conventional understanding of the OJIP transient is based mainly on the hypothesis discussed, in 1963, by Duysens and Sweers [60]. In their theory they assumed that Photosystem II (PSII) is responsible for Chl *a* variable fluorescence, and the rate of PSII photochemical conversion is limited by the electron acceptor side (i.e., the side that is reduced by PSII); further, the fluorescence yield was suggested to be controlled by a PSII acceptor quencher (called "Q"), later identified as the bound plastoquinone Q_A in its oxidized state (see e.g., van Gorkom and co-workers [61,62]). In this theory, the fast fluorescence rise is a reflection of the concentration of reduced Q_A, i.e., Q_A^-, as affected by the kinetics of several different redox reactions in the photosynthetic electron transport chain. Thus, the OJIP transient has the potential to be used for the characterization of the photochemical quantum yield of PSII photochemistry, and the electron transport activity. Further, the OJIPS Chl fluorescence transient has been an excellent monitor for the specific effects of various inhibitors, stressors, and mutations on the photosynthetic apparatus and its function. The involvement of other processes controlling the variable Chl *a* fluorescence during the fast phase of Chl *a* fluorescence induction, besides the Q_A quenching, has also been proposed: [63] for PSII connectivity; [64,65] for $P680^+$, the PSII reaction center in its oxidized state; [66,67] for pheophytin (Phe^-); [68] for non-photochemical quenching by the plastoquinone (PQ)-pool; and [69] for the influence of the electric field on the kinetics of some redox reactions and/or directly on the fluorescence yield; these will not be discussed in this review.

In photosynthetic samples, which have been kept in darkness, the electron acceptor side of PSII is mostly in the oxidized state (i.e., the PSII reaction centers are open, and the fluorescence intensity is minimal, $\mathbf{F}_o$ – represented on the fluorescence transient curve as O, for 'Origin', as mentioned earlier). The O to J rise, known as the photochemical phase, is very fast (approx. 2 ms), and depends strongly on the intensity of the exciting light, whereas J–I and I–P parts of the fluorescence curve, known as thermal phases (temperature sensitive), are much slower (especially the I–P portion) (see bottom graph in Fig. 1). (For an early discussion of photochemical and thermal phases, see e.g., Morin [70], and Delosme [71].) In less than 1 s, Chl *a* fluorescence reaches the peak P (also called $\mathbf{F}_M$ or $\mathbf{F}_{max}$, when the exciting light intensity is high and saturating). At the $\mathbf{F}_M$ level, in agreement with the hypothesis of the quencher 'Q', introduced by Duysens and Sweers [60], all Q_A molecules are completely reduced (i.e., all active PSIIs are closed), due to the reduction of the entire linear electron transport chain as a result of a traffic jam of electrons on the acceptor side of PSI (see Munday and Govindjee [72,73]; Schansker et al. [74]). At low light

Please cite this article in press as: A. Stirbet, Govindjee, On the relation between the Kautsky effect (chlorophyll *a* fluorescence induction) and Photosystem II: Basics and applications of the OJIP fluorescence transient, J. Photochem. Photobiol. B: Biol. (2011), doi:10.1016/j.jphotobiol.2010.12.010

intensities (see bottom graph in Fig. 1), the O–J part of the transient is not observed, and the fluorescence intensity at the P-level has a lower value than the maximum fluorescence $\mathbf{F}_M$ (see e.g., [50]). In this review we will discuss only the fast fluorescence induction curve measured under saturating excitation light (when P (or $\mathbf{F}_P$)$\equiv \mathbf{F}_M$), since important information regarding the photosynthetic activity can be obtained even by using just $\mathbf{F}_o$ and $\mathbf{F}_M$.

2. The empirical use of fluorescence induction data

2.1. Photosynthetic samples that had been kept in darkness

In numerous studies, fluorescence induction data, from samples that had been kept in darkness, are used empirically (i.e., without an explicit correlation with the biophysical processes taking place in the sample). The most common empirical parameters are either the $\mathbf{F}_o$ or the $\mathbf{F}_M$ values themselves, or expressions based on these two parameters. In normal non-stressed plant leaves, the ratio $\mathbf{F}_M/\mathbf{F}_o$ has a constant high value (5–6) under various physiological conditions [75]. In addition, the difference between $\mathbf{F}_M$ and $\mathbf{F}_o$, called the variable fluorescence, $\mathbf{F}_V$, and the ratio $\mathbf{F}_V/\mathbf{F}_M$ (in most higher plants having usually the value in the range of 0.78–0.84 [75]), are used extensively; the parameter $\mathbf{F}_V/\mathbf{F}_M$ has been related to the maximum quantum yield of primary PSII photochemistry [14,15,76–78]. Another parameter that is frequently used in graphical presentations of fluorescence induction data is the relative variable fluorescence at time t, $\mathbf{V}_t = (\mathbf{F}_t - \mathbf{F}_o)/(\mathbf{F}_M - \mathbf{F}_o)$; it is a double normalization of the fluorescence induction curve that allows a comparison of transients measured under different conditions and/or on different samples, turning absolute fluorescence intensities into relative contributions to the variable fluorescence. Considering the theory of Duysens and Sweers [60], and knowing the connectivity among different PSII units, i.e., excitation energy exchange migration among several PSIIs [79–85], the relative variable fluorescence $\mathbf{V}_t$ can be correlated with the fraction of closed PSII centers $\mathbf{B}_t = [Q_{\bar{A}}]_t/[Q_A]_{total}$, since $\mathbf{V}_t = \mathbf{B}_t/[1 + C \cdot (1 - \mathbf{B}_t)]$, where C is the connectivity parameter, whose value depends upon the overall probability of connectivity between the PSII units [79–83]. Therefore, $\mathbf{V}_t$ is $\equiv\mathbf{B}_t$ when there is no energetic connectivity between PSII units.

2.2. Fluorescence parameters for samples that are kept in light

Several other fluorescence parameters have been defined in studies that involve samples kept in light showing fluorescence induction, as mentioned earlier. Fluorometers working on the pulse amplitude modulation (PAM) principle, and supplemented with the saturation pulse method [28,86], are assumed to separate photochemical and the so-called non-photochemical quenching (Schreiber [21]); yet, this type of measurement can also be made using direct fluorescence instruments [17,18,87]. A pulse of intense light during the P to S phase of fluorescence induction leads to a transitory increase of the fluorescence to a maximum value, labeled as $\mathbf{F}'_M$, which is usually lower than $\mathbf{F}_M$ obtained with samples that had been in dark. In general, the decrease of the fluorescence maximum during the slow phase of fluorescence induction is attributed to non-photochemical processes [88]. However, Schansker et al. [87,89] have provided experimental evidence that, after the light activation of FNR (which happens 1–2 s after the onset of the light [74]), and in some cases even sooner [89]), $\mathbf{F}'_M$ ceases to be a true maximum (i.e., not all active PSII RCs are closed at $\mathbf{F}'_M$-level).

The $\mathbf{F}_o$ value of the fast transient of a sample, which was kept in light, is labeled as $\mathbf{F}'_o$, and it is different from $\mathbf{F}_o$ [90,91], being plant species, or even variety, dependent, but quite often this change is assumed to be small enough that $\mathbf{F}'_o = \mathbf{F}_o$.

Assuming the photochemical activity to be zero both at $\mathbf{F}_M$ and $\mathbf{F}'_M$ levels, a parameter NPQ, which stands for **n**on**p**hotochemical **q**uenching, is defined to be equal to $(\mathbf{F}_M - \mathbf{F}'_M)/\mathbf{F}'_M$ [92] (a formula in which $\mathbf{F}_o$ and $\mathbf{F}'_o$ values are not needed). However, we note that $\mathbf{F}'_M$ is affected, to some extent, by photochemical quenching also [87,89]. Based on the time range of the recovery from the quenching process, three major components of the non-photochemical quenching have been defined [93–95]: (1) the energy-dependent quenching **qE**, a quickly reversible component caused by ΔpH across the thylakoid membrane in the presence of PsbS protein, in many cases, and zeaxanthin (a carotenoid responsible for the increase of the light energy dissipation as heat in PSII antenna) [92,96–100]; (2) the so-called state transition quenching **qT**, due to the transition of the photosynthetic apparatus from the so-called State 1 (high fluorescent) to State 2 (low fluorescent), following reversible phosphorylation of the light-harvesting complex of PSII (LHCII) (see e.g. [93,101]); and (3) the quenching component related to the photoinhibition **qI** ([94,102–104]). The relative contributions of these components can vary, and the intensity of the light has been shown to be a very sensitive factor in controlling these events [105]. We note, however, especially in the **qT** and the **qI** cases, that the mechanisms behind them are still a matter of debate. For example, on the basis of combined fluorescence and 77 K measurement, and **qT**-determination, **qT** was related to the State transitions at low light intensities [106,107]. However, based on simultaneous measurements on fluorescence induction and transmission changes at 820 nm, Schansker et al. [87] related **qT** with the process of dark inactivation of FNR, than with LHCII-phosphorylation. Further, **qI** was shown to contain a contribution of State transitions.

Results obtained with samples, which had been kept in dark, can in addition serve as a reference for normalization of data obtained with samples that had been in light. An example is the expression for $\mathbf{q}_N$, also often used in the literature to characterize non-photochemical quenching [21]: $\mathbf{q}_N = 1 - (\mathbf{F}'_M - \mathbf{F}'_o)/(\mathbf{F}_M - \mathbf{F}_o)$. If we consider that $\mathbf{F}'_o = \mathbf{F}_o$, $\mathbf{q}_N$ becomes $(\mathbf{F}_M - \mathbf{F}'_M)/(\mathbf{F}_M - \mathbf{F}_o)$. The photochemical quenching, on the other hand, is expressed as: $\mathbf{q}_P = (\mathbf{F}'_M - \mathbf{F}_t)/(\mathbf{F}'_M - \mathbf{F}'_o)$. However, the symbols $\mathbf{q}_N$ and $\mathbf{q}_P$ lead to confusion, as they give the impression that the two terms are complementary, which is not the case (i.e., $\mathbf{q}_P + \mathbf{q}_N \neq 1$) (see discussion in [108]).

To understand the regulatory aspects of the energy distribution among PSIIs, a theoretical treatment known as "*energy partitioning in PSII complexes*" has been proposed by Kramer et al. [109], and Hendrickson et al. [110,111]. According to the energy partitioning approach (based on earlier work [76–78,108–113]), four energy fluxes have been defined: one is associated with the photochemical electron flow in active PSII reaction centers (J_{PSII}), the second with the thermal dissipation in photoinactivated, non-functional PSIIs (J_{NF}), the third with the light-regulated thermal dissipation in active PSIIs (J_{NPQ}), and the fourth is the combined flux of fluorescence and constitutive light-independent thermal dissipation ($J_{f,D}$). Each flux has its defined quantum efficiency that satisfies the relation $\Phi_{PSII} + \Phi_{NF} + \Phi_{NPQ} + \Phi_{f,D} = 1$. Hendrikson et al. [111] examined the correlation of the rate constant of photoinactivation, k_{pi}, with various fluxes, and found that the combined flux $J_{NPQ} + J_{f,D} (= J_{pi})$ is nicely correlated with k_{pi}, which led them to the conclusion that the ratio $\mathbf{F}_s/\mathbf{F}'_M$, where $\mathbf{F}_s$ is the steady state level of the fluorescence in the slow part of the fluorescence induction transient, is an appropriate predictor of the rate constant of PSII inactivation.

2.3. A conceptual treatment of fluorescence induction data

In general, experimental data can be used as such, empirically, or can be related in a theoretical manner to specific mechanisms. The latter approach has the advantage of helping the researchers

Please cite this article in press as: A. Stirbet, Govindjee, On the relation between the Kautsky effect (chlorophyll *a* fluorescence induction) and Photosystem II: Basics and applications of the OJIP fluorescence transient, J. Photochem. Photobiol. B: Biol. (2011), doi:10.1016/j.jphotobiol.2010.12.010

to handle, in a reasonable manner, the experimental results, and in planning new experiments. An analysis of the fast fluorescence transient (OJIP) developed by Reto J. Strasser and his collaborators (see e.g. [17,18,114–117]) is such an attempt; it is colloquially termed the JIP test, which uses the major inflection points in the fluorescence induction curve.

In this review we have attempted to present an objective view (with pros and cons) of this JIP test, and its connection with the structure and function of photosynthetic apparatus.

3. The analysis of fluorescence transient

3.1. Photosynthetic reactions: A background

Before we can analyze and understand the fluorescence induction (the Kautsky effect) in terms of photosynthetic reactions, we need to first provide a basic background of reactions related to photosynthesis, since there are many aspects of the process that are relevant to the interpretation of the fluorescence induction kinetics. The oxygenic photosynthesis involves two light reactions operating simultaneously at PSII and PSI reaction centers (see e.g., Hill and Bendall [118], and Duysens et al. [119]). Fig. 2 is a diagram of the well-known Z scheme for electron transfer from water to $NADP^+$ (see e.g., Fig. 1 in [120]; and Fig. 4 in [121]); the light energy, absorbed by the two photosystems, is converted into fluxes of electrochemical Gibbs free energy that is used to oxidize water to oxygen, reduce $NADP^+$, and produce ATP (for a basic background, see [122–124]). Most of the chlorophyll *a* fluorescence, at room temperature, originates in the antenna complexes of PSII (see e.g. [15]).

3.1.1. Light absorption and trapping

The first step of photosynthesis is the absorption of photons by antenna molecules within femtoseconds, leading to the formation of excited chlorophylls (Chl^*). The main function of the antenna (the light-harvesting complex) is to transfer excitation energy to the photosynthetic reaction centers (see a review [125]). Besides the transfer of excitons from excited antenna chlorophylls to the reaction centers (leading to photochemistry), part of the absorbed light energy is dissipated as heat and emitted as fluorescence (see Fig. 3). Primary charge separation occurs in both the PSI and PSII reaction center complexes, involving P700 and P680, respectively. Photochemistry is over within picoseconds, and all further reactions can proceed in darkness.

3.1.2. Photosynthetic electron transport

See reviews in [126,127]; and the web sites cited in [121]. The positive charges produced by PSII oxidize water to molecular O_2 at the oxygen evolving complex (OEC), via Y_z (tyrosine-161 on the D1 protein); the key water oxidation unit is represented in Fig. 2 as Mn_4O_5Ca. The negative charge (the electron) is first located on a pheophytin molecule, Phe, and is then passed on to the primary quinone Q_A, and then to the secondary quinone Q_B, which is a two-electron acceptor; the reduced Q_B, after it is protonated to become plastoquinol, PQH_2, exchanges with a PQ molecule from a pool of plastoquinone molecules, PQs (3–9 PQ per PSII) [128–130]. PQH_2 transfers one electron to cytochrome *f*, Cyt *f*, via Rieske iron-sulfur center, FeS, and another electron to the low-potential heme *b* (Cyt b_L, sometimes labeled as Cyt b_p, showing that it is situated on the electropositive part of the membrane, the lumen side); the reduced Cyt *f* reduces the copper protein plastocyanin, PC. In the Cyt b_6f complex, the reduced low-potential Cyt b_L transfers an electron to the high potential heme *b* (Cyt b_H, also denoted Cyt b_n, since it is situated on the electronegative side of the membrane). Cyt b_H reduces a PQ molecule, from the PQ-pool, to its semiquinone form, PQ^-; a second electron, extracted from another PQH_2 molecule and transferred to Cyt b_H via Cyt b_L, reduces PQ^- to PQH_2 after two protons are added to it. The electron transport from one reduced PQ molecule to Cyt b_6f complex and

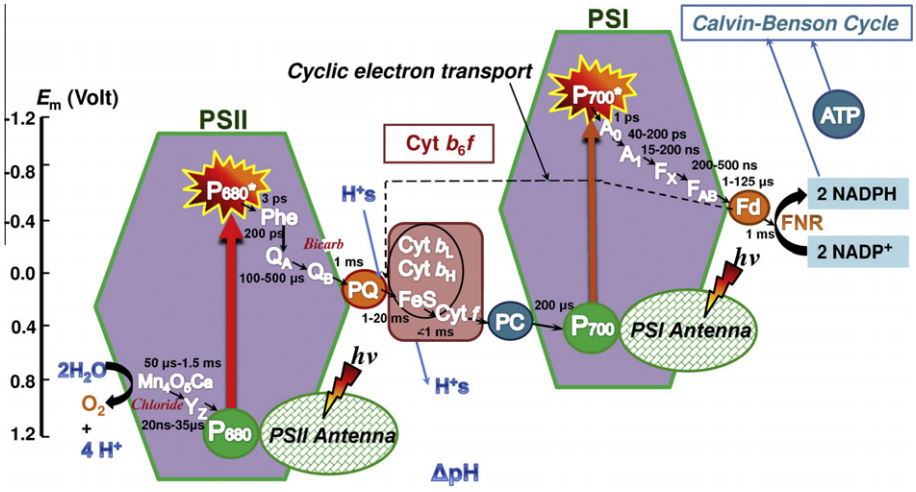

Fig. 2. A Z-Scheme for electron transport in photosynthesis, from water to nicotinamide adenine dinucleotide phosphate, $NADP^+$. Oxygenic photosynthesis uses two light reactions and two photosystems (PSII, photosystem II and PSI, photosystem I) – connected in series via a cytochrome b_6f (Cyt b_6f) complex. On the electron donor side of PSII, we have a tetranuclear manganese–oxygen–calcium cluster, Mn_4O_5Ca, and Y_z, tyrosine-161 on the D1 protein, and chloride ions. The reaction center chlorophyll of PSII is P680; it is the primary electron donor of PSII; $P680^*$ is the excited electronic state of P680; for a detailed view, see [95]. On the electron acceptor side of PSII, we have a pheophytin (Phe) molecule, the first electron acceptor of PSII, Q_A, a tightly bound one-electron acceptor plastoquinone, and Q_B, a two-electron acceptor plastoquinone that binds and unbinds from PSII; a bicarbonate (bicarb) ion is bound to a non-heme iron that sits between Q_A and Q_B. PQ in the scheme refers to a pool of mobile plastoquinone molecules. In the Cyt b_6f complex, we have an iron–sulfur (FeS) protein, known as Rieske FeS protein, a Cyt *f*, cytochrome *f*, and two cytochrome b molecules (a low (L) and a high (H) potential form). Plastocyanin molecule (PC) is a copper protein that transfers electrons from Cyt b_6f to PSI (cyanobacteria often employ $Cytc_6$ instead of PC); there is more than one PC molecule. In PSI, there is P700, the primary electron donor of PSI, whereas $P700^*$ is the excited electronic state of P700. On the electron acceptor side of PSI, we have A_0, a special chlorophyll *a* molecule; A_1, vitamin K_1; and F_X, F_A, F_B, three iron–sulfur centers. Fd represents ferredoxin; there is more than one Fd molecule, FNR is ferredoxin–$NADP^+$-reductase, and $NADP^+$ is nicotinamide–adenine dinucleotide phosphate. In this diagram, the ATP synthase is not shown. Estimated (or measured) half times for electron transport between intermediates are also shown. This diagram was modified from Fig. 1 (bottom) in Govindjee et al. [120]; also see Fig. 4 in [121].

Please cite this article in press as: A. Stirbet, Govindjee, On the relation between the Kautsky effect (chlorophyll *a* fluorescence induction) and Photosystem II: Basics and applications of the OJIP fluorescence transient, J. Photochem. Photobiol. B: Biol. (2011), doi:10.1016/j.jphotobiol.2010.12.010

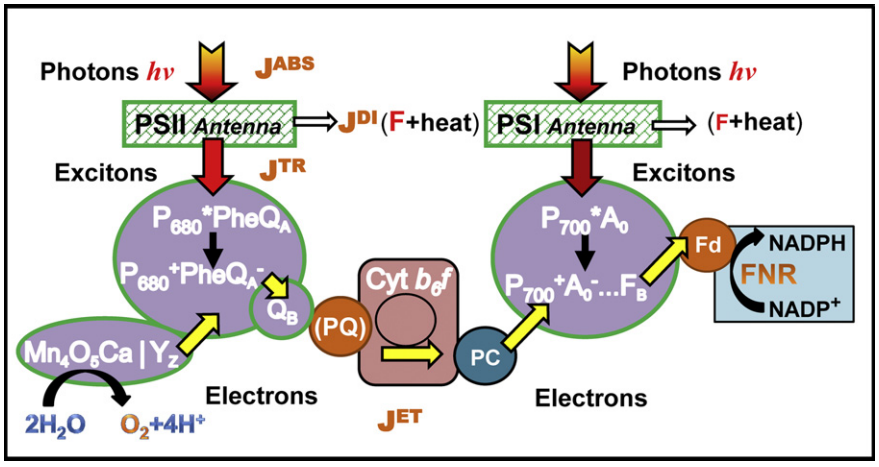

Fig. 3. A schematic representation of the main energy pathway related to chlorophyll (Chl) *a* fluorescence. Since most Chl *a* fluorescence originates in photosystem II (PSII) antenna, we have included here its absorbed photon flux, $\mathbf{J}^{ABS}$, which represents the rate of photon absorption by all PSII antenna pigments, the dissipated energy flux $\mathbf{J}^{DI}$, which represents the part of the absorbed photon flux dissipated through direct fluorescence (F) and other non-radiative processes (heat), and the trapped exciton flux, $\mathbf{J}^{TR}$, which represents the rate of exciton trapping by the PSII reaction center P680. The trapped energy is used to do charge separation (forming $P680^+PheQ_A^-$). The flux $\mathbf{J}^{ET}$ represents the rate of the photosynthetic electron transport from water to Fd, and eventually $NADP^+$ (or other Fd acceptors), at any moment t of the transient. Not shown in the figure are two values of $\mathbf{J}^{ET}$ estimated by the JIP test at two different moments during the OJIP rise (see Appendix A.1 for details): (i) $\mathbf{J}_o^{ET2}$ (ET_0 in the original notation of R.J. Strasser) that refers to the electron transport flux from Q_A to Q_B; and (ii) $\mathbf{J}_o^{RE1}$ (from ***re****duction* of PS***1*** electron acceptors – RE_0 in the original notation of R.J. Strasser), which is a recently introduced JIP parameter [117,160], characterizing the electron transport flux until PSI acceptors. See text and Fig. 2 (and its legend) for further details; also see R.J. Strasser and co-workers [17,18,117] for earlier schemes.

back to an oxidized PQ molecule, as described above, is known as the Q-cycle [131]. However, newer structural studies of Cyt b_6f [132] have revealed the presence of a fourth heme, of type *c*, situated in close proximity (~5 Å) of Cyt b_H, and also, a FNR molecule, both on the electronegative side of the membrane (not shown in Fig. 2). Two other possible cycles have been proposed to take place in the green plants, beside the Q-cycle [133]: (i) Cyt b_L transfers successively two electrons to the two-electron carrier formed by Cyt b_H and heme *c*, producing [Cyt b_H–*c*]$^{2-}$, which then reduces one PQ molecule from the pool, to PQH_2; (ii) the two-electron carrier [Cyt b_H–*c*] receives one electron from Cyt b_L, and another from the FNR molecule, via Fd^-, and then reduces one PQ molecule from the pool to PQH_2 (i.e., cyclic electron transport around PSI). Protons, H^+s, are released into the lumen during water oxidation, and on reoxidation of PQH_2 by the Cyt b_6f complex, both as a consequence of the linear electron transport, as well as the cycles around Cyt b_6f (see Crofts [131]). PCs (present in less than 1 PC/PSI in leaves with depressed carbon assimilation, and up to 5 PC/PSI in leaves with high carbon assimilation rates [134]) are located in the lumen, and, when in reduced state, act as electron donors to PSI. The positive charge produced by PSI is reduced by reduced PC, and the negative charge reduces ferredoxin, Fd (5–7 Fd molecules per PSI [35,135]) via a series of redox reactions involving, in the following order: the primary acceptor of PSI, A_0, a special chlorophyll *a* molecule; A_1, vitamin K_1; and F_X, F_A, and F_B, iron-sulfur centers. The reduction of $NADP^+$ by reduced Fd is catalyzed by FNR. In samples that had been in dark, FNR must be activated, a process that in higher plants takes several seconds, but algae, lichen and corals need only a few 100 ms (see e.g., [44,89]). Inactivation of FNR in the darkness is plant species dependent; it is completed within 15 min in pea leaves [136], and it may take as much as an hour in *Pinus halepensis* [89]. Reduced Fd can also act as an electron donor in other processes in stroma, like for example the Mehler reaction or the water–water-cycle [137,138] – not shown in Fig. 2. Cyclic electron transport around PSI occurs in competition with linear electron transport to the Calvin–Benson cycle and other processes just mentioned [80]; here reduced Fd, or NADPH, acts as a donor to the PQ-pool (see above). The physiological role of the cyclic electron flow is to contribute to the formation of the ΔpH across the thylakoid membranes, which drives ATP synthesis (see below). The pH of the lumen is also a regulator of heat dissipation in the antenna; it also affects Chl fluorescence (see e.g. [139,140]).

3.1.3. ATP synthesis

See e.g. Junge et al. [141]. ATP is produced from adenosine diphosphate, ADP, and inorganic phosphate, P_i, using the proton motive force, *pmf*, built across the thylakoid membrane (Mitchell [142]), and the enzyme ATP synthase. The *pmf* is made up of an electrical potential ($\Delta\psi$) across the thylakoid membrane, and a proton gradient (ΔpH). The proton gradient is basically from: (i) protons released into the lumen during water oxidation; (ii) proton translocation from the stroma side to the lumen during PQ reduction to PQH_2, and PQH_2 oxidation by Cyt b_6f complex; (iii) Q-cycle of Cyt b_6f complex (see [131–133]); and (iv) cyclic electron transport around PSI [133]. The protons are "driven out" from the thylakoid lumen through the central core of the enzyme ATP synthase (partially embedded in the membrane) causing conformational (rotational) changes in the enzyme, which catalyze phosphorylation of ADP and the release of ATP on the stromal side (see e.g.[143]).

3.1.4. The Calvin–Benson cycle

The reducing power generated via the so-called light reactions, NADPH, as well as the energy available from ATP hydrolysis, are critical for producing sugars from CO_2 through the Calvin–Benson cycle, a process that takes place in the stroma, with Rubisco (ribulose 1,5-bisphosphate carboxylase/oxygenase) as a key enzyme of the photosynthetic CO_2 assimilation (see e.g. Benson [144] and Bassham [145]). We do not present here the details of this process; it is important to know that light not only provides the energy for carbon assimilation, but it is also an important regulatory factor of the carbon metabolism. Chloroplasts have developed a light-dependent system for the control of the activities of key enzymes involved in the Calvin–Benson cycle, partly through the ferredoxin/thioredoxin system [146,147]; the central component of this regulatory system is the ferredoxin:thioredoxin reductase (FTR) (unique to oxygenic photosynthetic cells). For details of proteins involved, see [148,149]. The result of these activities is that the

Please cite this article in press as: A. Stirbet, Govindjee, On the relation between the Kautsky effect (chlorophyll *a* fluorescence induction) and Photosystem II: Basics and applications of the OJIP fluorescence transient, J. Photochem. Photobiol. B: Biol. (2011), doi:10.1016/j.jphotobiol.2010.12.010

Calvin–Benson cycle is adjusted constantly with changing light conditions.

3.2. How the dark/light transition and the stress influence the fluorescence induction

It is well-known that in samples kept in darkness, the connection between the light driven electron transfer (the production of NADPH and ATP), and the carbohydrate synthesis, through the Calvin–Benson cycle, is severed. When the light is turned on, this connection is reestablished in a relatively short time (hundreds of milliseconds to minutes) via specific regulatory processes, one being the ferredoxin/thioredoxin system (see the previous section; and Buchanan and co-workers [150,151]). Moreover, the photosynthetic systems in the dark state are extremely sensitive to light, and short-term strategies are put in place for the protection of the system; these include energy dissipation as heat following light absorption, leading to non-photochemical fluorescence quenching (see e.g. [152]). Another process taking place during dark/light transition is related to the regulation of energy distribution between the two photosystems (i.e., the so-called state transition [101], mentioned earlier). This affects mainly the slow phase of the fluorescence induction (see Section 2.2), and the photochemical activity changes following the activation of FNR and Calvin–Benson cycle. Yet, during the fast part of the transient, the OJIP phase, when the fluorescence rises in less than one second, the photosynthetic sample is assumed in general to preserve its initial state, and the variations in the fluorescence intensity are expected to be mostly due to changes in the redox state of the reaction center complex of PSII. The fast transient is affected, however, by changes occurring in the overall photosynthetic apparatus. Indeed, it is shown that the kinetics of the OJIP transient change when the photosynthetic samples are subjected to various environmental conditions, such as different light intensities [50,153–155], temperatures [45–47], drought [156], or when they are exposed to certain chemicals [157]. Extensive studies have established that, during exposure to prolonged sub-optimal environmental conditions, long-term strategies are brought to play by the organisms, as for example changes in protein expression, activation of new biochemical pathways, and repression of other pathways, which are characteristic of the unstressed state. As a result of sustained stress, the photosynthetic organism either acquires a new *homeostasis* (and eventually, later, protective metabolic adaptations alter physiological reactions of the whole plant) or, if the stress is severe, and the stress factor activity is not eliminated in time, a rapid damage of the plant occurs, leading to its death (see e.g., chapters in [158]). Some of the early mechanisms of acclimation to stress are oxygen radical scavenging, maintenance of ion uptake and water balance, and reactions altering carbon and nitrogen allocation, such that the reducing power is defused (see e.g., [159]). As a result, the OJIP fluorescence rise is affected in specific ways not only by structural, but also by other functional changes in the photosynthetic apparatus. This sensitivity of the fast fluorescence transient to the effects, caused by environmental factors, is very useful in studying different physiological states of plants.

In the next section, we review the analysis of only the fast part of the fluorescence induction transient.

4. Analysis of the fluorescence changes during the OJIP fluorescence rise

Reto J. Strasser and his collaborators [17,18,114,116,117] developed a computational tool to analyze the OJIP fluorescence transient in terms of the various PSII reactions, based on earlier general concepts of energy fluxes [81,83]. For simplicity, they called this test by an eye-catching name, *the JIP test*. In view of the extensive use of the JIP test in the published literature (~200–500 hits on Google search), we describe here the JIP test (i.e., analysis and understanding of the OJIP transient).

Fig. 3 is a schematic view (based on [117]) of the so-called energy fluxes, '**J**', related to the main phenomena occurring upon illumination of the PSII antenna in the photosynthetic sample. The JIP test, in its simplest form, assumes that there is no energy transfer between the PSII units, i.e., there is no connectivity between the PSII units, as if all the PSIIs exist independently, and thus it is called a '*separate package*' model. Inclusion of connectivity between 0 and 1 among PSII units is expected to affect the quantitative values of results, as the connectivity leads to a characteristic increase in the rate constant of Q_A reduction: $kL_t = kL_o \cdot (1 + C)/[1 + C\cdot(1 - \mathbf{B}_t)]$, where kL_t is the rate constant of Q_A reduction at any time t of the fluorescence transient, kL_o is the rate constant of Q_A reduction at $t = 0$, C is the connectivity parameter, and $\mathbf{B}_t$ is the fraction of closed PSII centers at any time t of the fluorescence transient (see e.g., Joliot and Joliot [79], and Strasser [81]). The details of the nomenclature of the terms we discuss here are described below (see also Table 1). To improve the clarity of terms, we have modified, in this review, the original notations for the energy fluxes used by Reto J. Strasser and collaborators [114,117] (see below, and the note in Appendix A). The total photon flux ***abs**orbed* by the PSII antenna pigments, $\mathbf{J}^{ABS}$ (ABS is the original notation), is partially ***tr**apped* by PSII reaction centers, $\mathbf{J}^{TR}$ (TR is the original notation), and partially ***di**ssipated* as e.g., heat and fluorescence, $\mathbf{J}^{DI}$ (DI is the original notation). The trapped exciton flux, $\mathbf{J}^{TR}$, represents the fraction of the absorbed photon flux used for the primary charge separation and stabilization of the reaction center II as $P680^+Q_A^-$ – i.e., 'closing' of PSII RCs. Lastly, the energy flux through the linear photosynthetic electron transport chain, from H_2O to Fd (and eventually to $NADP^+$ or other electron acceptors interacting with Fd), is represented by the electron transport flux $\mathbf{J}^{ET}$. This flux has a transient phase that coincides with the OJIPS Chl fluorescence induction period. The major changes in $\mathbf{J}^{ET}$ are mirrored by the variation in time of the fraction of Q_A reduction (in agreement with the theory of Duysens and Sweers [60]), especially during the fast OJIP phase.

All these energy fluxes (i.e., $\mathbf{J}^{ABS}$, $\mathbf{J}^{DI}$, $\mathbf{J}^{TR}$ and $\mathbf{J}^{ET}$) are interrelated, and are dependent on structural property and photosynthetic activity of the biological sample. Since the energy emitted as fluorescence by antenna chlorophylls is part of the dissipation energy flux, $\mathbf{J}^{DI}$, the fluorescence induction data can be theoretically related to the above energy fluxes [81,83,114].

The JIP test provides a number of parameters characterizing the photosynthetic sample, which are mainly estimates of energy fluxes per reaction center or per cross section (area) of the sample, ratios of different energy fluxes, and other mathematical expressions involving energy fluxes (see Table 1). These parameters are calculated using specific fluorescence values from the measured OJIP-transients, on the basis of a number of hypotheses regarding the photosynthetic apparatus and its function, such as excitation energy conversion, details of the electron transfer steps in the two photosynthetic systems, and of components that are expected to quench Chl *a* fluorescence (see Section 4.1 for the assumptions of the model).

We note that in this analysis only the maximum (initial) trapped exciton flux, $\mathbf{J}_o^{TR}$ (TR_0 is the original notation), is available, as evaluated from the initial slope of the relative variable fluorescence curve, $\mathbf{V_t}$, and the relative variable fluorescence value at the J-level, $\mathbf{V}_J$ (see bottom of Fig. 1, Table 1, and Section 4.2.1 Eq. (6), or Appendix A.1, Eq. (A15)). Also, two different values of the electron transport flux, $\mathbf{J}^{ET}$, have been estimated at two different moments during the fast fluorescence induction period (see Appendix A.1 for details): (i) $\mathbf{J}_o^{ET2}$ (ET_0 is the original notation) refers

Please cite this article in press as: A. Stirbet, Govindjee, On the relation between the Kautsky effect (chlorophyll *a* fluorescence induction) and Photosystem II: Basics and applications of the OJIP fluorescence transient, J. Photochem. Photobiol. B: Biol. (2011), doi:10.1016/j.jphotobiol.2010.12.010

Table 1
Equations and definitions of JIP parameters (based on information presented by Strasser and co-workers [18,114,116,117,160,175]). For reasons of clarity, several notations and definitions of JIP parameters used by Strasser and collaborators have been modified (for equivalence of notations, see text and Appendix A).

Information selected from the fast OJIP fluorescence induction (data necessary for the calculation of the so-called JIP parameters)	
$\mathbf{F_o} = \mathbf{F}_{20\mu s \text{ or } 50\mu s}$	First reliable fluorescence value after the onset of actinic illumination; used as initial value of the fluorescence
$\mathbf{F}_{300\mu s}$	Fluorescence value at 300 μs
$\mathbf{F_J} \equiv \mathbf{F}_{2ms}$	Fluorescence value at 2 ms (J-level)
$\mathbf{F_I} \equiv \mathbf{F}_{30ms}$	Fluorescence value at 30 ms (I-level)
$\mathbf{F_P}(\equiv \mathbf{F_M})$	Fluorescence value at the peak of OJIP curve; maximum value under saturating illumination
$\mathbf{t}_{Fmax}$	Time to reach the maximum fluorescence value $\mathbf{F_M}$
Area	Area between OJIP curve and the line $\mathbf{F} = \mathbf{F_M}$
Technical flurescence parameters	
$\mathbf{V_v} = \mathbf{F_t} - \mathbf{F_o}$	Variable Chl fluorescence
$\mathbf{F_V} = \mathbf{F_M} - \mathbf{F_o}$	Maximum variable Chl fluorescence
$\mathbf{V_t} = (\mathbf{F_t} - \mathbf{F_o})/(\mathbf{F_M} - \mathbf{F_o})$	Relative variable Chl fluorescence
$\mathbf{M_o} = (\Delta\mathbf{V}/\Delta\mathbf{t})_o = 4\ ms^{-1} \cdot (\mathbf{F}_{300\mu s} - \mathbf{F_o})/(\mathbf{F_M} - \mathbf{F_o})$	Approximate value of the initial slope of relative variable Chl fluorescence curve $\mathbf{V_t}$ (for $\mathbf{F_o} = \mathbf{F}_{50\mu s}$)
$\mathbf{S_m} \equiv \text{Area}/\mathbf{F_V}$	Normalized area (assumed proportional to the number of reduction and oxidation of one $\mathbf{Q_A}$-molecule during the fast OJIP transient, and therefore related to the number of electron carriers per electron transport chain)
Definitions of energy fluxes	
$\mathbf{J^{ABS}} = \mathbf{J^{TR}} + \mathbf{J^{DI}}$	Rate of photon absorption by total PSII antenna-denoted *as absorbed photon flux*
$\mathbf{J^{TR}}$	Rate of exciton trapping (leading to $\mathbf{Q_A}$ reduction) by all PSII RCs-denoted *trapped exciton flux*
$\mathbf{J_o^{TR}}$	Maximum (initial) trapped exciton flux
$\mathbf{J^{DI}}$	Rate of energy dissipation in all the PSIIs, in processes other than trapping – denoted as *dissipated energy flux*
$\mathbf{J_o^{ET2}}$	Electron transport flux from $\mathbf{Q_A}$ to $\mathbf{Q_B}$
$\mathbf{J_o^{RE1}}$	Electron transport flux until PSI acceptors (defined at t = 30 ms, corresponding to the I-level)
Quantum yields and efficiencies/probabilities	
$\varphi_{Po} \equiv \mathbf{J_o^{TR}}/\mathbf{J^{ABS}} = 1 - \mathbf{F_o}/\mathbf{F_M}$	Maximum quantum yield of primary PSII photochemistry
$\varphi_{Pt} \equiv J^{TR}/\mathbf{J^{ABS}} = 1 - \mathbf{F_t}/\mathbf{F_M} = \varphi_{Po} \cdot (1 - \mathbf{V_t})$	Quantum yield of primary PSII photochemistry
$\varphi_{ET2o} \equiv \mathbf{J_o^{ET2}}/\mathbf{J^{ABS}} = 1 - \mathbf{F_J}/\mathbf{F_M} = \varphi_{Po} \cdot (1 - \mathbf{V_J})$	Quantum yield of the electron transport flux from $\mathbf{Q_A}$ to $\mathbf{Q_B}$
$\varphi_{RE1o} \equiv \mathbf{J_o^{RE1}}/\mathbf{J^{ABS}} = 1 - \mathbf{F_I}/\mathbf{F_M} = \varphi_{Po} \cdot (1 - \mathbf{V_I})$	Quantum yield of the electron transport flux until the PSI electron acceptors
$\psi_{ET2o} \equiv \mathbf{J_o^{ET2}}/\mathbf{J_o^{TR}} = 1 - \mathbf{V_J}$	Efficiency/probability with which a PSII trapped electron is transferred from $\mathbf{Q_A}$ to $\mathbf{Q_B}$
$\psi_{RE1o} \equiv \mathbf{J_o^{RE1}}/\mathbf{J_o^{TR}} = 1 - \mathbf{V_I}$	Efficiency/probability with which a PSII trapped electron is transferred until PSI acceptors
$\delta_{RE1o} \equiv \mathbf{J_o^{RE1}}/\mathbf{J_o^{ET2}} = (1 - \mathbf{V_I})/(1 - \mathbf{V_J})$	Efficiency/probability with which an electron from $\mathbf{Q_B}$ is transferred until PSI acceptors
Specific energy fluxes (per active PSII reaction center)	
$\mathbf{J^{ABS}}/\mathbf{RC} = (\mathbf{M_o}/\mathbf{V_J}) \cdot (1/\varphi_{Po})$	Average absorbed photon flux per PSII reaction center (or also, apparent antenna size of an active PSII)
$\gamma_{RC2} \equiv \mathbf{Chl_{RC}}/\mathbf{Chl_{tot}}$	Probability that a PSII Chl functions as RC
$\mathbf{RC}/\mathbf{J^{ABS}} = \varphi_{Po} \cdot \mathbf{V_J}/\mathbf{M_o} = \gamma_{RC2}/(1 - \gamma_{RC2})$	Number of $\mathbf{Q_A}$ reducing RCs per PSII antenna Chl
$\mathbf{J_o^{TR}}/\mathbf{RC} = \mathbf{M_o}/\mathbf{V_J}$	Maximum trapped exciton flux per PSII
$\mathbf{J_o^{ET2}}/\mathbf{RC} = (\mathbf{M_o}/\mathbf{V_J}) \cdot (1 - \mathbf{V_J})$	Electron transport flux from $\mathbf{Q_A}$ to $\mathbf{Q_B}$ per PSII
$\mathbf{J_o^{RE1}}/\mathbf{RC} = (\mathbf{M_o}/\mathbf{V_J}) \cdot (1 - \mathbf{V_I})$	Electron transport flux until PSI acceptors per PSII
Phenomenological energy fluxes/activities (per excited cross section CS)	
$\mathbf{J^{ABS}}/\mathbf{CS_o} = \mathbf{F_o}$ or $\mathbf{J^{ABS}}/\mathbf{CS_M} = \mathbf{F_M}$	Absorbed photon flux per cross section (or also, apparent PSII antenna size)
$\mathbf{RC}/\mathbf{CS} = (\mathbf{RC}/\mathbf{J^{ABS}}) \cdot (\mathbf{J^{ABS}}/\mathbf{CS})$	The number of active PSII RCs per cross section
$\mathbf{J_o^{TR}}/\mathbf{CS} = (\mathbf{J_o^{TR}}/\mathbf{J^{ABS}}) \cdot (\mathbf{J^{ABS}}/\mathbf{CS})$	Maximum trapped exciton flux per cross section
$\mathbf{J_o^{ET2}}/\mathbf{CS} = (\mathbf{J_o^{ET2}}/\mathbf{J^{ABS}}) \cdot (\mathbf{J^{ABS}}/\mathbf{CS})$	Electron transport flux from $\mathbf{Q_A}$ to $\mathbf{Q_B}$ per cross section
$\mathbf{J_o^{RE1}}/\mathbf{CS} = (\mathbf{J_o^{RE1}}/\mathbf{J^{ABS}}) \cdot (\mathbf{J^{ABS}}/\mathbf{CS})$	Electron transport flux until PSI acceptors per cross section
De-excitation rate constants of PSII antenna	
$\mathbf{k_N} = \mathbf{k_F} \cdot \mathbf{J^{ABS}}/\mathbf{F_M}$	Non-photochemical de-excitation rate constant; $\mathbf{k_F}$ being the rate constant for fluorescence emission
$\mathbf{k_P} = \mathbf{k_F} \cdot \mathbf{J^{ABS}} \cdot \mathbf{F_V}/(\mathbf{F_o} \cdot \mathbf{F_M}) = \mathbf{k_N} \cdot \mathbf{F_V}/\mathbf{F_o}$	Photochemical de-excitation rate constant
"Performance" indexes (combination of parameters)	
$\mathbf{PI_{ABS}} = [\gamma_{RC2}/(1 - \gamma_{RC2})] \cdot [\varphi_{Po}/(1 - \varphi_{Po})] \cdot [\psi_{ET2o}/(1 - \psi_{ET2o})]$	Performance index for energy conservation from photons absorbed by PSII antenna, to the reduction of $\mathbf{Q_B}$
$\mathbf{PI_{ABS}^{total}} = \mathbf{PI_{ABS}} \cdot [\delta_{RE1o}/(1 - \delta_{RE1o})]$	Performance index for energy conservation from photons absorbed by PSII antenna, until the reduction of PSI acceptors
$\mathbf{PI_{CSo}^{total}} = \mathbf{F_o} \cdot \mathbf{PI_{ABS}^{total}}$; $\mathbf{PI_{CSM}^{total}} = \mathbf{F_M} \cdot \mathbf{PI_{ABS}^{total}}$	Performance index on cross section basis
Driving forces (total driving forces for photochemical activity)	
$\mathbf{DF_{ABS}^{total}} = \log(\mathbf{PI_{ABS}^{total}})$	Driving force on absorption basis
$\mathbf{DF_{CS}^{total}} = \log(\mathbf{PI_{CS}^{total}})$	Driving force on cross section basis

to the electron transport flux from Q_A to Q_B and (ii) $\mathbf{J_o^{RE1}}$ (from the ***re***duction of PS***1*** electron acceptors-RE_0 original notation), which is a recently introduced JIP parameter [117,160], refers to the electron transport flux until the PSI acceptors.

In the following sections we provide a detailed description of the JIP test (i.e., analysis and understanding of the OJIP transient), by first presenting the main assumptions that form the theoretical basis of this model (Section 4.1), and then introducing the various parameters and their derivations (see Table 1, Section 4.2, and the Appendix A).

4.1. The assumptions

In order to appreciate the analysis reviewed here, we present all the assumptions made for a realistic understanding of this method. Due to the obvious limitations that Chl *a* fluorescence is only one of the pathways of de-excitation of the excited state of Chl *a*, a number of assumptions and restrictions must be imposed in the analysis of the fluorescence induction data, and the derivation of the JIP parameters that provide information on PSII reactions. Below we specify the main theoretical hypotheses on which this analysis is

Please cite this article in press as: A. Stirbet, Govindjee, On the relation between the Kautsky effect (chlorophyll *a* fluorescence induction) and Photosystem II: Basics and applications of the OJIP fluorescence transient, J. Photochem. Photobiol. B: Biol. (2011), doi:10.1016/j.jphotobiol.2010.12.010

based (see Strasser and co-workers [17,18,114,116,117]). A discussion of the implications for the accuracy of JIP parameters, and the limits of the JIP test method for the study of photosynthetic activity, will be briefly described in Section 5 (Pros and Cons of the JIP test).

The assumptions (with relevant discussion) are:

(1) The structural–functional view of the photosynthetic apparatus presented in Fig. 2 is correct.

(2) The fluorescence of PSI is constant [15,60,161], and at room temperature its contribution to the total fluorescence signal is very low [162–166]; thus, PSI fluorescence can be neglected in most cases, especially because we deal with variable fluorescence that originates specifically in PSII.

(3) In order to simplify the theoretical approach, PSII units are considered to be homogeneous and active (i.e., all of them are capable of photochemical activity). See, however, Sections 4.3.2 and 4.3.3 that show how we can obtain information on heterogeneity of PSIIs and on inactive PSIIs from the fast fluorescence induction data.

(4) In the same physiological state (i.e., in a sample kept in darkness or in light), an open PSII center (i.e., with oxidized Q_A) has a low (minimum) fluorescence emission, and a closed PSII (i.e., with reduced Q_A) has a high fluorescence emission (see [60]). The increase in the fluorescence intensity is therefore assumed to be due mainly to the reduction of Q_A, which determines the entire shape of the OJIP curve. The contributions of oxidized PSII reaction center chlorophyll ($P680^+$), and reduced pheophytin (Phe^-) to the fluorescence quenching are ignored, since their contributions in this time range are expected to be negligible (see [64,65] for ($P680^+$); for a different view on Phe^-, see [67]). In addition, the possible non-photochemical quenching by the oxidized plastoquinone PQ-pool observed by Vernotte et al. [68] (which most probably takes place only in samples in which the integrity of the photosynthetic apparatus is compromised, as in thylakoids and PSII preparations [167]), and the eventual non-photochemical quenching effect of the local electrical field at the P680 level [58], are also neglected in the current JIP test.

(5) Although all the measured fluorescence is from the antenna pigment complex, the organization of the antenna pigments proteins is ignored in the current analysis; they are considered to form homogeneous "blocks" of Chl *a* molecules serving each RC. Further, in the analysis, the contributions of accessory pigments (e.g., Chl *b*; carotenoids; and the phycobilins), if any, are ignored. In green algae and higher plants, the efficiency of excitation energy transfer from Chl *b* to Chl *a* is 100% (Duysens [168]); for cyanobacteria, which contain phycobilins, see e.g., Nedbal et al. [169].

(6) The PSII reaction centers are considered independent, and thus, not connected to each other (however, see Section 4.3.1, where it is shown how we can obtain information on connectivity between the PSII antenna from the fast fluorescence induction data).

(7) The fluorescence rise from the O to the P-level is assumed to be so fast that no significant change of the physiological state of the sample occurs, i.e., it is assumed that the structure and conformation of the photosynthetic apparatus remain constant during this fast transient.

(8) In samples that had been kept in darkness for a few minutes, Q_A as well as the PQ-pool are considered to be in the oxidized state. (We know that there are cases where this is not true, and, thus, care must be exercised in interpreting data from different samples.)

(9) It is assumed that all active PSII reaction centers close with a sufficiently strong light pulse. Therefore, when the maximum fluorescence $\mathbf{F}_M \equiv \mathbf{F}_P$ is measured at the end of the OJIP transient, all Q_A molecules are considered to be in reduced state, Q_A^-, in the active PSIIs. This hypothesis is not always valid, as for example in the case of light adapted samples [89], or severely heat-treated plants [170].

(10) The well-known formula for the photochemical quantum yield of PSII photochemistry, $\varphi_{Pt} = 1 - \mathbf{F}_t/\mathbf{F}_M$ [76–78] is derived in the context of the JIP test theory [17], considering the assumption that the dissipated energy flux, $\mathbf{J}^{DI}$, is directly proportional to the measured fluorescence $\mathbf{F}$: $\mathbf{J}_t^{DI} = \alpha \cdot \mathbf{F}_t$, where α is the proportionality constant (see Appendix A.1, Eq. (A2), and [17]).

Different ways to obtain the photochemical quantum yield of PSII photochemistry have been proposed [see e.g., 14,15,17,18,76–78,83]. In this review the formula for φ_{Pt} was obtained using an assumption written as: $\mathbf{J}^{DI} = \alpha_{op} \cdot F^{op} + \alpha_{cl} \cdot F^{cl}$, where F^{op} and F^{cl} represent the fluorescence emitted, respectively, by the open and closed PSIIs, and α_{op} and α_{cl} are their specific proportionality constants (see Appendix A.6).

(11) The trapped exciton flux, $\mathbf{J}^{TR}$, represents the fraction of the absorbed photon flux used for PSII primary charge separation *and stabilization* as $P680^+Q_A^-$. Therefore, the number of electrons transferred to Q_A, in the photosynthetic sample, is equal to the number of excitons trapped by PSII RCs. With this definition of the exciton trapping, the possible occurrence of charge recombination between the primary reaction center pair $P680^+$ and Phe^- is not expected to affect the value of $\mathbf{J}^{TR}$ (see Section 4.2.1 Eq. (2), and Appendix A.1, Eq. (A12)).

(12) Q_A is reduced only once (i.e., it undergoes a single turnover) as the fluorescence rises to the J-level; in strong light, it reaches its maximum at ~2 ms ($\mathbf{F}_J = \mathbf{F}_{2ms}$) (see bottom graph in Fig. 1). The justification for this hypothesis is based on the experimental evidence obtained by Strasser and Strasser [114], suggesting that the O–J phase of the relative variable fluorescence of a normal photosynthetic sample, normalized to $\mathbf{V}_J$, is very similar to the relative variable fluorescence obtained in the presence of 3-(3′,4′dichlorophenyl)-1,1′dimethylurea (DCMU), when the electron transfer from Q_A to Q_B is blocked (see e.g. [171]); in the presence of DCMU, Q_A is known to be reduced only once until the fluorescence rises to $\mathbf{F}_M$. Therefore, the initial slope of the relative variable fluorescence curve of a DCMU treated sample, $\mathbf{M}_{o\_DCMU}$, is approximated with the ratio $\mathbf{M}_o/\mathbf{V}_J$, where $\mathbf{M}_o$ and $\mathbf{V}_J$ are respectively, the initial slope, and the J-level value of the relative variable fluorescence curve $\mathbf{V}_t$ of the untreated sample (see Section 4.2.1 Eq. (6), and Appendix A.1, Eq. (A15)). As a result, the specific rate of the electron transport from Q_A to Q_B, labeled as $\mathbf{J}_o^{ET2}/\mathbf{RC}$, is obtained theoretically *as depending on the* $\mathbf{V}_J$ *value* (i.e., a fraction of the maximum specific trapped exciton flux: $\mathbf{J}_o^{ET2}/\mathbf{RC} = (\mathbf{J}_o^{TR}/\mathbf{RC}) \cdot (1 - \mathbf{V}_J)$ – see Section 4.2.2, Eq. (10), and Appendix A.1, Eq. (A19)).

(13) Studies of the OJIP transient through numerical simulations [53,55,56,172] suggest that, during the initial part of the J–I phase of fluorescence transient (see the bottom graph in Fig. 1), the PQ-pool begins to be reduced. On the other hand, simultaneous measurements of the fluorescence transient and the transmission changes at 820 nm, due to PC and P700 (see [74]), indicate that, at the end of this phase (i.e., at the I-level), the electrons generated by PSII just reach PC, and start to be transferred to the end of the electron acceptor side of PSI (see Fig. 2; and also [173]); in the case of samples kept in the dark, in which FNR is inactive for 1–2 s after the onset of the light [74], Fd can be considered

Please cite this article in press as: A. Stirbet, Govindjee, On the relation between the Kautsky effect (chlorophyll *a* fluorescence induction) and Photosystem II: Basics and applications of the OJIP fluorescence transient, J. Photochem. Photobiol. B: Biol. (2011), doi:10.1016/j.jphotobiol.2010.12.010

as the end PSI electron acceptor in the linear photosynthetic electron transport chain during the OJIP transient. Consequently, a specific electron transport flux, labeled $\mathbf{J}_o^{RE1}/\mathbf{RC}$, can also be defined at the time of the I-level (t = 30 ms), also as a fraction of the maximum specific PSII trapped exciton flux: $\mathbf{J}_o^{RE1}/\mathbf{RC} = (\mathbf{J}_o^{TR}/\mathbf{RC}) \cdot (1 - \mathbf{V}_I)$ (see Table 1 and Appendix A.1, Eq. (A24)); this represents the specific electron transport flux until PSI acceptors.

(14) The normalized area between the fast fluorescence induction curve and the upper line defined by the $\mathbf{F}_M$ level, $\mathbf{S}_m = \mathbf{Area}/(\mathbf{F}_M - \mathbf{F}_o)$, is proportional to the number of electrons passing through the electron transport chain, with $N = \mathbf{S}_m/\mathbf{S}_s$ (where $\mathbf{S}_s$ represents the normalized area for single turnover events), meaning the number of times Q_A becomes reduced and re-oxidized again, until the maximum fluorescence intensity $\mathbf{F}_M$ is reached (i.e., the turnover number) (see Malkin and Kok [174] and Schreiber et al. [21]).

(15) The absorbed photon flux, $\mathbf{J}^{ABS}$, approximates PSII antenna chlorophyll content of the measured sample, Chl_{ant} (see Appendix A.1, A.1.3, Eq. (A47)).

(16) The fluorescence value of $\mathbf{F}_o$ (or $\mathbf{F}_M$) approximates the phenomenological absorbed photon flux, expressed as the ratio $\mathbf{J}^{ABS}/\mathbf{CS}$, where **CS** represents the excitation cross section of PSII (see Table 1 and Appendix A.2, Eqs. (A28) and (A29)).

(17) The inverse of the initial slope of the relative variable fluorescence curve of a DCMU treated sample $(\mathbf{M}_{o,DCMU})^{-1}$, approximates the normalized area over the fluorescence transient, $\mathbf{S}_S$ (see Appendix A.4, Eq. (A45)).

4.2. Fluorescence parameters

Changes in Chl *a* fluorescence intensity when plants kept in darkness are exposed to continuous light can be recorded with a high time resolution, from microseconds to seconds, using commercial instruments such as the PEA (Plant Efficiency Analyser), HandyPEA, M-PEA, or PocketPEA (Hansatech Instruments, Kings Lynn Norfolk, UK). (Other available instruments are not mentioned, as they were not used for the data presented in this review.) For the HandyPEA and the PEA, the actinic light (peak at 650 nm) is supplied by an array of three or six light emitting diodes, respectively, and is focused on the sample surface to provide a homogeneous irradiation of the exposed area (4 mm diameter). A maximum intensity of 600 Wm^{-2} (3200 μmol photons m^{-2} s^{-1}) is routinely used in most experiments [18].

The polyphasic Chl *a* fluorescence rise during the first second of illumination is characteristic of the majority of the oxygenic photosynthetic organisms (see Papageorgiou et al. [22] for differences between different organisms). For their JIP test, Strasser and Strasser [114] used raw fluorescence data collected during the first second of illumination; seven selected values were stored separately in order to be processed into the JIP parameters (see also Table 1): (1) the first reliable fluorescence value in the transient (e.g., the fluorescence at t = 20 μs when using HandyPEA, M-PEA or PoketPEA instruments, or 50 μs for PEA) is used as the initial fluorescence value, $\mathbf{F}_o$, for samples that had been kept in darkness for a few minutes; (2) $\mathbf{F}_M$, the maximum fluorescence level of the OJIP transient, measured under saturating light conditions; (3, 4 and 5) three intermediate fluorescence values measured at 300 μs, 2 ms, and 30 ms, and labeled as $\mathbf{F}_{300\mu s}$, $\mathbf{F}_J$, and $\mathbf{F}_I$, respectively; (6) the time following the onset needed to reach the maximum fluorescence value, t_{Fmax}; and (7) the area between the fluorescence curve and the level of the maximum intensity $\mathbf{F}_M$ (measured in ms · fluorescence relative units), labeled **Area**.

The summary of the JIP parameters, calculated with these selected fluorescence data, is shown in Table 1 (based on publications by Strasser and co-workers [17,18,114,116,117,175]). The table is divided into several main categories: technical fluorescence data; quantum efficiencies and energy flux ratios; specific energy fluxes or activities (defined per reaction center); phenomenological energy fluxes or activities (defined per cross section); de-excitation constants; performance indexes and driving forces. The detailed derivation of all the JIP parameters is shown in the Appendix A. Below, we present only the derivation of the maximum specific trapped exciton flux, $\mathbf{J}_o^{TR}/\mathbf{RC}$, and that of the specific electron transport flux from Q_A to Q_B, $\mathbf{J}_o^{ET2}/\mathbf{RC}$, which are central to this analysis. We will also present information on what is called the performance index, **PI**, an important parameter to plant biologists.

4.2.1. The maximum flux of excitons trapped per PSII (leading to Q_A reduction), designated as the specific maximum trapped exciton flux, $\mathbf{J}_o^{TR}/\mathbf{RC}$

The (maximum) trapped exciton flux, $\mathbf{J}_o^{TR}$, is obtained from the initial slope of the relative variable fluorescence measured on DCMU treated samples, in which the electron transfer from Q_A^- to Q_B is blocked (since Q_B is displaced by DCMU [176,177]). The slope, $\mathbf{M}_{o,DCMU} = (dV/dt)_o$, can be approximated from the experimental data as $\Delta\mathbf{V}_o/\Delta t_o$:

$$\mathbf{M}_{o,DCMU} = (dV/dt)_o \cong \Delta\mathbf{V}_o/\Delta t_o = \Delta\{[Q_A^-]/[Q_A]_{total}\}_o/\Delta t_o \quad (1)$$

With this slope, which equals the rate of increase of the fraction of closed RCs (Eq. 1) we can evaluate the maximum trapped exciton flux, $\mathbf{J}_o^{TR}$ (see below) only when the PSII units are not connected.

Since all PSII units are considered homogeneous (assumption (**3**), Section 4.1), every active PSII has a Q_A, and the total number of active PSII reaction centers (**RC**) in the measured area of the sample is equal to $[Q_A]_{total}$. Therefore the initial slope $M_{o,DCMU}$ can be written also as:

$$\mathbf{M}_{o,DCMU} \cong \Delta\{[Q_A^-]/\mathbf{RC}\}_o/\Delta t_o = \{\Delta[Q_A^-]_o/\Delta t_o\}/\mathbf{RC}, \quad (2)$$

where $\Delta[Q_A^-]_o/\Delta t_o$ approximates the initial rate of Q_A reduction, or in other words, the initial rate of closure of the PSII reaction centers. Consistent with the definition of $\mathbf{J}^{TR}$ (see assumption (**11**), Section 4.1), one RC is closed ($Q_A \rightarrow Q_A^-$) for every exciton trapped, and the initial rate of Q_A reduction will be a measure of the (maximum) trapped exciton flux, $\mathbf{J}_o^{TR}$:

$$\mathbf{J}_o^{TR} = (d[Q_A^-]/dt)_o \cong \Delta[Q_A^-]_o/\Delta t_o \quad (3)$$

Then, from Eq. (2) and (3), the maximum specific (per PSII reaction center) trapped exciton flux will be:

$$\mathbf{J}_o^{TR}/\mathbf{RC} = \mathbf{M}_{o,DCMU} \cong \Delta\mathbf{V}_o/\Delta t_o \quad (4)$$

In order to have an accurate estimate of the initial slope $\mathbf{M}_{o,DCMU}$, the time interval Δt_o must be very small, since Δt_o is an approximation of dt_o, which is an infinitesimal small time interval. In the JIP test [114], the time interval of 0.25 ms has been used (Δt_o = 0.3–0.05 ms). However, the fluorescence curve of photosynthetic samples has a sigmoidal shape, due to PSII connectivity [77,79,81] which can affect the evaluation of $\mathbf{M}_{o,DCMU}$. $\mathbf{F}_{300\mu s}$ is a good choice for this evaluation, because numerous experimental data show that its value is least affected by the connectivity ([17,1,178,179]; also see Section 4.3.1). Thus:

$$\mathbf{J}_o^{TR}/\mathbf{RC} \cong \mathbf{M}_{o,DCMU} \cong \Delta\mathbf{V}_o/\Delta t_o = 4\ ms^{-1} \cdot (\mathbf{F}_{0.3ms} - \mathbf{F}_{0.05ms})/(\mathbf{F}_M - \mathbf{F}_{0.05ms}) \quad (5)$$

Please cite this article in press as: A. Stirbet, Govindjee, On the relation between the Kautsky effect (chlorophyll *a* fluorescence induction) and Photosystem II: Basics and applications of the OJIP fluorescence transient, J. Photochem. Photobiol. B: Biol. (2011), doi:10.1016/j.jphotobiol.2010.12.010

For practical reasons, $\mathbf{M}_{o,DCMU}$ cannot be directly measured under field experiments. Nevertheless, it can be evaluated using fluorescence data obtained on samples untreated with DCMU. In this case, the initial slope of the relative variable fluorescence curve, $\mathbf{M}_o$, is smaller than $\mathbf{M}_{o,DCMU}$, because the relative fluorescence at $t = 0.3$ ms is lowered by reoxidation of Q_A^- as a result of electron transfer to Q_B (see the electron transfer chain in Fig. 2). However, some experimental results [114] suggest that $M_{o,DCMU}$ can be approximated with the ratio $\mathbf{M}_o/\mathbf{V}_J$ (assumption (**12**), Section 4.1). Hence, for control samples (i.e., not treated with DCMU), the maximum specific trapped exciton flux $\mathbf{J}_o^{TR}/\mathbf{RC}$ can be obtained as follows:

$$\begin{aligned}\mathbf{J}_o^{TR}/\mathbf{RC} &= \mathbf{M}_o/\mathbf{V}_J \\ &= 4\ \mathrm{ms}^{-1}\cdot[(\mathbf{F}_{0.3ms}-\mathbf{F}_{0.05ms})/(\mathbf{F}_M-\mathbf{F}_{0.05ms})]/ \\ &\quad [(\mathbf{F}_{2ms}-\mathbf{F}_{0.05ms})/(\mathbf{F}_M-\mathbf{F}_{0.05ms})] \\ &= 4\mathrm{ms}^{-1}\cdot(\mathbf{F}_{0.3ms}-\mathbf{F}_{0.05ms})/(\mathbf{F}_{2ms}-\mathbf{F}_{0.05ms}) \qquad (6)\end{aligned}$$

$\mathbf{J}_o^{TR}/\mathbf{RC}$ represents the initial rate of the closure of photoactive RCs per total number of photoactive RCs. However, under stress conditions, some of the PSII centers are inactivated (i.e., are no longer capable of reducing Q_A to Q_A^-), being transformed into so-called 'silent' reaction centers (see e.g. [180]; and also the Section 4.3.2). Nonetheless, $\mathbf{J}_o^{TR}/\mathbf{RC}$ still refers only to the active PSII centers. The same is valid for all the JIP parameters expressed as a function of **RC** (i.e., specific JIP parameters), since their derivation is based on $\mathbf{J}_o^{TR}/\mathbf{RC}$.

Using the maximum quantum yield of primary PSII photochemistry, $\varphi_{Po} \equiv \mathbf{J}_o^{TR}/\mathbf{J}^{ABS} = \mathbf{F}_V/\mathbf{F}_M$ (see [8,76–78]; also Appendix A.1, Eq. (A7)), the average absorbed photon flux per reaction center, $\mathbf{J}^{ABS}/\mathbf{RC}$, can be evaluated as:

$$\mathbf{J}^{ABS}/\mathbf{RC} = (\mathbf{J}_o^{TR}/\mathbf{RC})/(\mathbf{J}_o^{TR}/\mathbf{J}^{ABS}) = (\mathbf{J}_o^{TR}/\mathbf{RC})\cdot(1/\varphi_{Po}) \qquad (7)$$

Then:

$$\mathbf{J}_o^{TR}/\mathbf{RC} = \varphi_{Po}\cdot\mathbf{J}^{ABS}/\mathbf{RC} \qquad (8)$$

Based on Eq. (8), the JIP parameter $\mathbf{J}^{ABS}/\mathbf{RC}$ is regarded also as a measure of the apparent antenna size, i.e. the average amount of absorbing antenna chlorophylls per fully active (Q_A-reducing) reaction center, $Chl_{ant}/\mathbf{RC}$ [114]. However, because $\mathbf{J}^{ABS}/\mathbf{RC}$ is not equal, but only proportional, to the amount of absorbing Chl antenna molecules per active RC, it can be used as a measure of $Chl_{ant}/\mathbf{RC}$ *only* in a comparative manner. As φ_{Po} represents an average maximum photochemical quantum yield of all different types of PSII RCs in the sample, this 'antenna size' is also an average. Nevertheless, it offers a way to detect eventual inactivation of RCs (see Section 4.3.2).

4.2.2. Specific electron transport flux from Q_A to Q_B, $\mathbf{J}_o^{ET2}/\mathbf{RC}$

For normal photosynthetic samples, the initial slope of the relative variable fluorescence curve, $\mathbf{M}_o$, indicates the net rate of the closure of PSII RCs. The exciton trapping increases the number of closed centers, and the electron transport from Q_A to Q_B decreases it:

$$\mathbf{M}_o = \mathbf{J}_o^{TR}/\mathbf{RC} - \mathbf{J}_o^{ET2}/\mathbf{RC} \quad \text{and then} \quad \mathbf{J}_o^{ET2}/\mathbf{RC} = \mathbf{J}_o^{TR}/\mathbf{RC} - \mathbf{M}_o \qquad (9)$$

Using Eq. (6), the specific electron transport flux from Q_A to Q_B, $\mathbf{J}_o^{ET2}/\mathbf{RC}$, is calculated as:

$$\begin{aligned}\mathbf{J}_o^{ET2}/\mathbf{RC} &= (\mathbf{M}_o/\mathbf{V}_J) - \mathbf{M}_o = (\mathbf{M}_o/\mathbf{V}_J)\cdot(1-\mathbf{V}_J) \\ &= (\mathbf{J}_o^{TR}/\mathbf{RC})\cdot(1-\mathbf{V}_J) \qquad (10)\end{aligned}$$

4.2.3. Performance index (**PI**), an important JIP parameter, and the driving force (log **PI**)

In general, in a large number of photosynthetic studies, the ratio $\mathbf{F}_V/\mathbf{F}_M = (\mathbf{F}_M - \mathbf{F}_o)/\mathbf{F}_M$ is used as a stress indicator. However, this empirical parameter, based on $\mathbf{F}_o$ and $\mathbf{F}_M$ fluorescence values, is not always sensitive enough to observe differences between diverse samples. Srivastava et al. [116] (see also [17,18,117]) used a new, more responsive, and important, parameter, named performance index **PI**. This JIP parameter is based on a different approach, as in Goldman-equation, in which it is assumed that the total potential of a system can be calculated by multiplying the Nernst-equations for the individual components (Goldman [181]; also see Hodgkin and Katz [182]). The performance index, **PI**, is calculated in the same way as a Goldman-equation, from three (or four) components, which depends on the reaction center density, the trapping efficiency, and the electron transport efficiency (see below). Consequently, if a stress affects any of these components, the effect will show up in the performance index, which therefore has a higher sensitivity than that achieved by any of its isolated components. A driving force, expressed as log (**PI**) can then be calculated, just as is done in chemistry. In many cases [183–187], the expressions of **PI** and the driving force have been shown to be very sensitive to different stresses, and therefore very useful for physiological, environmental and biotechnological screening.

4.2.4. Performance index on absorption basis, PI_{ABS}

Initially, the product of three independent JIP parameters, combining structural properties of PSII (i.e., $\mathbf{RC}/\mathbf{J}^{ABS}$, φ_{Po}, and ψ_{ET2o}; see Table 1), was used to define an expression, called "structure–function index" $\mathbf{SFI}_{Po(ABS)}$ [43]:

$$\mathbf{SFI}_{Po(ABS)} = (\mathbf{RC}/\mathbf{J}^{ABS})\cdot\varphi_{Po}\cdot\psi_{ET2o} \qquad (11)$$

Since $\mathbf{J}^{ABS}/\mathbf{RC}$ is also regarded as a measure of the apparent antenna size, i.e., the amount of absorbing antenna chlorophylls per fully active (Q_A-reducing) reaction center (see Appendix A.1, A.1.3), then:

$$\begin{aligned}\mathbf{RC}/\mathbf{J}^{ABS} &\cong Chl_{RC}/Chl_{ant} = Chl_{RC}/(Chl_{tot}-Chl_{RC}) \\ &= (Chl_{RC}/Chl_{tot})/(1-Chl_{RC}/Chl_{tot}) \qquad (12)\end{aligned}$$

where Chl_{RC} represents the total PSII RC chlorophylls, and Chl_{tot} the total PSII Chl. Expressing the fraction of PSII RC chlorophylls relative to the total PSII chlorophyll as $\gamma_{RC2} = Chl_{RC}/Chl_{tot}$, we have:

$$\mathbf{RC}/\mathbf{J}^{ABS} = \gamma_{RC2}/(1-\gamma_{RC2}) \qquad (13)$$

And:

$$\mathbf{SFI}_{Po(ABS)} = [\gamma_{RC2}/(1-\gamma_{RC2})]\cdot\varphi_{Po}\cdot\psi_{ET2o} \qquad (14)$$

Srivastava et al. [116] presented the performance index, on absorption basis, $\mathbf{PI}_{ABS}$, in which all the constitutive terms were introduced as ratios, similar to Eq. (14) (a yield divided by its complementary function):

$$\mathbf{PI}_{ABS} = [\gamma_{RC2}/(1-\gamma_{RC2})]\cdot[\varphi_{Po}/(1-\varphi_{Po})]\cdot[\psi_{ET2o}/(1-\psi_{ET2o})] \qquad (15)$$

The total performance index, $\mathbf{PI}^{total}$, is obtained by multiplying Eq. (15) with a fourth term, characterizing the efficiency of the electron transport flux until PSI acceptors, δ_{RE1o} (see Table 1 and [117,160]):

$$\begin{aligned}\mathbf{PI}_{ABS}^{total} &= \mathbf{PI}_{ABS}\cdot\delta_{RE1o}/(1-\delta_{RE1o}) \\ &= [\gamma_{RC}/(1-\gamma_{RC})]\cdot[\varphi_{Po}/(1-\varphi_{Po})]\cdot[\psi_{ET2o}/(1-\psi_{ET2o})] \\ &\quad\cdot[\delta_{RE1o}/(1-\delta_{RE1o})] \qquad (16)\end{aligned}$$

4.2.5. Performance index on cross section basis, PI_{CS}

The performance index on cross section basis, $\mathbf{PI}_{CS}$, is obtained by multiplying the performance index on absorption basis $\mathbf{PI}_{ABS}$ (Eq. (16)), by the phenomenological energy flux, $\mathbf{J}^{ABS}/\mathbf{CS} = \mathbf{F}_o$ (or $\mathbf{F}_M$):

Please cite this article in press as: A. Stirbet, Govindjee, On the relation between the Kautsky effect (chlorophyll *a* fluorescence induction) and Photosystem II: Basics and applications of the OJIP fluorescence transient, J. Photochem. Photobiol. B: Biol. (2011), doi:10.1016/j.jphotobiol.2010.12.010

$$\mathbf{PI}^{\text{total}}_{\text{CS,o}} = \mathbf{F}_\text{o} \cdot [\gamma_\text{RC}/(1-\gamma_\text{RC})] \cdot [\varphi_\text{Po}/(1-\varphi_\text{Po})] \cdot [\psi_\text{ET2o}/(1-\psi_\text{ET2o})] \cdot [\delta_\text{RE1o}/(1-\delta_\text{RE1o})] \quad (17)$$

$$\mathbf{PI}^{\text{total}}_{\text{CS,M}} = \mathbf{F}_\text{M} \cdot [\gamma_\text{RC}/(1-\gamma_\text{RC})] \cdot [\varphi_\text{Po}/(1-\varphi_\text{Po})] \cdot [(\psi_\text{ET2o}/(1-\psi_\text{ET2o})] \cdot [\delta_\text{RE1o}/(1-\delta_\text{RE1o})] \quad (18)$$

4.2.6. Driving forces: $\mathbf{DF}_{ABS}$ and $\mathbf{DF}_{CS}$

The performance index was especially designed (see Eqs. (15)–(18)) as a product of terms in the form $p_i/(1-p_i)$, similar to what is done for the Nernst equation. Extrapolating this concept from chemistry, the log(**PI**) can be considered as the total *driving force* for the photochemical activity of the observed system; it would be the sum of the partial driving forces for the events involved in OJIP fluorescence rise. Therefore:

$$\mathbf{DF}^{\text{total}}_{\text{ABS}} = \log(\mathbf{PI}^{\text{total}}_{\text{ABS}}) = log(\mathbf{RC}/\mathbf{J}^{\text{ABS}}) + \log[\varphi_\text{Po}/(1-\varphi_\text{Po})] + \log[\psi_\text{ET2o}/(1-\psi_\text{ET2o})] + \log[\delta_\text{RE1o}/(1-\delta_\text{RE1o})] \quad (19)$$

$$\mathbf{DF}^{\text{total}}_{\text{CS}} = \log\left(\mathbf{PI}^{\text{total}}_{\text{CS}}\right) = \log\left(\mathbf{PI}^{\text{total}}_{\text{ABS}}\right) + \log\left(\mathbf{J}^{\text{ABS}}/\mathbf{CS}\right) \quad (20)$$

4.3. Additional information obtained from OJIP fluorescence transient

Reto J. Strasser and collaborators have designed several original methods to obtain, based on the fast fluorescence induction data, structural and functional information on the photosynthetic organisms: the overall probability for the connectivity of PSII units; the evaluation of the fraction of non Q_A-reducing PSII reaction centers; and the evaluation of the fraction of non-Q_B-reducing PSII. These are reviewed below.

4.3.1. Evaluation of the overall probability for the connectivity of PSII units

The shape of the OJIP fluorescence induction curve is influenced by excitation energy transfer among PSII units, commonly called as PSII connectivity [77,79,63], or as grouping ([81]). The quantitative relation between the relative variable chlorophyll fluorescence, $\mathbf{V}(t) = (\mathbf{F}(t) - \mathbf{F}_\text{o})/(\mathbf{F}_\text{M} - \mathbf{F}_\text{o})$, and the fraction of PSII with reduced Q_A, $\mathbf{B}(t)$, has an hyperbolic form in the case of single turnover situation (DCMU treatment), and is described by the relation [81,83]:

$$\mathbf{V}(t) = \mathbf{B}(t)/[1 + \text{C} \cdot (1 - \mathbf{B}(t))], \quad (21)$$

where C is the parameter for the curvature of the hyperbola, being dependent on the overall probability of the connectivity between the PSII units, p:

$$\text{C} = p \cdot (\mathbf{F}_\text{as} - \mathbf{F}_\text{o})/\mathbf{F}_\text{o} = p \cdot [(\mathbf{F}_\text{M} - \mathbf{F}_\text{o})/\mathbf{F}_\text{o}] \cdot \mathbf{V}_\text{as} \quad (22)$$

with $\mathbf{F}_\text{as}$ being the fluorescence value used in the normalization of the fluorescence curve (the **as**ymptote).

Eq. (21) shows that for the unconnected photosystems (separate package model), with $p = 0$ and therefore C = 0, the relative variable fluorescence is identical to the fraction of closed reaction centers of PSII, and the fast kinetics of the fluorescence transient becomes exponential:

$$\mathbf{V}_\text{E}(t) = \mathbf{B}_\text{E}(t) = 1 - \exp[-k \cdot (t - t_\text{o})] \quad (23)$$

The exponential constant k can be calculated using the exponential fluorescence curve, $\mathbf{F}_\text{E}(t)$, as:

$$k = [1/(t - t_\text{o})] \cdot \ln[(\mathbf{F}_\text{as} - \mathbf{F}_\text{o})/(\mathbf{F}_\text{as} - \mathbf{F}_\text{E}(t))] \quad (24)$$

Here we present a method to evaluate the overall connectivity constant p from an experimental OJIP fluorescence induction curve, measured *in vivo*, on a sample that has been kept in darkness, under physiological conditions (for detailed information, see Stirbet et al. [178]; Strasser and Stirbet [179]). Fig. 4 shows the fast fluorescence transient of a normal pea leaf (the OJIP curve), and of the DCMU treated pea leaf (the DCMU curve), on a logarithmic time scale. As mentioned earlier (assumption (**12**), Section 4.1), Strasser and Strasser [114] proposed that the O–J part of relative variable fluorescence curve measured *in vivo* in control samples, normalized to $\mathbf{V}_\text{J}$, can be considered very similar to the relative variable fluorescence rise measured on DCMU treated samples. Naming $\mathbf{W}(t)$ the normalized $\mathbf{V}(t)$ curve of the normal sample, we have:

$$\mathbf{W}(t) = \mathbf{V}(t)/\mathbf{V}_\text{J} = (\mathbf{F}(t) - \mathbf{F}_\text{o})/(\mathbf{F}_\text{J} - \mathbf{F}_\text{o}) \quad (25)$$

In the inset of Fig. 4, the sigmoidal form of the curve $\mathbf{W}(t)$ can be clearly seen, proving the existence of an energetic connectivity among PSII centers of the sample. An exponential curve, with the asymptote $\mathbf{V}_\text{as} = \mathbf{V}_\text{J}$, can be constructed, for a hypothetical unconnected PSII population, which undergoes a single Q_A reduction (see Eq. (26), and the curve $\mathbf{W}_\text{E}(t)$ in the inset of Fig. 4):

$$\mathbf{W}_\text{E}(t) = \mathbf{V}_\text{E}(t)/\mathbf{V}_\text{J} = (\mathbf{F}_\text{E}(t) - \mathbf{F}_\text{o})/(\mathbf{F}_\text{J} - \mathbf{F}_\text{o}) = 1 - \exp[-k \cdot (t - t_\text{o})] \quad (26)$$

The curves $\mathbf{W}(t)$ and $\mathbf{W}_\text{E}(t)$ have a common point, besides the origin (an intersection point), $\mathbf{W}_\text{com} = (\mathbf{W}_\text{E})_\text{com}$, which can be used in equation Eq. (24) for the evaluation of the exponential constant k:

$$k = [1/(t_\text{com} - t_\text{o})] \cdot \ln[(\mathbf{F}_\text{J} - \mathbf{F}_\text{o})/(\mathbf{F}_\text{J} - \mathbf{F}_\text{com})] = [1/(t_\text{com} - t_\text{o})] \cdot \ln(1 - \mathbf{W}_\text{com}) \quad (27)$$

The value $t_\text{com} = 0.3$ ms was chosen to evaluate the exponential constant k, and construct the exponential curve $\mathbf{W}_\text{E}(t)$ using Eq. (26).

The difference between the experimental and simulated curve, $\mathbf{W}_\text{E}(t) - \mathbf{W}(t) = \Delta\mathbf{W}(t)$ can be calculated (see the inset of Fig. 4; for clarity, the curve has been magnified 10 times); it shows the effect of energetic connectivity between the photosynthetic units. The relative variable fluorescence $\mathbf{V}(t)$ and $\mathbf{V}_\text{E}(t)$, or $\mathbf{W}(t)$ and $\mathbf{W}_\text{E}(t)$, are expressed as functions of the fraction of closed reaction

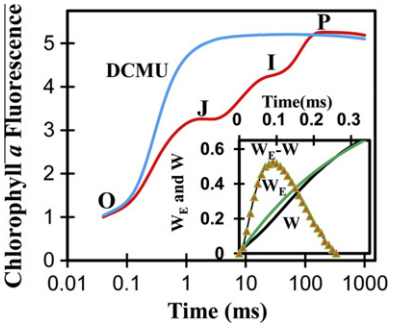

Fig. 4. The OJIP chlorophyll *a* fluorescence transient at room temperature of a control, and a DCMU (3-(3′, 4′ dichlorophenyl)-1,1′dimethylurea) treated pea leaf, presented on a logarithmic time scale. For the DCMU treatment, a droplet of 500 µl (170 µM DCMU in distilled water) was added on the axial side of the leaf, and the leaf was kept in the dark for 24 h. The excitation light intensity was 3200 µmol photons m^{-2} s^{-1} (wavelength, 650 nm). Fluorescence is given in arbitrary units. The inset shows three curves presented on a linear time scale: (1) **W** is a normalized OJIP curve of the form $\mathbf{W}_t = \mathbf{V}_t/\mathbf{V}_\text{J}$, where the relative variable fluorescence of the control sample, $\mathbf{V}_t$, is calculated as $\mathbf{V}_t = (\mathbf{F}_t - \mathbf{F}_\text{o})/(\mathbf{F}_\text{M} - \mathbf{F}_\text{o})$; (2) $\mathbf{W}_\text{E}$ is a theoretically constructed exponential curve of the form $\mathbf{W}_\text{E}(t) = 1 - \exp[-k \cdot (t - t_\text{o})]$, where $k = [1/(t_{0.3\text{ms}} - t_\text{o})] \cdot \ln(1 - \mathbf{W}_{0.3\text{ms}})$; and (3) $\mathbf{W}_\text{E} - \mathbf{W}$ is the difference between the $\mathbf{W}_\text{E}(t)$ and $\mathbf{W}_t$ curves (multiplied by 10). See text for further details. Source of the original figure: Stirbet et al. [178]; modified by A.S.

Please cite this article in press as: A. Stirbet, Govindjee, On the relation between the Kautsky effect (chlorophyll *a* fluorescence induction) and Photosystem II: Basics and applications of the OJIP fluorescence transient, J. Photochem. Photobiol. B: Biol. (2011), doi:10.1016/j.jphotobiol.2010.12.010

centers. For short time intervals, up to $t = 0.3$ ms, **B** is considered equal to $\mathbf{B}_E$; therefore:

$$\mathbf{B} = \mathbf{B}_E = \mathbf{V}_E = \mathbf{W}_E \cdot \mathbf{V}_J \quad (28)$$

Thus, the curvature constant of the hyperbola C can be derived, based on Eqs. (21), (23) and (26) as:

$$C = (\mathbf{B} - \mathbf{V})/[\mathbf{V} \cdot (1 - \mathbf{B})] = (\mathbf{B}_E - \mathbf{V})/[\mathbf{V} \cdot (1 - \mathbf{B}_E)]$$
$$= (\mathbf{V}_E - \mathbf{V})/[\mathbf{V} \cdot (1 - \mathbf{V}_E)] = (\mathbf{W}_E - \mathbf{W})/[\mathbf{W} \cdot (1 - \mathbf{W}_E\mathbf{V}_J)] \quad (29)$$

The value of C is obtained using $\mathbf{W}_E$ and **W**, calculated at $t = 0.1$ ms, when $\Delta\mathbf{W}$ is maximum (see the curve $\Delta\mathbf{W} = \mathbf{W}_E - \mathbf{W}$ in the inset of Fig. 4).

Finally, the overall probability of the connectivity between PSII units, p, is calculated using Eq. (22):

$$p = C \cdot [\mathbf{F}_o/(\mathbf{F}_J - \mathbf{F}_o)] \quad (30)$$

The results obtained with this method show that p from the analysis of the OJIP transient has a value close to that obtained using the DCMU transient ($p = 0.23$ and 0.26 respectively, for the fluorescence transients presented in Fig. 4 [178].

4.3.2. Evaluation of the fraction of non-Q_A-reducing PSIIs, or the so-called 'silent' reaction centers

The "JIP test" (see above) of fluorescence transient in photosynthetic organisms, exposed for short times to light, heat or other abiotic stress ([43]; see also [188,189]) revealed a marked decrease in $\varphi_{Po} = \mathbf{J}_o^{TR}/\mathbf{J}^{ABS}$, measured as $\mathbf{F}_V/\mathbf{F}_M$, a stable (unchanged) $\mathbf{J}_o^{TR}/\mathbf{RC}$, measured as $\mathbf{M}_o/\mathbf{V}_J$, and no change in the absorption photon flux $\mathbf{J}^{ABS}$. Tsimilli-Michael et al. [43] (also see [190], and the review [17]) proposed that this apparently inconsistent result was due to the transformation of some active PSII reaction centers to inactive RCs, which act as efficient exciton traps, but dissipate all their excitation energy as heat (also see inactive PSIIs described by Cleland et al. [191], and Krause et al. [180]). The $\mathbf{F}_V/\mathbf{F}_M$ of the sample represents an average value of the trapped exciton flux, but $\mathbf{J}_o^{TR}/\mathbf{RC}$ is calculated based on the kinetics of the variable fluorescence, and therefore refers only to photochemically active RCs (i.e., those that can reduce Q_A). Moreover, a concomitant increase of $\mathbf{J}^{ABS}/\mathbf{RC}$ does not imply a true increase of the antenna size, but refers to an increase of the '*apparent*' antenna size (i.e., of the total absorption divided by the 'active RCs').

Strasser and Tsimilli-Michael [190] proposed the use of the term "*silent RCs*" for such inactive reaction centers, because they neither reduce Q_A, nor contribute to the variable fluorescence. Their fluorescence yield remains low, equal to that of open RCs. This type of inactivation is reversible soon after the stress, which had provoked the transformation, is removed. If the number of ***a**ctive* and *silent* PSII centers in the sample are, respectively, $\mathbf{RC}_a$ and $\mathbf{RC}_{silent}$, and the parameters of the ***con**trol* sample (i.e., the sample as it was before the application of the stress) are referred to as 'ct', the fraction of PSII transformed to silent RCs, $\mathbf{RC}_{silent}/(\mathbf{RC}_a)_{ct}$, can be calculated as follows (see details in [190]):

$$\mathbf{RC}_a/(\mathbf{RC}_a)_{ct} = (\mathbf{J}^{ABS}/\mathbf{RC}_a)_{ct}/(\mathbf{J}^{ABS}/\mathbf{RC}_a) \quad (31)$$

Further, the fraction of active PSII centers, $\mathbf{RC}_a/(\mathbf{RC}_a)_{ct}$, can be calculated using the relation $\mathbf{J}^{ABS}/\mathbf{RC} = (\mathbf{M}_o/\mathbf{V}_J)/(1 - \mathbf{F}_o/\mathbf{F}_M)$ (see Appendix A.1, A.1.3), as:

$$\mathbf{RC}_a/(\mathbf{RC}_a)_{ct} = [(\mathbf{M}_o/\mathbf{V}_J)_{ct}/(1 - \mathbf{F}_o/\mathbf{F}_M)_{ct}]/[(\mathbf{M}_o/\mathbf{V}_J)/(1 - \mathbf{F}_o/\mathbf{F}_M)] \quad (32)$$

Knowing that $\mathbf{RC}_a/(\mathbf{RC}_a)_{ct} + \mathbf{RC}_{silent}/(\mathbf{RC}_a)_{ct} = 1$, the fraction of the inactive (silent) PSII will be:

$$\mathbf{RC}_{silent}/(\mathbf{RC}_a)_{ct} = 1 - \mathbf{RC}_a/(\mathbf{RC}_a)_{ct} \quad (33)$$

It is important to note that the above interpretation of the discrepancies between $\varphi_{Po} = \mathbf{J}_o^{TR}/\mathbf{J}^{ABS}$ (measured as $\mathbf{F}_V/\mathbf{F}_M$), $\mathbf{J}_o^{TR}/\mathbf{RC}$ (measured as $\mathbf{M}_o/\mathbf{V}_J$), and the absorption photon flux $\mathbf{J}^{ABS}$, are justified only if $\mathbf{F}_o$ and P(=$\mathbf{F}_M$), measured on stressed samples, represent true fluorescence minimum (i.e., all PSIIs open), and maximum (i.e., all active PSIIs closed). Indeed, Tóth et al. [170] show that, in the case of severely heat-stressed leaves (i.e., after a heat treatment at 48–50 °C for 20–40 s), the fast fluorescence transient doesn't reach the maximum fluorescence value, due to an early activation of FNR. The activation of FNR, before the maximum fluorescence $\mathbf{F}_P$ is reached, leads to an increased rate of the electron transport, which prevents the creation of the transient electron transport block leading to the complete reduction of Q_A [72–74], and therefore to $\mathbf{F}_M$. Thus, in those situations when the JIP parameters are not well correlated, it is important to verify not only that $\mathbf{J}^{ABS}$ is unchanged, but also that all active PSIIs are closed at the P-level (e.g., by using DCMU treatment), and that $\mathbf{F}_o$ is not changed. Only if this is confirmed, the hypothesis of a possible inactivation can be considered.

4.3.3. Evaluation of the fraction of the non-Q_B-reducing PSII centers

PSII reaction centers are considered homogeneous in the simple model used (assumption (**4**), Section 4.1), but we know that *in vivo* there are several types of PSII heterogeneities, such as different antenna size (i.e., α- and β-PSII centers), and inactive Q_A or Q_B (see [192–194]). Exposure to different abiotic stresses affects these heterogeneities, altering the fractions of different PSII centers. Non-Q_B-reducing centers are known to have a specific influence on the fluorescence transient, especially the O–J part, which has been sustained through numerical simulation [195]. A fast test for the evaluation of the non-Q_B-reducing PSII fraction was proposed by Strasser and co-workers [190,196,197], based on the fact that these centers have a slow relaxation kinetics in the dark. The test necessitates the measurement of two successive fluorescence transients, induced by two subsequent identical light pulses (each of 1 s duration), separated by a short (maximum ~500 ms) dark relaxation interval (see the detailed description of the method in [190]). The main assumption in this method was that the normal Q_B reducing centers are all open during the dark relaxation period, but not the non-Q_B-reducing centers (which need more than 1–2 s to open through recombination of Q_A^- with the oxygen evolving complex (OEC) in the S_2 state). However, studies of dark-adaptation kinetics of the OJIP-transient [74] showed that, after the first second of illumination, the PQ-pool becomes reduced, and that it remains reduced after a dark relaxation period of 500 ms. Therefore, the PSII centers that remain closed after the dark relaxation interval are not only non-Q_B-reducing centers, but also normal Q_B-reducing centers, as the forward electron transfer reaction from Q_A^- to Q_B is blocked, due to the PQ-pool being in the reduced state; this leads to an overestimation of the non-Q_B-reducing fraction. As a result, this method can eventually be used only qualitatively, when comparing two samples, but we recommend using another alternative method (see [198,199], and the references therein).

Schansker and Strasser [199] have used a different approach to evaluate the non-Q_B-reducing fraction of PSII, in which the photosynthetic sample, kept in dark, was first preilluminated with far-red light ($\lambda = 718$ nm) at a low intensity (80 μmol photons m^{-2} s^{-1}) for a short period of time (10 s), in order to oxidize the PQ-pool. Here, the far-red light-induced increase in $\mathbf{F}_o$ (measured as the fluorescence value at 20 μs) was considered to be due not only to the non-Q_B-reducing PSII, but also to a small fraction of closed Q_B-reducing centers (related to the equilibrium effect). Analyzing the dark-adaptation kinetics of $\mathbf{F}_{20\mu s}$ for pea leaves, the 4–5% increase of the fluorescence yield had two components: ~2.5% due to the equilibrium effect; and only 1.8–3% due to the non-Q_B-reducing centers [199].

Please cite this article in press as: A. Stirbet, Govindjee, On the relation between the Kautsky effect (chlorophyll *a* fluorescence induction) and Photosystem II: Basics and applications of the OJIP fluorescence transient, J. Photochem. Photobiol. B: Biol. (2011), doi:10.1016/j.jphotobiol.2010.12.010

5. Pros and Cons of the analysis of the OJIP transient by the so-called JIP test

The JIP test is based on a well-structured theory, and in order to accept it, we must agree on its assumptions, and the restrictions associated with them (see Section 4.1 on *Assumptions*). The major assumption that we must accept, assumption (**4**), is the thesis that the variation of chlorophyll fluorescence intensity is due mainly to the reduction of Q_A (Duysens and Sweers [60]). This is still the most accepted view on the subject (see reviews in Papageorgiou and Govindjee [3]). However, considering that Q_A may not be the only component influencing the variable fluorescence, Vredenberg ([59,200]; and references cited there) has presented quite a different model. As we already know, there are a number of theories considering additional involvement of non-photochemical fluorescence quenching of different origins during the OJIP transient (see e.g., [58,64,65,67,68,200]), which all, more or less, affect the validity of JIP test. Further, the slow fluorescence transient, the PSMT transient, not discussed here, is significantly affected by changes other than that related to Q_A (e.g. for the slow fluorescence decrease from $\mathbf{F}_P$ to $\mathbf{F}_S$: conformational changes, changing k_P and k_N, or absorption changes, J^{ABS}, based on some modifications of spectroscopic propreties of the photosynthetic sample).

Some of the assumptions, as for example the non-consideration of PSI fluorescence (assumption (**2**), Section 4.1), of homogeneity of PSII units (assumption (**3**)), of the non-inclusion of non-photochemical processes in the fluorescence quenching (assumption (**4**)), of homogeneous antenna pigment structure (assumption (**5**)), or of non-connectivity between PSII units (assumption (**6**)), have been used often in different mathematical models simulating the fast fluorescence induction, in order to simplify the theoretical approach [16,24,51,59,172,201–203]. However, these processes do affect the shape of the OJIP fluorescence transient, and at the same time the values of the fluorescence intensities used in the JIP test to calculate the JIP parameters (i.e., $\mathbf{F}_o$, $\mathbf{F}_{300\mu s}$, $\mathbf{F}_J$, $\mathbf{F}_I$ and $\mathbf{F}_M$). Thus, the values of the JIP parameters are certainly affected (see Section 4.2.2, Eq. (10)). The same is true for assumption (**8**), where in the samples that had been kept in darkness for a few minutes, Q_A as well as PQ-pool are considered to be in the oxidized state. We are aware that in some other cases, Q_A and the PQ-pool may not be completely oxidized even when the samples have been in dark for a long time, like in some algae and higher plants that have high chlororespiratory activity [204]. Assumption (**14**) in which the normalized complementary area of the fast fluorescence induction curve is considered to be proportional to the number of electrons passing through the electron transport chain, *N* (the turnover number) (see Appendix A.4), also requires proof, even if it is still used (see e.g., [205]).

Some of the assumptions are specific to the JIP test, the most important being the assumptions (**12**) and (**13**) (see Section 4.1). The assumption (**12**) states that during the O–J part of the fluorescence transient of a normal sample that had been kept in darkness, Q_A undergoes only a single turnover, as in the DCMU treated sample. However, numerical simulations of the fast fluorescence transient [53–56,172,206] show that a non-negligible fraction of Q_A (up to 50%) is reduced a second time during the O–J time interval of the OJIP transient. As a result, at the $\mathbf{F}_J$ level, instead of a hypothetical mixture of PSII centers in the redox states $Q_A^-Q_B$, and $Q_AQ_B^-$ based on the assumption (**12**), there will be a mixture of PSII centers with $Q_A^-Q_B$, $Q_AQ_B^-$ and $Q_A^-Q_B^-$ (Stirbet et al. [53], Zhu et al. [56], Chang-Peng Xin, Jin Yang, and Xin-Guang Zhu (personal communication, 2010, to one of us, G)), The resemblance between the O–J phase of the OJIP transient, and the fluorescence transient of DCMU treated sample, is not so close as it has been assumed in the current JIP test analysis. Assumption (**13**) states that the rate of the electron transport flux per RC at the I-level of the fast fluorescence transient (t = 30 ms), labeled as specific electron transport flux until PSI acceptors, can be described as $\mathbf{J}_o^{RE1}/\mathbf{RC} = (\mathbf{J}_o^{TR}/\mathbf{RC}) \cdot (1 - \mathbf{V}_I)$ (see Appendix A.1, Eq. (A24)). The $\mathbf{J}_o^{RE1}$, where RE1 refers to the ***re***duction of the PS***1*** acceptors, is based on the experimental observations of Schansker et al. [74] suggesting that at the I-level the electrons generated by PSII reaction centers have reached PCs, and they have begun to reduce PSI acceptors. This suggestion is supported by results on mathematical simulation of both the OJIP transient and changes in 820 nm-transmittance signal (Lazár [206]); we note however, that the model proposed by Lazár [206] includes the PQ-pool quenching, even if the experimental results used in the simulations were obtained *in situ* on leaves, in which case the PQ-pool quenching is most probably absent [167].

A small number of JIP test approximations are rather bold, i.e., they have been used for simplicity, in order to extract the maximum possible information from the routinely measured fluorescence induction data alone, especially in those studies that involve a large number of samples, as for example in the experiments needed under field conditions. These assumptions (see Section 4.1) are explicitly: (i) assumption (**15**) – the approximation of PSII antenna chlorophyll content of the measured sample, Chl_{ant}, with the absorbed photon flux, $\mathbf{J}^{ABS}$ (see Appendix A.1, A.1.3); (ii) assumption (**16**) – the approximation of the phenomenological absorbed photon flux $\mathbf{J}^{ABS}/\mathbf{CS}$ with $\mathbf{F}_o$ or $\mathbf{F}_M$ values (see Appendix A.2, Eqs. (A28) and (A29)); and (iii) assumption (**17**) – the approximation of the normalized complementary area of DCMU treated samples, $\mathbf{S}_S$, with $(\mathbf{M}_{o,DCMU})^{-1}$ (see Appendix A.4, Eq. (A45)). The assumption (**16**) has important repercussions, as all phenomenological JIP parameters are derived based on $\mathbf{J}^{ABS}/\mathbf{CS}$ value (see Table 1, and Appendix A.2).

Even if in the basic JIP test, the connectivity between the RCs and the heterogeneity of PSII units are neglected, they have been considered separately, as presented in Sections 4.3.1–4.3.3, and determined quantitatively based on fluorescence induction data. These additions to JIP test parameters help to characterize more completely the photosynthetic samples under study. On the other hand, the method proposed earlier [190] for the calculation of the non-Q_B-reducing fraction using OJIP transient (see Section 4.3.3), largely overestimates it, due to the reduced state of the PQ-pool. The other method (discussed earlier) to evaluate this fraction, used by Schansker and Strasser [199], involving 10 s preillumination of the sample with far-red light, can be considered as one of the most precise for the moment, but it is too complicated to be used in screening studies, where the basic JIP test is more useful. Regarding the assessment of the inactive PSII centers, which can result following a stress period [43,188,189], based on the observed discrepancies between $\varphi_{Po} = \mathbf{J}_o^{TR}/\mathbf{J}^{ABS}$ (measured as $\mathbf{F}_V/\mathbf{F}_M$), $\mathbf{J}_o^{TR}/\mathbf{RC}$ (measured as $\mathbf{M}_o/\mathbf{V}_J$), and the absorption photon flux $\mathbf{J}^{ABS}$ (see Section 4.3.2), it is important to verify that the values of $\mathbf{F}_o$ and $\mathbf{F}_M$, measured in the case of stressed samples, are truly the minimum (i.e., all PSIIs being open) and maximum (i.e., all active PSIIs being closed) of the fluorescence, since the calculated JIP parameters are affected by them. *In fact this is an important requirement when utilizing JIP test that must be assured in all cases.*

Finally, it is generally accepted today that Chl *a* fluorescence is a signature of photosynthesis, but that is only true when all aspects of fluorescence (e.g., kinetics; spectra; lifetimes; and many other parameters) are exploited; see Papageorgiou and Govindjee [3]. *The JIP test, in this context, is nothing more than a systematic method, to be used as a practical tool, to obtain quick information on various possibilities of effects on photosynthesis, particularly on PSII, and to a limited extent on PSI.* By itself it cannot be used to obtain detailed information on the entire system, without direct measurements on electron transport, and overall photosynthesis rates. Currently, this

Please cite this article in press as: A. Stirbet, Govindjee, On the relation between the Kautsky effect (chlorophyll *a* fluorescence induction) and Photosystem II: Basics and applications of the OJIP fluorescence transient, J. Photochem. Photobiol. B: Biol. (2011), doi:10.1016/j.jphotobiol.2010.12.010

is being attempted, to a limited extent, through utilization of new improved instruments that measure simultaneously, *in vivo*, the prompt Chl fluorescence induction and 820-nm transmission changes reflecting PSI changes [44,74,87,89,136,160,167,170,173,197,199,207,208], or lately, with the multi signal instrument mPEA of Hansatech Instruments, also the delayed fluorescence (that measures back reactions of PSII) [160], which offers new opportunities for the development and improvement of this analysis of OJIP transients.

6. Conclusions

The availability of user-friendly portable direct fluorescence *Fluorometers*, and the specialized software for the analysis of raw experimental data, make the so-called JIP test, which is nothing more than a systematic tool for evaluating fluorescence rise kinetics, very attractive; further, it allows quick measurements even in the field conditions. Extremely rich information about the PSII photochemical activity, electron transport events, and different regulatory processes, is contained in the Chl *a* fluorescence induction transient, and can be revealed through a systematic theoretical treatment of the fluorescence curves. This is illustrated not only through large number of the fluorescence parameters available in the extensive literature, but more importantly, through the numerous results obtained in both basic and applied studies carried out all over the world (see for JIP parameters, Refs. [187,208–217]). The analysis of the photosynthetic activity based on the energy flux theory, of which Reto J. Strasser is a pioneer, has the potential of further development, and (we are) sure that the JIP test will expand even more in the future, especially because it is being combined with parallel optical measurements on the electron carriers in both Photosystems I and II.

Acknowledgments

We are grateful to Reto J. Strasser for having given both of us opportunity to work with him and to have shared the excitement in his wonderful laboratory in Geneva, Switzerland. We were considered a part of his family; we thank Norma Strasser for her wonderful hospitality during our visit there. We thank Gert Schansker and Alaka Srivastava, former associates of Reto, for their comments and suggestions to improve our manuscript. We are equally thankful to three anonymous readers who provided criticisms of parts of our review, several of which could not be incorporated here. If there are any errors, they are ours.

Appendix A

In the following, as well as in the main paper, we have used the published material on JIP test (see e.g., [17,18,114,116,117,160]), but departed, for clarity and convenience, from the original nomenclature for some of the terms. We have used: (1) $\mathbf{J}^{ABS}$, instead of **ABS**, for the PSII absorption photon flux; (2) $\mathbf{J}^{DI}$, instead of **DI**, for the PSII energy dissipation flux; (3) $\mathbf{J}^{TR}$, instead of **TR**, for the PSII exciton trapping flux; (4) $\mathbf{J}_o^{ET2}$, instead of $\mathbf{ET}_0$, for the electron transport flux from Q_A to Q_B; and (5) $\mathbf{J}_o^{RE1}$ instead of $\mathbf{RE}_0$, for the electron transport flux until PSI acceptors.

A.1. The JIP test parameters expressed as quantum efficiencies, specific energy fluxes, and flux ratios (see Table 1)

A.1.1. The quantum yield of primary PSII photochemistry, $\varphi_P = \mathbf{J}^{TR}/\mathbf{J}^{ABS}$

One of the most important parameters used in fluorescence induction studies is the ratio of variable to maximum fluorescence, the $\mathbf{F}_v/\mathbf{F}_M$ ratio. It represents the quantum yield of the primary PSII photochemistry, φ_P [8,76–78]. Here we show the derivation of this parameter in the framework of the so-called JIP test (see also [17]).

Based on the general law of energy conservation, the total photon flux absorbed by all PSII antenna pigments in the measured area of the photosynthetic sample can be written as the sum of the trapped exciton flux, $\mathbf{J}^{TR}$, and the dissipation energy flux, $\mathbf{J}^{DI}$:

$$\mathbf{J}_t^{ABS} = \mathbf{J}_t^{TR} + \mathbf{J}_t^{DI} \quad (A1)$$

Considering the physiological state of the sample to be unchanged during the fast fluorescence transient (assumption (**7**), Section 4.1, main text), and a constant illumination of the sample, the absorbed photon flux $\mathbf{J}^{ABS}$ will be also constant (i.e., $\mathbf{J}_t^{ABS} \equiv \mathbf{J}^{ABS}$). In this case, any change in $\mathbf{J}^{TR}$ will be compensated by a change in $\mathbf{J}^{DI}$, or *vice versa*.

The dissipation energy flux, $\mathbf{J}_t^{DI}$, is assumed to be proportional to the fluorescence emission at any time t of the fast fluorescence transient, since in the JIP test, the non-radiative contributions to $\mathbf{J}_t^{DI}$ are considered constant during the OJIP fluorescence rise (assumption (**10**), Section 4.1). Thus:

$$\mathbf{J}_t^{DI} = \alpha \cdot \mathbf{F}_t \quad (A2)$$

where α is a proportionality constant.[1]

In samples that had been kept in darkness, all PSIIs are assumed to be open at the beginning of the fluorescence transient (i.e., all Q_A molecules in the system are in the oxidized state – assumption (4), Section 4.1). Under this condition, the fluorescence intensity is minimal, $\mathbf{F}_o$, and the trapped exciton flux, $\mathbf{J}_o^{TR}$, is maximal. Moreover, at the P-level (in saturating light, when $t = t_{Fmax}$), all active PSIIs are closed (i.e., all Q_A molecules of Q_A-reducing PSIIs are in the reduced state, Q_A^- – assumption (**4**)), the fluorescence intensity is maximal, $\mathbf{F}_M$, and the trapped exciton flux is zero, $\mathbf{J}_{Fmax}^{TR} = 0$.

The substitution of $\mathbf{J}_t^{DI}$ in Eq. (A1) with its value given by Eq. (A2), gives:

$$\mathbf{J}^{ABS} = \mathbf{J}_t^{TR} + \alpha \cdot \mathbf{F}_t \quad \text{and then} \quad \mathbf{F}_t = \mathbf{J}^{ABS}/\alpha - \mathbf{J}_t^{TR}/\alpha \quad (A3)$$

For $t = t_{Fmax}$ the trapped exciton flux is zero (i.e., $\mathbf{J}_{Fmax}^{TR} = 0$), and Eq. (A3) becomes:

$$\mathbf{F}_M = \mathbf{J}^{ABS}/\alpha \quad (A4)$$

Hence, the normalized fluorescence $\mathbf{F}_t/\mathbf{F}_M$, obtained by dividing Eq. (A3) by equation Eq. (A4), is:

$$\mathbf{F}_t/\mathbf{F}_M = 1 - \mathbf{J}_t^{TR}/\mathbf{J}^{ABS} \quad (A5)$$

On the other hand, the ratio of the output energy flux from PSII antenna pigments (represented by the trapped exciton flux, $\mathbf{J}_t^{TR}$) to the total PSII input energy flux (represented by the absorbed photon flux $\mathbf{J}^{ABS}$) corresponds to the quantum yield of primary PSII photochemistry, φ_{Pt}, whose value can be therefore estimated as:

$$\varphi_{Pt} \equiv \mathbf{J}_t^{TR}/\mathbf{J}^{ABS} = 1 - \mathbf{F}_t/\mathbf{F}_M \quad (A6)$$

At $t = 0$ the quantum yield of the primary PSII photochemistry is maximum thus:

$$\varphi_{Po} \equiv \mathbf{J}_o^{TR}/\mathbf{J}^{ABS} = 1 - \mathbf{F}_o/\mathbf{F}_M = \mathbf{F}_V/\mathbf{F}_M \quad (A7)$$

[1] This assumption seems to be too restrictive, because even in the hypothesis of homogeneous PSII, during the fluorescence transient their fluorescence properties change, and the open PSII (with oxidized Q_A) have low fluorescence yield, and the closed PSII (with reduced Q_A) have high fluorescence yield. We have verified a similar alternative assumption, in which the dissipation energy flux has two parts: $\mathbf{J}_t^{DI} = \alpha_{op} \cdot F_t^{op} + \alpha_{cl} \cdot F_t^{cl}$, where F_t^{op} and F_t^{cl} represent, respectively, the fluorescence of open and closed PSII centers, and α_{op} and α_{cl} are the respective proportionality constants. However, this alternative assumption leads to the same formula for the quantum yield of the primary PSII photochemistry (i.e., Eq. (A6)) which was obtained with the original assumption $\mathbf{J}_t^{DI} = \alpha \cdot \mathbf{F}_t$ (see Appendix A.6).

Please cite this article in press as: A. Stirbet, Govindjee, On the relation between the Kautsky effect (chlorophyll *a* fluorescence induction) and Photosystem II: Basics and applications of the OJIP fluorescence transient, J. Photochem. Photobiol. B: Biol. (2011), doi:10.1016/j.jphotobiol.2010.12.010

Further, by dividing Eq. (A6) by Eq. (A7), we obtain:

$$\varphi_{Pt}/\varphi_{Po} = (1 - \mathbf{F}_t/\mathbf{F}_M)/(1 - \mathbf{F}_o/\mathbf{F}_M) = (\mathbf{F}_M - \mathbf{F}_t)/(\mathbf{F}_M - \mathbf{F}_o)$$
$$= [\mathbf{F}_M - \mathbf{F}_o - (\mathbf{F}_t - \mathbf{F}_o)]/(\mathbf{F}_M - \mathbf{F}_o)$$
$$= 1 - (\mathbf{F}_t - \mathbf{F}_o)/(\mathbf{F}_M - \mathbf{F}_o) = 1 - \mathbf{V}_t, \quad (A8)$$

where $\mathbf{V}_t$ is the relative variable fluorescence, which in the JIP test represents also the fraction of the closed reaction centers (i.e., $\mathbf{V}_t = [Q_A^-]_t/[Q_A]_{total}$), due to the fact that PSII units are considered unconnected with each other (assumption (**6**), in Section 4.1).

Therefore, the quantum yield of the primary PSII photochemistry at any time t of the fluorescence transient is, in terms of the maximum quantum yield φ_{Po}:

$$\varphi_{Pt} = \varphi_{Po} \cdot (1 - \mathbf{V}_t) \quad (A9)$$

We note that this equation has been often used, where the connectivity between the PSIIs has been assumed to be zero, but the relation is valid in the case of connected PSIIs (see e.g., Paillotin [77]).

A.1.2. The maximum flux of excitons trapped per PSII (leading to Q_A reduction), given as the maximum specific trapped exciton flux, $\mathbf{J}_o^{TR}/\mathbf{RC}$

The maximum trapped exciton flux, $\mathbf{J}_o^{TR}$, is obtained from the initial slope of the relative variable fluorescence rise measured in DCMU treated samples, in which the electron transfer from Q_A^- to Q_B is blocked (since Q_B is replaced by DCMU [176,177]). This slope, $\mathbf{M}_{o,DCMU} = (dV/dt)_o$, can be approximated from the experimental data as $\Delta\mathbf{V}_o/\Delta t_o$:

$$\mathbf{M}_{o,DCMU} = (dV/dt)_o \cong \Delta\mathbf{V}_o/\Delta t_o = \Delta\{[Q_A^-]/[Q_A]_{total}\}_o/\Delta t_o \quad (A10)$$

This slope, that is equal to the rate of increase of the fraction of closed RCs (Eq. (A10)), gives the maximum trapped exciton flux, $\mathbf{J}_o^{TR}$ only if the PSII units are not connected.

Since all PSII units are considered homogeneous (assumption (**3**), Section 4.1), every PSII has a Q_A, and the total number of PSII reaction centers in the measured area of the sample (denoted **RC**) is equal to $[Q_A]_{total}$. Therefore the initial slope $\mathbf{M}_{o,DCMU}$ can be written also as:

$$\mathbf{M}_{o,DCMU} \cong \Delta([Q_A^-]/\mathbf{RC})_o/\Delta t_o = (\Delta[Q_A^-]_o/\Delta t_o)/\mathbf{RC}, \quad (A11)$$

where $\Delta[Q_A^-]_o/\Delta t_o$ approximates the initial rate of Q_A reduction, or in other words, the initial rate of closure of the PSII reaction centers. Consistent with the definition of $\mathbf{J}^{TR}$ (see assumption (**11**), Section 4.1), one RC is closed ($Q_A \rightarrow Q_A^-$) for every exciton trapped, and the initial rate of Q_A reduction will be a measure of the maximum trapped exciton flux, $\mathbf{J}_o^{TR}$:

$$\mathbf{J}_o^{TR} = (d[Q_A^-]/dt)_o \cong \Delta[Q_A^-]_o/\Delta t_o \quad (A12)$$

Then, from Eq. (A11) and (A12), the maximum specific (per PSII reaction center) trapped exciton flux will be:

$$\mathbf{J}_o^{TR}/\mathbf{RC} = \mathbf{M}_{o,DCMU} \cong \Delta\mathbf{V}_o/\Delta t_o \quad (A13)$$

In order to have an accurate estimate of the initial slope $\mathbf{M}_{o,DCMU}$, the time interval Δt_o must be very small, since Δt_o is an approximation of dt_o, which is an infinitesimal small time interval. In the JIP test, originally proposed by Strasser and Strasser [114], the time interval of 0.25 ms was used (Δt_o = 0.3–0.05 ms). However, the fluorescence curve of photosynthetic samples has a sigmoidal shape, due to PSII connectivity [77,79,81] which can affect the evaluation of $\mathbf{M}_{o,DCMU}$. $\mathbf{F}_{300\mu s}$ is a good choice for this evaluation because experimental data show that its value is less affected by the connectivity ([17,18,178,179]; see also Section 4.3.1). Thus:

$$\mathbf{J}_o^{TR}/\mathbf{RC} \cong \mathbf{M}_{o,DCMU} \cong \Delta\mathbf{V}_o/\Delta t_o$$
$$= 4\ ms^{-1} \cdot (\mathbf{F}_{0.3ms} - \mathbf{F}_{0.05ms})/(\mathbf{F}_M - \mathbf{F}_{0.05ms}) \quad (A14)$$

For practical reasons, $\mathbf{M}_{o,DCMU}$ cannot be directly measured under field experiments. Nevertheless, it can be 'evaluated' using fluorescence data obtained on samples untreated with DCMU. In this case, the initial slope of the relative variable fluorescence curve, $\mathbf{M}_o$, is smaller than $\mathbf{M}_{o,DCMU}$, because the relative fluorescence at t = 0.3 ms is lowered by the reoxidation of Q_A^- as a result of electron transfer to Q_B (see the electron transfer chain in Fig. 2). However, some experimental results, [114], suggest that $\mathbf{M}_{o,DCMU}$ can be approximated with the ratio $\mathbf{M}_o/\mathbf{V}_J$ (assumption (**12**), Section 4.1). Hence, for control samples (i.e., not treated with DCMU), the maximum specific trapped exciton flux $\mathbf{J}_o^{TR}/\mathbf{RC}$ can be evaluated as:

$$\mathbf{J}_o^{TR}/\mathbf{RC} \cong \mathbf{M}_o/\mathbf{V}_J$$
$$\cong 4\ ms^{-1} \cdot [(\mathbf{F}_{0.3ms} - \mathbf{F}_{0.05ms})/(\mathbf{F}_M - \mathbf{F}_{0.05ms})]$$
$$/[(\mathbf{F}_{2ms} - \mathbf{F}_{0.05ms})/(\mathbf{F}_M - \mathbf{F}_{0.05ms})]$$
$$= 4\ ms^{-1} \cdot (\mathbf{F}_{0.3ms} - \mathbf{F}_{0.05ms})/(\mathbf{F}_{2ms} - \mathbf{F}_{0.05ms}) \quad (A15)$$

$\mathbf{J}_o^{TR}/\mathbf{RC}$ represents the initial rate of the closure of photoactive RCs per total number of photoactive RCs. However, under stress conditions, some of the PSII centers are inactivated (i.e., are no longer capable of reducing Q_A to Q_A^-), being transformed into so-called 'silent' reaction centers (see e.g. [180]; and Section 4.3.2). Nonetheless, $\mathbf{J}_o^{TR}/\mathbf{RC}$ still refers only to the active PSII centers. The same is valid for all specific JIP parameters (see Table 1) since their derivation is based on $\mathbf{J}_o^{TR}/\mathbf{RC}$.

A.1.3. The average absorbed photon flux per reaction center, given as specific absorbed photon flux, $\mathbf{J}^{ABS}/\mathbf{RC}$

The average absorbed photon flux per reaction center can be obtained using Eq. (A15) and (A7):

$$\mathbf{J}^{ABS}/\mathbf{RC} = (\mathbf{J}_o^{TR}/\mathbf{RC})/(\mathbf{J}_o^{TR}/\mathbf{J}^{ABS}) = (\mathbf{J}_o^{TR}/\mathbf{RC})/\varphi_{Po}$$
$$\cong (\mathbf{M}_o/\mathbf{V}_J)/(1 - \mathbf{F}_o/\mathbf{F}_M) \quad (A16)$$

Based on the relation $\mathbf{J}_o^{TR}/\mathbf{RC} = \varphi_{Po} \cdot \mathbf{J}^{ABS}/\mathbf{RC}$, the JIP parameter $\mathbf{J}^{ABS}/\mathbf{RC}$ is also regarded as a measure of the apparent antenna size, i.e. the average amount of absorbing antenna chlorophylls per fully active (Q_A-reducing) reaction center, $Chl_{ant}/\mathbf{RC}$,[114]. However, because $\mathbf{J}^{ABS}/\mathbf{RC}$ is not equal, but only proportional, to the amount of absorbing Chl antenna molecules per active RC, it can be used as a measure of $Chl_{ant}/\mathbf{RC}$ *only* in a comparative manner. As φ_{Po} represents an average maximum photochemical quantum yield of all different types of PSII RCs in the sample, this 'antenna size' is also an average. Nevertheless, it offers a way to detect an eventual inactivation of RCs (see Section 4.3.2).

A.1.4. The specific electron transport flux from Q_A to Q_B, $\mathbf{J}_o^{ET2}/\mathbf{RC}$

For normal photosynthetic samples, the initial slope of the relative variable fluorescence curve, $\mathbf{M}_o$, indicates the net rate of the closure of PSII RCs. The exciton trapping increases the number of closed centers, and the electron transport from Q_A to Q_B decreases it:

$$\mathbf{M}_o = \mathbf{J}_o^{TR}/\mathbf{RC} - \mathbf{J}_o^{ET2}/\mathbf{RC} \quad \text{and then} \quad \mathbf{J}_o^{ET2}/\mathbf{RC} = \mathbf{J}_o^{TR}/\mathbf{R}C - \mathbf{M}_o \quad (A17)$$

Using Eq. (A15), the specific electron transport flux from Q_A to Q_B, $\mathbf{J}_o^{ET2}/\mathbf{RC}$, is calculated as:

$$\mathbf{J}_o^{ET2}/\mathbf{RC} = (\mathbf{M}_o/\mathbf{V}_J) - \mathbf{M}_o = (\mathbf{M}_o/\mathbf{V}_J) \cdot (1 - \mathbf{V}_J) \quad (A18)$$

Please cite this article in press as: A. Stirbet, Govindjee, On the relation between the Kautsky effect (chlorophyll *a* fluorescence induction) and Photosystem II: Basics and applications of the OJIP fluorescence transient, J. Photochem. Photobiol. B: Biol. (2011), doi:10.1016/j.jphotobiol.2010.12.010

A.1.5. The efficiency/probability with which the initial PSII trapped electron is transferred from Q_A to Q_B, i.e., $\psi_{ET2o} \equiv \mathbf{J}_o^{ET2}/\mathbf{J}_o^{TR}$

Using Eq. (A15), Eq. (A17) can be written as:

$$\mathbf{J}_o^{ET2}/\mathbf{RC} = (\mathbf{M}_o/\mathbf{V}_J)\cdot(1-\mathbf{V}_J) = (\mathbf{J}_o^{TR}/\mathbf{RC})\cdot(1-\mathbf{V}_J) \quad (A19)$$

And therefore:

$$\psi_{ET2o} \equiv \mathbf{J}_o^{ET2}/\mathbf{J}_o^{TR} = 1-\mathbf{V}_J \quad (A20)$$

A.1.6. The quantum yield of the electron transport flux from Q_A to Q_B, $\varphi_{ET2o} \equiv \mathbf{J}_o^{ET2}/\mathbf{J}^{ABS}$

The quantum yield of the electron transport flux from Q_A to Q_B, $\mathbf{J}_o^{ET2}/\mathbf{J}^{ABS}$, can be obtained easily using Eqs. (A7) and (A20):

$$\varphi_{ET2o} \equiv \mathbf{J}_o^{ET2}/\mathbf{J}^{ABS} = \left(\mathbf{J}_o^{ET2}/\mathbf{J}_o^{TR}\right)\cdot(\mathbf{J}_o^{TR}/\mathbf{J}^{ABS}) = \psi_{ET2o}\cdot\varphi_{Po} = \varphi_{Po}\cdot(1-\mathbf{V}_J) \quad (A21)$$

Using Eq. (A7) (for φ_{Po} as a function of fluorescence values), and the definition of the relative variable fluorescence $\mathbf{V}_J$, Eq. (A21) can also be written as:

$$\varphi_{ET2o} = [(\mathbf{F}_M-\mathbf{F}_o)/\mathbf{F}_M]\cdot[1-(\mathbf{F}_J-\mathbf{F}_o)/(\mathbf{F}_M-\mathbf{F}_o)] = [(\mathbf{F}_M-\mathbf{F}_o)/\mathbf{F}_M]\cdot[(\mathbf{F}_M-\mathbf{F}_o-\mathbf{F}_J+\mathbf{F}_o)/(\mathbf{F}_M-\mathbf{F}_o)] = (\mathbf{F}_M-\mathbf{F}_J)/\mathbf{F}_M = 1-\mathbf{F}_J/\mathbf{F}_M \quad (A22)$$

Also, using Eq. (A6) for the particular case $\mathbf{F}_t = \mathbf{F}_J$, the following equality is evident:

$$\varphi_{Pj} = 1-\mathbf{F}_J/\mathbf{F}_M = \varphi_{ET2o} \quad (A23)$$

A.1.7. The specific electron transport flux until PSI acceptors, $\mathbf{J}_o^{RE1}/\mathbf{RC}$

Based on experimental results showing that at the I-level of OJIP transient,electrons generated by PSII have reached plastocyanin molecules, PCs, and just start to be transferred all the way up to the end of electron acceptor side of PSI [74], an energy flux, labeled as the specific electron transfer flux until PSI acceptors, $\mathbf{J}_o^{RE1}/\mathbf{RC}$, is defined in a similar manner as $\mathbf{J}_o^{ET2}/\mathbf{RC}$ (see assumption (**13**), Section 4.1, and (A19)).

$$\mathbf{J}_o^{RE1}/\mathbf{RC} = (\mathbf{J}_o^{TR}/\mathbf{RC})\cdot(1-\mathbf{V}_I) = (\mathbf{M}_o/\mathbf{V}_J)\cdot(1-\mathbf{V}_I) \quad (A24)$$

A.1.8. The efficiency/probability with which a PSII trapped electron is transferred until PSI acceptors, $\psi_{RE1o} \equiv \mathbf{J}_o^{RE1}/\mathbf{J}_o^{TR}$

The efficiency/probability with which a PSII trapped electron is transferred until PSI acceptors, ψ_{RE1o}, is calculated using Eq. (A24) as:

$$\psi_{RE1o} \equiv \mathbf{J}_o^{RE1}/\mathbf{J}_o^{TR} = 1-\mathbf{V}_I \quad (A25)$$

A.1.9. The quantum yield of the electron transport flux until PSI acceptors, $\varphi_{RE1o} \equiv \mathbf{J}_o^{RE1}/\mathbf{J}^{ABS}$

Using Eqs. (A7) and (A25), the quantum yield of the electron transport flux until PSI acceptors, φ_{RE1o} can be obtained as:

$$\varphi_{RE1o} \equiv \mathbf{J}_o^{RE1}/\mathbf{J}^{ABS} = (\mathbf{J}_o^{RE1}/\mathbf{J}_o^{TR})\cdot(\mathbf{J}_o^{TR}/\mathbf{J}^{ABS}) = \psi_{RE1o}\cdot\varphi_{Po} = \varphi_{Po}\cdot(1-\mathbf{V}_I) \quad (A26)$$

A.1.10. The efficiency/probability with which an electron from Q_B is transferred until PSI acceptors, $\delta_{RE1o} = \mathbf{J}_o^{RE1}/\mathbf{J}_o^{ET2}$

$\mathbf{J}_o^{RE1}/\mathbf{J}_o^{ET2}$ is obtained easily using Eqs. (A20) and (A25):

$$\delta_{RE1o} \equiv \mathbf{J}_o^{RE1}/\mathbf{J}_o^{ET2} = (\mathbf{J}_o^{RE1}/\mathbf{J}_o^{TR})/(\mathbf{J}_o^{ET2}/\mathbf{J}_o^{TR}) = (1-\mathbf{V}_I)/(1-\mathbf{V}_J) \quad (A27)$$

A.2. JIP parameters defined in terms of fluxes and activities per cross section of the sample

Different energy fluxes measured per excited cross section of the photosynthetic sample, **CS**, as $\mathbf{J}_{ABS}/\mathbf{CS}$, $\mathbf{J}_o^{TR}/\mathbf{CS}$, $\mathbf{J}^{DI}/\mathbf{CS}$, $\mathbf{J}_o^{ET2}/\mathbf{CS}$, and $\mathbf{J}_o^{RE1}/\mathbf{CS}$ (see below for the definitions), are descriptions of the observed phenomena, and are denoted as phenomenological energy fluxes. Since a photosynthetic sample is usually not optically homogeneous, and contains many cell layers of different depths, the term 'excited cross section' has been used instead of 'optical cross section' (the latter being suitable only for an optically homogeneous sample).

A.2.1. The absorbed photon flux per excited cross section, $\mathbf{J}^{ABS}/\mathbf{CS}$

The value of the absorbed photon flux $\mathbf{J}^{ABS}/\mathbf{CS}$ can be 'determined' experimentally, being a measure of $^{PSII}\mathbf{Chl}_{ant}/\mathbf{CS}$, in which case, it is denoted as $\mathbf{J}^{ABS}/\mathbf{CS}_{Chl}$. However, in the JIP test, which can be used in large-scale field experiments, the initial fluorescence $\mathbf{F}_o$ is assumed to be an approximation of $\mathbf{J}^{ABS}/\mathbf{CS}$ [114], for convenience:

$$\mathbf{J}^{ABS}/\mathbf{CS}_o = \mathbf{F}_o \quad (A28)$$

$\mathbf{J}^{ABS}/\mathbf{CS}$ is measured in relative units, being meaningful only in studies in which several samples are compared, and that too, for samples having the same fluorescence yield at $\mathbf{F}_o$, φ_{Fo}.

Since the cross section, **CS**, may be affected by changes taking place during the light period, one must be cautious in comparing these fluxes based on $\mathbf{F}_o$ values. Moreover, in order to have a very accurate value of $\mathbf{F}_o$, a separate experiment is necessary under low light conditions, with instruments that allow precise measurements of true $\mathbf{F}_o$.

A similar relationship as that for Eq. (A28) can be obtained for $t = t_{Fmax}$:

$$\mathbf{J}^{ABS}/\mathbf{CS}_M = \mathbf{F}_M \quad (A29)$$

Here also, care must be taken to measure true $\mathbf{F}_M$, as in the case of $\mathbf{F}_o$.

The use of phenomenological fluxes must certainly be made with great care. In studies using different treatments, it is important to check the stability of $\mathbf{F}_o$ and $\mathbf{F}_M$, in order to decide between using $\mathbf{CS}_o$ or $\mathbf{CS}_M$; it is necessary to select only the stable values. Because $\mathbf{J}^{ABS}/\mathbf{CS}$ is included in the definition of all other phenomenological JIP parameters (see below), they are affected by the same degree of imprecision as $\mathbf{J}^{ABS}/\mathbf{CS}$ is.

A.2.2. The maximum trapped exciton flux per excited cross section, $\mathbf{J}_o^{TR}/\mathbf{CS}_o$

The maximum PSII trapped exciton flux is calculated using Eqs. (A7) and (A28):

$$\mathbf{J}_o^{TR}/\mathbf{CS}_o = (\mathbf{J}_o^{TR}/\mathbf{J}^{ABS})\cdot(\mathbf{J}^{ABS}/\mathbf{CS}_o) = \varphi_{Po}\cdot\mathbf{F}_o = (1-\mathbf{F}_o/\mathbf{F}_M)\cdot\mathbf{F}_o \quad (A30)$$

A.2.3. The electron transport flux from Q_A to Q_B, per excited cross section, $\mathbf{J}_o^{ET2}/\mathbf{CS}_o$

The electron transport flux from Q_A to Q_B per excited cross section of the sample is calculated using Eqs. (A23) and (A28):

$$\mathbf{J}_o^{ET2}/\mathbf{CS}_o = (\mathbf{J}_o^{ET2}/\mathbf{J}^{ABS})\cdot(\mathbf{J}^{ABS}/\mathbf{CS}_o) = \varphi_{ET2o}\cdot\mathbf{F}_o) = \varphi_{Pj}\cdot\mathbf{F}_o = (1-\mathbf{F}_J/\mathbf{F}_M)\cdot\mathbf{F}_o \quad (A31)$$

A.2.4. The electron transport flux until PSI acceptors, per excited cross section, $\mathbf{J}_o^{RE1}/\mathbf{CS}_o$

The electron transport flux until PSI acceptors per excited cross section of the sample is calculated using Eqs. (A24) and (A28):

Please cite this article in press as: A. Stirbet, Govindjee, On the relation between the Kautsky effect (chlorophyll *a* fluorescence induction) and Photosystem II: Basics and applications of the OJIP fluorescence transient, J. Photochem. Photobiol. B: Biol. (2011), doi:10.1016/j.jphotobiol.2010.12.010

$$\mathbf{J}_o^{RE1}/\mathbf{CS}_o = (\mathbf{J}_o^{RE1}/\mathbf{J}^{ABS}) \cdot (\mathbf{J}^{ABS}/\mathbf{CS}_o) = \boldsymbol{\varphi}_{RE1o} \cdot \mathbf{F}_o = \boldsymbol{\varphi}_{Pi} \cdot \mathbf{F}_o = (1 - \mathbf{F}_I/\mathbf{F}_M) \cdot \mathbf{F}_o \quad (A32)$$

*A.2.5. The number of active PSII per excited cross section, **RC/CS**$_o$*

The number of active PSII per excited cross section is (using Eqs. (A16) and (A28)):

$$\mathbf{RC}/\mathbf{CS}_o = (\mathbf{J}^{ABS}/\mathbf{CS}_o)/(\mathbf{J}^{ABS}/\mathbf{RC}) = \mathbf{F}_o \cdot \boldsymbol{\varphi}_{Po} \cdot \mathbf{V}_J/\mathbf{M}_o = \mathbf{F}_o \cdot (1 - \mathbf{F}_o/\mathbf{F}_M) \cdot \mathbf{V}_J/\mathbf{M}_o \quad (A33)$$

A.3. De-excitation constant k_P (for photochemistry) and k_N (for all non-photochemical processes)

Each energy flux ($\mathbf{J}^{TR}$, $\mathbf{J}^{DI}$, or the fluorescence **F**) is proportional to the corresponding de-excitation rate constant, k_i, and to the concentration of the excited antenna chlorophyll [Chl*]:

$$\mathbf{J}^i \approx k_i \cdot [\text{Chl}^*] \quad (A34)$$

Using k_N as the sum of all non-photochemical rate constants (i.e., the sum of k_H, for heat dissipation, k_F for fluorescence emission, and k_X, for energy migration to PSI), and k_P the photochemical rate constant, the sum of all rate constants is:

$$\Sigma k_i = k_P + k_N \quad (A35)$$

The absorption flux $\mathbf{J}^{ABS}$, which is equal to the sum of all de-excitation fluxes, can be therefore written, based on Eq. (A35), as:

$$\mathbf{J}^{ABS} \approx (k_N + k_P) \cdot [\text{Chl}^*] \quad (A36)$$

On the other hand, the maximum trapping flux $\mathbf{J}_o^{TR}$ (when all reaction centers are open) can be expressed as:

$$\mathbf{J}_o^{TR} \approx k_P \cdot [\text{Chl}^*] \quad (A37)$$

Hence, the ratio $\mathbf{J}_o^{TR}/\mathbf{J}^{ABS}$ is:

$$\mathbf{J}_o^{TR}/\mathbf{J}^{ABS} = \boldsymbol{\varphi}_{Po} = k_P/(k_N + k_P) = 1 - (\mathbf{F}_o/\mathbf{F}_M) = \mathbf{F}_V/\mathbf{F}_M \quad (A38)$$

Other expressions, based on fluorescence values $\mathbf{F}_o$ and $\mathbf{F}_M$, can be obtained for the photochemical rate constant k_P, and the non-photochemical rate constant k_N (see Havaux et al. [108]), as for example:

$$k_N = (\mathbf{J}^{ABS}/\mathbf{CS}) \cdot k_F \cdot (1/\mathbf{F}_M) \quad (A39)$$

$$k_N + k_P = (\mathbf{J}^{ABS}/\mathbf{CS}) \cdot k_F \cdot (1/\mathbf{F}_o) \quad (A40)$$

$$k_P = (\mathbf{J}^{ABS}/\mathbf{CS}) \cdot k_F \cdot (1/\mathbf{F}_o - 1/\mathbf{F}_M) \quad (A41)$$

We note that the ratio of Eqs. (A40) and (A39) gives the well-known relation for the maximum quantum yield of PSII primary photoreaction:

$$k_P/(k_P + k_N) = [(\mathbf{J}^{ABS}/\mathbf{CS}) \cdot k_F \cdot (1/\mathbf{F}_o - 1/\mathbf{F}_M)]/[(\mathbf{J}^{ABS}/\mathbf{CS}) \cdot k_F \cdot (1/\mathbf{F}_o)] = 1 - (\mathbf{F}_o/\mathbf{F}_M) = \boldsymbol{\varphi}_{Po} = \mathbf{J}_o^{TR}/\mathbf{J}^{ABS} \quad (A42)$$

A.4. The complementary area and the turnover number

The area over the OJIP fluorescence transient curve until the line $\mathbf{F}_t = \mathbf{F}_M$, from $t = 0$ to t_{Fmax}, the complementary area, is calculated from the fluorescence rise as:

$$\mathbf{Area} = \int_0^{t_{Fmax}} (\mathbf{F}_M - \mathbf{F}_t)\mathrm{d}t \quad (A43)$$

This **Area** is normalized by $\mathbf{F}_V = \mathbf{F}_M - \mathbf{F}_o$, in order to compare different samples. The normalized expression is:

$$\mathbf{S}_m = \mathbf{Area}/(\mathbf{F}_M - \mathbf{F}_o) = \int_0^{t_{Fmax}} (1 - \mathbf{V}_t)\mathrm{d}t \quad (A44)$$

The subscript "m" on "S" refers to the multiple turnover of Q_A reduction. In DCMU treated samples, Q_A is reduced only once, and the normalized area is minimal (denoted $\mathbf{S}_S$, where the index 's' indicates a single turnover). The ratio between $\mathbf{S}_m$ and $\mathbf{S}_S$, measured on the same sample, gives the total number of electrons transferred into the electron transport chain, the so-called turnover number $\mathbf{N} = \mathbf{S}_m/\mathbf{S}_S$. The relation $\mathbf{N} = \mathbf{S}_m/\mathbf{S}_S$ is true only if one assumes a strict proportionality between the normalized area $\mathbf{S}_m$ and **N**, which is not a generally accepted idea.

Here also, for practical reasons, $\mathbf{S}_S$ cannot be directly measured under field experiments, but it is approximated as $(\mathbf{M}_{o,DCMU})^{-1}$ (see assumption (**17**), Section 4.1). We note however, that although this is a rough approximation, it can be useful in qualitative comparative studies.

Finally, applying the relation $\mathbf{M}_{o,DCMU} = \mathbf{M}_o/\mathbf{V}_J$ (see assumption (**12**), Section 4.1), **N** can be calculated as:

$$\mathbf{N} = \mathbf{S}_m/\mathbf{S}_S = \mathbf{S}_m/(\mathbf{M}_{o,DCMU})^{-1} = \mathbf{S}_m/(\mathbf{M}_o/\mathbf{V}_J)^{-1} \quad (A45)$$

*A.5. Performance index (**PI**), an important JIP parameter, and the driving force (log **PI**)*

In general, in a large number of photosynthetic studies, the ratio $\mathbf{F}_V/\mathbf{F}_M = (\mathbf{F}_M - \mathbf{F}_o)/\mathbf{F}_M$ is used as a stress indicator. However, this empirical parameter, based on $\mathbf{F}_o$ and $\mathbf{F}_M$ fluorescence values, is not always sensitive enough to observe differences between different samples. Srivastava et al. [116] used a new, more responsive, and important, fluorescence parameter, named performance index **PI**. This JIP parameter is based on a different approach, as in Goldman-equation, in which it is assumed that a total potential of a system can be calculated by multiplying the Nernst-equation for the individual components [181,182]). The performance index, **PI**, is calculated in the same way as a Goldman-equation, from three (or four) components which depend on the reaction center density, the trapping efficiency, and the electron transport efficiency (see below). Consequently, if a stress affects any of these components, the effect will show up in the performance index, which therefore has a higher sensitivity than that achieved by any of its isolated components. A driving force, expressed as log (**PI**) can then be calculated, just as is done in chemistry.

*A.5.1. The performance index on an absorption basis, **PI**$_{ABS}$*

Initially, the product of three independent JIP parameters combining structural properties of PSII (i.e., $\mathbf{RC}/\mathbf{J}^{ABS}$, $\boldsymbol{\varphi}_{Po}$, and $\boldsymbol{\psi}_{ET2o}$) was used to define an expression "structure function index", $\mathbf{SFI}_{Po(ABS)}$ (Tsimilli-Michael et al. [43]):

$$\mathbf{SFI}_{Po(ABS)} = (\mathbf{RC}/\mathbf{J}^{ABS}) \cdot \boldsymbol{\varphi}_{Po} \cdot \boldsymbol{\psi}_{ET2o} \quad (A46)$$

Since $\mathbf{J}^{ABS}/\mathbf{RC}$ is also regarded as a measure of the apparent antenna size, i.e., the amount of absorbing antenna chlorophylls per fully active (Q_A-reducing) reaction center (see Appendix A.1, A.1.3), then:

$$\mathbf{RC}/\mathbf{J}^{ABS} \cong \text{Chl}_{RC}/\text{Chl}_{ant} = \text{Chl}_{RC}/(\text{Chl}_{tot} - \text{Chl}_{RC}) = (\text{Chl}_{RC}/\text{Chl}_{tot})/(1 - \text{Chl}_{RC}/\text{Chl}_{tot}), \quad (A47)$$

where Chl_{RC} represents the total PSII RC chlorophylls, and Chl_{tot} represents the total PSII Chl. Expressing the fraction of PSII RC chlorophylls relative to the total PSII chlorophyll as $\gamma_{RC2} = \text{Chl}_{RC}/\text{Chl}_{tot}$ we have:

$$\mathbf{RC}/\mathbf{J}^{ABS} = \gamma_{RC2}/(1 - \gamma_{RC2}) \quad (A48)$$

And therefore:

$$\mathbf{SFI}_{Po(ABS)} = \gamma_{RC2}/(1 - \gamma_{RC2}) \cdot \boldsymbol{\varphi}_{Po} \cdot \boldsymbol{\psi}_{ET2o} \quad (A49)$$

Please cite this article in press as: A. Stirbet, Govindjee, On the relation between the Kautsky effect (chlorophyll *a* fluorescence induction) and Photosystem II: Basics and applications of the OJIP fluorescence transient, J. Photochem. Photobiol. B: Biol. (2011), doi:10.1016/j.jphotobiol.2010.12.010

The performance index, on absorption basis, $\mathbf{PI}_{ABS}$, as presented by Srivastava et al. [116], in which all the constitutive terms were introduced as ratios, similar to Eq. (A48) (a yield divided by its complementary function) is:

$$\mathbf{PI}_{ABS} = [\gamma_{RC2}/(1-\gamma_{RC2})] \cdot [\varphi_{Po}/(1-\varphi_{Po})] \cdot [\psi_{ET2o}/(1-\psi_{ET2o})] \quad (A50)$$

The total performance index, $\mathbf{PI}^{total}$, is obtained by multiplying Eq. (A50) with a fourth term, characterizing the efficiency of the electron transport flux until PSI acceptors, δ_{RE1o} (see [117,160]):

$$\begin{aligned}\mathbf{PI}^{total}_{ABS} &= \mathbf{PI}_{ABS} \cdot \delta_{RE1o}/(1-\delta_{RE1o}) \\ &= [\gamma_{RC}/(1-\gamma_{RC})] \cdot [\varphi_{Po}/(1-\varphi_{Po})] \cdot [\psi_{ET2o}/(1-\psi_{ET2o})] \\ &\quad \cdot [\delta_{RE1o}/(1-\delta_{RE1o})]\end{aligned} \quad (A51)$$

A.5.2. Performance index on cross section basis, $\mathbf{PI}_{CS}$

The performance index on cross section basis, $\mathbf{PI}_{CS}$, is obtained by multiplying the performance index on absorption basis $\mathbf{PI}_{ABS}$ (Eq. (A51)), by the phenomenological energy flux, $\mathbf{J}^{ABS}/\mathbf{CS} = \mathbf{F}_o$ (or $\mathbf{F}_M$):

$$\begin{aligned}\mathbf{PI}^{total}_{CS,o} &= \mathbf{F}_o \cdot [\gamma_{RC}/(1-\gamma_{RC})] \cdot [\varphi_{Po}/(1-\varphi_{Po})] \\ &\quad \cdot [\psi_{ET2o}/(1-\psi_{ET2o})] \cdot [\delta_{RE1o}/(1-\delta_{RE1o})]\end{aligned} \quad (A52)$$

$$\begin{aligned}\mathbf{PI}^{total}_{CS,M} &= \mathbf{F}_M \cdot [\gamma_{RC}/(1-\gamma_{RC})] \cdot [\varphi_{Po}/(1-\varphi_{Po})] \\ &\quad \cdot [\psi_{ET2o}/(1-\psi_{ET2o})] \cdot [\delta_{RE1o}/(1-\delta_{RE1o})]\end{aligned} \quad (A53)$$

A.5.3. Driving forces: $\mathbf{DF}_{ABS}$ and $\mathbf{DF}_{CS}$

In chemistry, an expression of the form $\log [p_i/(1-p_i)]$ is sometimes used, where p_i is a probability or fraction of a component; when p_i is the fraction of the reduced compound i, and $(1-p_i)$ the fraction of the oxidized compound i, the expression represents the potential, or driving force, for the corresponding oxido-reduction reaction (Nernst's equation). The performance index was especially designed as a product of terms in the form $p_i/(1-p_i)$ (see Eqs. (A50)–(A53)). Extrapolating this concept from chemistry, the log (**PI**) can be considered as the total *driving force* for the photochemical activity of the observed system; it would be the sum of the partial driving forces for the events involved in OJIP fluorescence rise. Therefore we can write:

$$\begin{aligned}\mathbf{DF}^{total}_{ABS} &= \log(\mathbf{PI}^{total}_{ABS}) \\ &= log(\mathbf{RC}/\mathbf{J}^{ABS}) + \log[\varphi_{Po}/(1-\varphi_{Po})] \\ &\quad + \log[\psi_{ET2o}/(1-\psi_{ET2o})] + \log[\delta_{RE1o}/(1-\delta_{RE1o})]\end{aligned} \quad (A54)$$

$$\mathbf{DF}^{total}_{CS} = log(\mathbf{PI}^{total}_{CS}) = log(\mathbf{PI}^{total}_{ABS}) + \log(\mathbf{J}^{ABS}/\mathbf{CS}) \quad (A55)$$

*A.6. The demonstration of the equivalence between the assumption $\mathbf{J}_t^{DI} = \alpha \cdot \mathbf{F}_t$ used in Appendix A.1 for the derivation of the quantum yield of the primary PSII photochemistry (see Eq. (A2), assumption (**10**) in Section 4.1, and Ref. [17]), and the similar assumption $\mathbf{J}^{DI}_t = \alpha_{op}F^{op}_t + \alpha_{cl}F^{cl}_t$*

We consider the fluorescence measured at time t, $\mathbf{F}_t$, as the sum of the fluorescence of open, F^{op}_t, and closed, F^{cl}_t, PSII units (based on Duysens and Sweers theory [60], and neglecting PSI fluorescence; see assumptions (**2**) and (**4**) in Section 4.1):

$$\mathbf{F}_t = F^{op}_t + F^{cl}_t \quad (A56)$$

Using the original assumption, $\mathbf{J}^{DI}_t = \alpha \cdot \mathbf{F}_t$, for each component of $\mathbf{F}_t$ in Eq. (A56), we obtain:

$$\mathbf{J}^{DI}_t = \alpha_{op}F^{op}_t + \alpha_{cl}F^{cl}_t \quad (A57)$$

where α_{op} and α_{cl} are specific proportionality constants for the open and closed PSII RCs.

Next, we follow the same logic used to obtain the formula of the quantum yield of primary PSII photochemistry, φ_P, as presented in Appendix A.1, A.1.1 (see also [17]).

Based on the law of energy conservation and Eq. (A57) we can write:

$$\mathbf{J}^{ABS} = \mathbf{J}^{TR}_t + \mathbf{J}^{DI}_t = \mathbf{J}^{TR}_t + \alpha_{op} \cdot F^{op}_t + \alpha_{cl} \cdot F^{cl}_t \quad (A58)$$

At $t = 0$ all PSIIs are open. Therefore, $F^{cl}_o = 0$ and $\mathbf{F}_o = F^{op}_o$. The relation (A58) becomes:

$$\mathbf{J}^{ABS} = \mathbf{J}^{TR}_o + \alpha_{op} \cdot F^{op}_o = \mathbf{J}^{TR}_o + \alpha_{op} \cdot \mathbf{F}_o \quad (A59)$$

And therefore:

$$\alpha_{op} = (\mathbf{J}^{ABS} - \mathbf{J}^{TR}_o)/\mathbf{F}_o \quad (A60)$$

At $t = t_{Fmax}$ all PSIIs are closed. Therefore, $\mathbf{J}^{TR}_M = 0$, $F^{op}_M = 0$ and $F^{cl}_M = \mathbf{F}_M$. Therefore, Eq. (A59) becomes:

$$\mathbf{J}^{ABS} = \alpha_{cl} \cdot \mathbf{F}_M \quad (A61)$$

and then:

$$\alpha_{cl} = \mathbf{J}^{ABS}/\mathbf{F}_M \quad (A62)$$

Substituting in Eq. (A57) the proportionality parameters α_{op} and α_{cl} with their values calculated in Eqs. (A60) and (A62), we obtain:

$$\mathbf{J}^{ABS} = \mathbf{J}^{TR}_t + [(\mathbf{J}^{ABS} - \mathbf{J}^{TR}_o)/\mathbf{F}_o] \cdot F^{op}_t + [\mathbf{J}^{ABS}/\mathbf{F}_M] \cdot F^{cl}_t \quad (A63)$$

Based on the relation $\mathbf{F}_t = F^{op}_t + F^{cl}_t$ (Eq. (A56)), we have:

$$F^{cl}_t = \mathbf{F}_t - F^{op}_t \quad (A64)$$

Substituting F^{cl}_t given by Eq. (A64) in Eq. (A63):

$$\mathbf{J}^{ABS} = \mathbf{J}^{TR}_t + [(\mathbf{J}^{ABS} - \mathbf{J}^{TR}_o)/\mathbf{F}_o] \cdot F^{op}_t + [\mathbf{J}^{ABS}/\mathbf{F}_M] \cdot (\mathbf{F}_t - F^{op}_t) \quad (A65)$$

Or, rearranging the terms in Eq. (A65):

$$\mathbf{J}^{ABS} - \mathbf{J}^{TR}_t = F^{op}_t \cdot (\mathbf{J}^{ABS} - \mathbf{J}^{TR}_o)/\mathbf{F}_o + \mathbf{J}^{ABS} \cdot (\mathbf{F}_t - F^{op}_t)/\mathbf{F}_M \quad (A66)$$

Rearranging further the terms in Eq. (A66) leads to the expression:

$$\mathbf{J}^{ABS} - \mathbf{J}^{TR}_t = F^{op}_t \cdot \mathbf{J}^{ABS} \cdot [1/\mathbf{F}_o - 1/\mathbf{F}_M - \mathbf{J}^{TR}_o/(\mathbf{J}^{ABS} \cdot \mathbf{F}_o)] + \mathbf{J}^{ABS} \cdot (\mathbf{F}_t/\mathbf{F}_M) \quad (A67)$$

Dividing Eq. (A67) by $\mathbf{J}^{ABS}$ we obtain:

$$1 - \mathbf{J}^{TR}_t/\mathbf{J}^{ABS} = \mathbf{F}_t/\mathbf{F}_M + (F^{op}_t/\mathbf{F}_o) \cdot (\mathbf{1} - \mathbf{F}_o/\mathbf{F}_M - \mathbf{J}^{TR}_o/\mathbf{J}^{ABS}) \quad (A68)$$

Considering the term $(F^{op}_t/\mathbf{F}_o) \cdot (\mathbf{1} - \mathbf{F}_o/\mathbf{F}_M - \mathbf{J}^{TR}_o/\mathbf{J}^{ABS})$ small enough to be taken as zero, we obtain:

$$\mathbf{J}^{TR}_t/\mathbf{J}^{ABS} = 1 - \mathbf{F}_t/\mathbf{F}_M = \varphi_{Pt} \quad \text{and} \quad \mathbf{J}^{TR}_o/\mathbf{J}^{ABS} = 1 - \mathbf{F}_o/\mathbf{F}_M = \varphi_{Po}$$

which are the same, respectively, Eqs. (A6) and (A7), obtained with the assumption $\mathbf{J}^{DI}_t = \alpha \cdot \mathbf{F}_t$ (see Appendix A.1, A.1.1, assumption (**10**) in Section 4.1, and [17]).

References

[1] H.-W. Trissl, Y. Gao, K. Wulf, Theoretical fluorescence induction curves derived from coupled differential equations describing the primary photochemistry of photosystem II by an exciton-radical pair equilibrium, Biophys. J. 64 (1993) 974–988.
[2] Govindjee, J. Amesz, D.C. Fork (Eds.), Light Emission by Plants and Bacteria, Academic Press, Orlando, 1986, 638pp.
[3] G.C. Papageorgiou, Govindjee (Eds.), Chlorophyll a Fluorescence: A Signature of Photosynthesis, Advances in Photosynthesis and Respiration, vol. 19, Springer, Dordrecht, The Netherlands, 2004, 818pp.
[4] W.L. Butler, Fluorescence yield in photosynthetic systems and its relation to electron transport, Curr. Top. Bioenerg. 1 (1966) 49–73.
[5] Govindjee, G.C. Papageorgiou, Chlorophyll fluorescence and photosynthesis: fluorescence transients, Photophysiology 6 (1971) 1–50.

Please cite this article in press as: A. Stirbet, Govindjee, On the relation between the Kautsky effect (chlorophyll *a* fluorescence induction) and Photosystem II: Basics and applications of the OJIP fluorescence transient, J. Photochem. Photobiol. B: Biol. (2011), doi:10.1016/j.jphotobiol.2010.12.010

[6] J.H.C. Goedheer, Fluorescence in relation to photosynthesis, Annu. Rev. Plant Physiol. 23 (1972) 87–112.
[7] Govindjee, G. Papageorgiou, E. Rabinowitch, Chlorophyll Fluorescence and Photosynthesis, in: G.G. Guilbault (Ed.), Practical Fluorescence Theory, Methods, and Techniques, Marcel Dekker Inc., New York, 1973, pp. 543–575.
[8] W.L. Butler, Energy distribution in the photochemical apparatus of photosynthesis, Annu. Rev. Plant Physiol. 29 (1978) 345–378.
[9] Govindjee, P. Jursinic, Photosynthesis and fast changes in light emission by green plants, Photochem. Photobiol. Rev. 4 (1979) 125–205.
[10] J.-M. Briantais, C. Vernotte, G.H. Krause, E. Weis, Chlorophyll a fluorescence of higher plants: chloroplasts and leaves, in: Govindjee, J. Amesz, D.C. Fork (Eds.), Light Emission by Plants and Bacteria, Academic Press, New York, 1986, pp. 539–583.
[11] G. Renger, U. Schreiber, Practical applications of fluorometric methods to algae and higher plant research, in: Govindjee, J. Amesz, D.C. Fork (Eds.), Light Emission by Plants and Bacteria, Academic Press, Orlando, 1986, pp. 587–619.
[12] P. Horton, J.R. Bowyer, Chlorophyll fluorescence transients, in: J.L. Harwood, J.R. Bowyer (Eds.), Methods in Plant Biochemistry, vol. 4, Academic Press, New York, 1990, pp. 259–296.
[13] G.H. Krause, E. Weis, Chlorophyll fluorescence and photosynthesis: the basics, Annu. Rev. Plant Physiol. Plant Mol. Biol. 42 (1991) 313–349.
[14] Govindjee, Sixty-three years since Kautsky: chlorophyll a fluorescence, Aust. J. Plant Physiol. 22 (1995) 131–160.
[15] Govindjee, Chlorophyll a fluorescence: a bit of basics and history, in: G.C. Papageorgiou, Govindjee (Eds.), Chlorophyll a Fluorescence: A Signature of Photosynthesis, Advances in Photosynthesis and Respiration, vol. 19, Springer, Dordrecht, The Netherlands, 2004, pp. 1–41.
[16] D. Lazár, Chlorophyll a fluorescence induction, Biochim. Biophys. Acta 1412 (1999) 1–28.
[17] R.J. Strasser, A. Srivastava, M. Tsimilli-Michael, The fluorescence transient as a tool to characterize and screen photosynthetic samples, in: M. Yunus, U. Pathre, P. Mohanty (Eds.), Probing Photosynthesis: Mechanism, Regulation and Adaptation, Taylor and Francis, London, UK, 2000, pp. 443–480.
[18] R.J. Strasser, M. Tsimilli-Michael, A. Srivastava, Analysis of the chlorophyll fluorescence transient, in: G.C. Papageorgiou, Govindjee (Eds.), Chlorophyll Fluorescence: A Signature of Photosynthesis, Advances in Photosynthesis and Respiration, vol. 19, Springer, Dordrecht, The Netherlands, 2004, pp. 321–362.
[19] K. Maxwell, G.N. Johnson, Chlorophyll fluorescence-a practical guide, J. Exp. Bot. 51 (2000) 659–668.
[20] E. Rosenqvist, O. van Kooten, Chlorophyll fluorescence: a general description and nomenclature, in: J.R. DeEll, P.M.A. Toivonen (Eds.), Practical Applications of Chlorophyll Fluorescence in Plant Biology, Kluwer Academic Publishers, Dordrecht, The Netherlands, 2003, pp. 31–78.
[21] U. Schreiber, Pulse-amplitude-modulation (PAM) fluorometry and saturation pulse method: an overview, in: G.C. Papageorgiou, Govindjee (Eds.), Chlorophyll a Fluorescence: A Signature of Photosynthesis, Advances in Photosynthesis and Respiration, vol. 19, Springer, Dordrecht, The Netherlands, 2004, pp. 279–319.
[22] G.C. Papageorgiou, M. Tsimilli-Michael, K. Stamatakis, The fast and slow kinetics of chlorophyll a fluorescence induction in plants, algae and cyanobacteria: a viewpoint, Photosynth. Res. 94 (2007) 275–290.
[23] N.R. Baker, Chlorophyll fluorescence: a probe of photosynthesis *in vivo*, Annu. Rev. Plant Biol. 59 (2008) 659–668.
[24] D. Lazár, G. Schansker, Models of chlorophyll a fluorescence transients, in: A. Laisk, L. Nedbal, Govindjee (Eds.), Photosynthesis *in Silico*: Understanding Complexity from Molecules to Ecosystems, Advances in Photosynthesis and Respiration, vol. 29, Springer, Dordrecht, The Netherlands, 2009, pp. 85–123.
[25] R. Röttgers, Comparison of different variable chlorophyll a fluorescence techniques to determine photosynthetic parameters of natural phytoplankton, Deep-Sea Res. I 54 (2007) 437–451.
[26] R.J. Strasser, Govindjee, The F_o and the O–J–I–P fluorescence rise in higher plants and algae, in: J.H. Argyroudi-Akoyunoglou (Ed.), Regulation of Chloroplast Biogenesis, Plenum Press, New York, 1991, pp. 423–426.
[27] R.J. Strasser, Govindjee, On the O–J–I–P fluorescence transients in leaves and D1 mutants of *Chlamydomonas reinhardtii*, in: N. Murata (Ed.), Research in Photosynthesis, vol. II, Kluwer Academic Publishers, Dordrecht, The Netherlands, 1992, pp. 39–42.
[28] U. Schreiber, U. Schliwa, W. Bilger, Continuous recording of photochemical and nonphotochemical chlorophyll fluorescence quenching with a new type of modulation fluorometer, Photosynth. Res. 10 (1986) 51–62.
[29] D. Mauzerall, Light-induced changes in *Chlorella*, and the primary photoreaction for the production of oxygen, Proc. Natl. Acad. Sci. USA 69 (1972) 1358–1362.
[30] P.G. Falkowski, K. Wyman, A.C. Ley, D. Mauzerall, Relationship of steady state photosynthesis to fluorescence in eucaryotic algae, Biochim. Biophys. Acta 849 (1986) 183–192.
[31] Z.S. Kolber, O. Prášil, P.G. Falkowski, Measurements of variable chlorophyll fluorescence using fast repetition rate techniques: defining methodology and experimental protocols, Biochim. Biophys. Acta 1367 (1998) 88–106.
[32] R.J. Olson, A.M. Chekalyuk, H.M. Sosik, Phytoplankton photosynthetic characteristics from fluorescence induction assays of individual cells, Limnol. Oceanogr. 41 (1996) 1253–1263.
[33] M.Y. Gorbunov, P.G. Falkowski, Fluorescence induction and relaxation (FIRe) technique and instrumentation for monitoring photosynthetic processes and primary production in aquatic ecosystems, in: A. van der Est, D. Bruce (Eds.), Photosynthesis: Fundamental Aspects to Global Perspectives, Proc. 13th International Congress of Photosynthesis, Montreal, August 29–September 3, 2004, Allen Press, Springer, 2005, pp. 1029-1031.
[34] Z. Johnson, Description and application of the background irradiance gradient single turnover fluorometer (BIG STf), Marine Ecol. Prog. Ser. 283 (2004) 73–80.
[35] A. Chekalyuk, M. Hafez, Advanced laser fluorometry of natural aquatic environments, Limnol. Oceanogr.: Methods 6 (2008) 591–609.
[36] H. Kautsky, A. Hirsch, Neue Versuche zur Kohlensäureassimilation, Naturwissenschaften 19 (1931) 964.
[37] F. Rappaport, D. Béal, A. Joliot, P. Joliot, On the advantages of using green light to study fluorescence yield changes in leaves, Biochim. Biophys. Acta 1767 (2007) 56–65.
[38] R.J. Strasser, Dissipative Strukturen als thermodynamischer Regelkreis des Photosyntheseapparates, Ber. Deutsche Bot. Ges. Bd. 98 (1985) 53–72.
[39] A. Srivastava, H. Greppin, R.J. Strasser, Acclimation of land plants to diurnal changes in temperature and light, in: P. Mathis (Ed.), Photosynthesis: From Light to Biosphere, vol. 4, Kluwer Academic Publishers, The Netherlands, 1995, pp. 909–912.
[40] G.C. Papageorgiou, Govindjee, Light induced changes in the fluorescence yield of chlorophyll a *in vivo*. I. *Anacystis nidulans*, Biophys. J. 8 (1968) 299–1315.
[41] G.C. Papageorgiou, Govindjee, Light induced changes in the fluorescence yield of chlorophyll a *in vivo*. II. *Chlorella pyrenoidosa*, Biophys. J. 8 (1968) 1316–1328.
[42] Govindjee, K. Satoh, Fluorescence properties of chlorophyll b- and chlorophyll c-containing algae, in: Govindjee, J. Amesz, D.C. Fork (Eds.), Light Emission by Plants and Bacteria, Academic Press, Orlando, 1986, pp. 497–537.
[43] M. Tsimilli-Michael, M. Pêcheux, R.J. Strasser, Vitality and stress adaptation of the symbionts of coral reef and temperate foraminifers probed *in hospite* by the fluorescence kinetics OJIP, Archs. Sci. Genève 51 (1998) 205–240.
[44] P. Ilík, G. Schansker, E. Kotabová, P. Váczi, R.J. Strasser, M. Bártak, A dip in the chlorophyll fluorescence induction at 0.2–2 s in *Trebouxia*-possesing lichens reflects a fast reoxidation of photosystem I.A comparison with higher plants, Biochim. Biophys. Acta 1757 (2006) 12–20.
[45] B. Guissé, A. Srivastava, R.J. Strasser, The polyphasic rise of the chlorophyll *a* fluorescence (O–K–J–I–P) in heat stressed leaves, Arch. Sci. Genève 48 (1995) 147–160.
[46] A. Srivastava, B. Guissé, H. Greppin, R.J. Strasser, Regulation of antenna structure and electron transport in PSII of *Pisum sativum* under elevated temperature probed by the fast polyphasic chlorophyll a fluorescence transient OKJIP, Biochim. Biophys. Acta 1320 (1997) 95–106.
[47] B.J. Strasser, Donor side capacity of photosystem II probed by chlorophyll a fluorescence transients, Photosynth. Res. 52 (1997) 147–155.
[48] J.C. Munday Jr., Govindjee, Fluorescence transients in *Chlorella*: effects of supplementary light, anaerobiosis and methyl viologen, Prog. Photosynth. Res. II (1969) 913–922.
[49] C. Neubauer, U. Schreiber, The polyphasic rise of chlorophyll fluorescence upon onset of strong continuous illumination. I. Saturation characteristics and partial control by the photosystem II acceptor side, Z. Naturforsch. 42c (1987) 1246–1254.
[50] R.J. Strasser, A. Srivastava, Govindjee, Polyphasic chlorophyll a fluorescent transient in plants and cyanobacteria, Photochem. Photobiol. 61 (1995) 32–42.
[51] E. Baake, J.P. Schloder, Modeling the fast fluorescence rise of photosynthesis, Bull. Math. Biol. 54 (1992) 999–1021.
[52] H.-W. Trissl, Y. Gao, K. Wulf, Theoretical fluorescence induction curves derived from coupled differential equations describing the primary photochemistry of photosystem II by an excition-radical pair equilibrium, Biophys. J. 64 (1993) 974–988.
[53] A. Stirbet, Govindjee, B.J. Strasser, R.J. Strasser, Chlorophyll *a* fluorescence induction in higher plants: modelling and numerical simulation, J. Theor. Biol. 193 (1998) 131–151.
[54] G.V. Lebedeva, N.E. Belyaeva, G.Y. Riznichenko, A.B. Rubin, O.V. Demin, Kinetic model of photosystem II of higher plants, Russ. J. Phys. Chem. 74 (2000) 1702–1710.
[55] D. Lazár, Chlorophyll *a* fluorescence rise induced by high light illumination of dark-adapted plant tissue studied by means of a model of photosystem II and considering photosystem II heterogeneity, J. Theor. Biol. 220 (2003) 469–503.
[56] X.-G. Zhu, Govindjee, N.R. Baker, E. deSturler, D. R Ort, S.P. Long, Chlorophyll *a* fluorescence induction kinetics in leaves predicted from a model describing each discrete step of excitation energy and electron transfer associated with photosystem II, Planta 223 (2005) 114–133.
[57] W.J. Vredenberg, Algorithm for analysis of OJDIP fluorescence induction curves in terms of photo- and electrochemical events in photosystems of plant cells. Derivation and application, J. Photochem. Photobiol. B 91 (2008) 58–65.
[58] A. Rubin, G. Riznichenko, Modeling of the primary processes in a photosynthetic membrane, in: A. Laisk, L. Nedbal, Govindjee (Eds.), Photosynthesis *in Silico*: Understanding Complexity from Molecules to Ecosystems, Advances in Photosynthesis and Respiration, vol. 29, Springer, Dordrecht, The Netherlands, 2009, pp. 151–176.
[59] W. Vredenberg, O. Prášil, Modeling of chlorophyll a fluorescence kinetics in plant cells: derivation of a descriptive algorithm, in: A. Laisk, L. Nedbal, Govindjee (Eds.), Photosynthesis *in Silico*: Understanding Complexity from

Please cite this article in press as: A. Stirbet, Govindjee, On the relation between the Kautsky effect (chlorophyll *a* fluorescence induction) and Photosystem II: Basics and applications of the OJIP fluorescence transient, J. Photochem. Photobiol. B: Biol. (2011), doi:10.1016/j.jphotobiol.2010.12.010

Molecules to Ecosystems, Advances in Photosynthesis and Respiration, vol. 29, Springer, Dordrecht, The Netherlands, pp. 125–149.
[60] L.M.N. Duysens, H.E. Sweers, Mechanism of the two photochemical reactions in algae as studied by means of fluorescence, in: Japanese Society of Plant Physiologists (Ed.), Studies on Microalgae and Photosynthetic Bacteria, University of Tokyo Press, Tokyo, 1963, pp. 353–372.
[61] H.J. van Gorkom, M.P.J. Pulles, A.-L. Étienne, Fluorescence and absorbance changes in Tris-washed chloroplasts, in: H. Metzner (Ed.), Photosynthetic Oxygen evolution, Academic Press, London, UK, 1978, pp. 135–145.
[62] H.J. van Gorkom, Fluorescence measurements in the study of photosystem II electron transport, in: Govindjee, J. Amesz, D.C. Fork (Eds.), Light Emission by Plants and Bacteria, Academic Press, Ontario, 1986, pp. 267–289.
[63] P. Joliot, A. Joliot, Excitation transfer between photosynthetic units: the 1964 experiment, Photosynth. Res. 76 (2003) 241–245.
[64] W.L. Butler, On the primary nature of fluorescence yield changes associated with photosynthesis, Proc. Natl. Acad. Sci. USA 69 (1972) 3420–3422.
[65] V.P. Shinkarev, Govindjee, Insight into the relationship of chlorophyll *a* fluorescence yield to the concentration of its natural quenchers in oxygenic photosynthesis, Proc. Natl. Acad. Sci. USA 90 (1993) 7466–7469.
[66] V.V. Klimov, A.V. Klevanik, V.A. Shuvalov, A.A. Krasnovsky, Reduction of pheophytin in the primary light reaction of photosystem II, FEBS Lett. 82 (1977) 183–186.
[67] W.J. Vredenberg, System analysis of photoelectrochemical control of chlorophyll fluorescence in terms of trapping models of photosystem II: a challenging view, in: G.C. Papageorgiou, Govindjee (Eds.), Chlorophyll a Fluorescence: A Signature of Photosynthesis, Advances in Photosynthesis and Respiration, vol. 19, Springer, Dordrecht, The Netherlands, 2004, pp. 133–172.
[68] C. Vernotte, A.-L. Étienne, J.-M. Briantais, Quenching of the system II chlorophyll fluorescence by the plastoquinone pool, Biochim. Biophys. Acta 545 (1979) 519–527.
[69] N.E. Belyaeva, G.V. Lebedeva, G. Yu, Riznichenko, Kinetic model of primary photosynthetic processes in chloroplasts. Modeling of thylakoid membranes electric potential, in: G.Yu. Riznichenko (Ed.), Mathematics Computer Education, vol. 10, Progress-Traditsiya, Moscow, 2003, pp. 263–276.
[70] P. Morin, Études des cinétiques de fluorescence de la chlorophylle in vivo, dans les premiers instants qui suivent le début de l'illumination, J. Chim. Phys. 61 (1964) 674–680.
[71] R. Delosme, Étude de l'induction de fluorescence des algues vertes et des chloroplastes au début d'une illumination intense, Biochim. Biophys. Acta 143 (1967) 108–128.
[72] J.C. Munday Jr., Govindjee, Light-induced changes in the fluorescence yield of chlorophyll *a* in vivo III. The dip and the peak in the fluorescence transient of *Chlorella pyrenoidosa*, Biophys. J. 9 (1969) 1–21.
[73] J.C. Munday Jr., Govindjee, Light-induced changes in the fluorescence yield of chlorophyll *a* in vivo IV. The effect of preillumination on the fluorescence transient of *Chlorella pyrenoidosa*, Biophys. J. 9 (1969) 22–35.
[74] G. Schansker, S.Z. Tóth, R.J. Strasser, Methylviologen and dibromothymoquinone treatments of pea leaves reveal the role of photosystem I in the Chl *a* fluorescence rise OJIP, Biochim. Biophys. Acta 1706 (2005) 250–261.
[75] O. Bjorkman, B. Demmig, Photon yield of O_2 evolution and chlorophyll fluorescence characteristics at 77 K among vascular plants of diverse origins, Planta 170 (1987) 489–504.
[76] W.L. Butler, M. Kitajima, Fluorescence quenching in photosystem II of chloroplasts, Biochim. Biophys. Acta 376 (1975) 116–125.
[77] G. Paillotin, Movement of excitations in the photosynthetic domains of photosystem II, J. Theor. Biol. 58 (1976) 237–252.
[78] B. Genty, J.-M. Briantais, N.R. Baker, The relationship between the quantum yield of photosynthetic electron transport and quenching of chlorophyll fluorescence, Biochim. Biophys. Acta 990 (1989) 87–92.
[79] A. Joliot, P. Joliot, Etude cinétique de la réaction photochimique libérant l'oxygène au cours de la photosynthèse, C.R. Acad. Sci. Paris 258 (1964) 4622–4625.
[80] P. Joliot, A. Joliot, Quantification of cyclic and linear electron flows in plants, Proc. Natl. Acad. Sci. USA 102 (2005) 4913–4918.
[81] R.J. Strasser, The grouping model of plant photosynthesis, in: G. Akoyunoglou, J.H. Argyroudi-Akoyunoglou (Eds.), Chloroplast Development, Elsevier Biomedical, 1978, pp. 513–538.
[82] W.L. Butler, Energy transfer between photosystem II units in a connected package model of the photochemical apparatus of photosynthesis, Proc. Natl. Acad. Sci. USA 77 (1980) 4694–4701.
[83] R.J. Strasser, The grouping model of plant photosynthesis: heterogeneity of photosynthetic units in thylakoids, in: G. Akoyunoglou (Ed.), Photosynthesis: Proceedings of the Vth International Congress on Photosynthesis, Halkidiki, Greece 1980, Structure and Molecular Organisation of the Photosynthetic Apparatus, vol. III, Balaban International Science Services, Philadelphia, 1981, pp. 727–737.
[84] H.-W. Trissl, J. Lavergne, Fluorescence induction from photosystem II: analytical equations for the yields of photochemistry and fluorescence derived from analysis of a model including exciton radical pair equilibrium and restricted energy transfer between photosynthetic units, Aust.J. Plant Physiol. 22 (1994) 183–193.
[85] J. Lavergne, H.-W. Trissl, Theory of fluorescence induction in photosystem II: derivation of analytical expressions in a model including exciton-radical-pair equilibrium and restricted energy transfer between photosynthetic units, Biophys. J. 68 (1995) 2474–2492.
[86] U. Schreiber, Detection of rapid induction kinetics with a new type of high-frequency modulated chlorophyll fluorometer, Photosynth. Res. 9 (1986) 261–272.
[87] G. Schansker, S.Z. Tóth, R.J. Strasser, Dark-recovery of the Chl *a* fluorescence transient (OJIP) after light adaptation: the qT-component of nonphotochemical quenching is related to an activated photosystem I acceptor side, Biochim. Biophys. Acta 1757 (2006) 787–797.
[88] G.H. Krause, P. Jahns, Non-photochemical energy dissipation determined by chlorophyll fluorescence quenching: characterization and function, in: G.C. Papageorgiou, Govindjee (Eds.), Chlorophyll a Fluorescence: A Signature of Photosynthesis, Advances in Photosynthesis and Respiration, vol. 19, Springer, The Netherlands, 2004, pp. 463–495.
[89] G. Schansker, Y. Yuan, R.J. Strasser, Chl *a* fluorescence and 820 nm transmission changes occurring during a dark-to-light transition in pine needles and pea leaves: a comparison, in: J.F. Allen, B. Osmond, J.H. Golbeck, E. Gantt (Eds.), Energy from the Sun, Springer, Dordrecht, 2008, pp. 945–949.
[90] W. Bilger, U. Schreiber, Energy-dependent quenching of dark level chlorophyll fluorescence in intact leaves, Photosynth. Res. 10 (1986) 303–308.
[91] P. Horton, A.V. Ruban, Delta pH-dependent quenching of the F_o level of chlorophyll fluorescence in spinach leaves, Biochim. Biophys. Acta 1142 (1993) 203–206.
[92] W. Bilger, O. Björkman, Role of the xanthophyll cycle in photoprotection elucidated by measurements of light-induced absorbance changes, fluorescence and photosynthesis in leaves of *Hedera canariensis*, Photosynth. Res. 25 (1990) 173–185.
[93] W.P. Quick, M. Stitt, An examination of factors contributing to non-photochemical quenching of chlorophyll fluorescence in barley leaves, Biochim. Biophys. Acta 977 (1989) 287–296.
[94] P.G. Walters, P. Horton, Theoretical assessment of alternative mechanisms for non-photochemical quenching of PSII fluorescence in barley leaves, Photosynth. Res. 36 (1993) 119–139.
[95] P. Müller, X.-P. Li, K.K. Niyogi, Non-photochemical quenching. A response to excess light energy, Plant Physiol. 125 (2001) 1558–1566.
[96] P. Horton, A.V. Ruban, R.G. Walters, Regulation of light harvesting in green plants, Annu. Rev. Plant Physiol. Plant Mol. Biol. 47 (1996) 655–684.
[97] K.K. Niyogi, X.P. Li, V. Rosenberg, H.S. Jung, Is PsbS the site of non-photochemical quenching in photosynthesis?, J Exp. Bot. 56 (2005) 375–382.
[98] B. Demmig-Adams, Carotenoids and photoprotection: a role for the xanthophyll zeaxanthin, Biochim. Biophys. Acta 1020 (1990) 1–24.
[99] A. Gilmore, V.P. Shinkarev, T.L. Hazlett, Govindjee, Quantitative analysis of the effects of intrathylakoid pH and the xanthophyll cycle pigments on chlorophyll a fluorescence lifetime distributions and intensity in thylakoids, Biochemistry 37 (1998) 13582–13593.
[100] B. Demmig-Adams, W.W. Adams III, A.K. Mattoo (Eds.), Photoprotection, Photoinhibition, Gene Regulation, and Environment, in: Govindjee (Ser. Ed.), Advances in Photosynthesis and Respiration, vol. 21, Springer, Dordrecht, 2005, 390pp. (reprinted in 2008).
[101] J.F. Allen, C.W. Mullineaux, Probing the mechanism of state transitions in oxygenic photosynthesis by chlorophyll fluorescence spectroscopy, kinetics and imaging, in: G.C. Papageorgiou, Govindjee (Eds.), Chlorophyll a Fluorescence: A Signature of Photosynthesis, Springer, Dordrecht, The Netherlands, 2004, pp. 447–461.
[102] H.Y. Lee, Y.-N. Hong, W.S. Chow, Photoinactivation of photosystem II and photoprotection by non-functional neighbours in *Capiscum annuum* L. leaves, Planta 212 (2001) 332–342.
[103] N. Adir, H. Zer, S. Shochat, I. Ohad, Photoinhibition – a historical perspective, Photosynth. Res. 76 (2003) 343–370.
[104] S. Matsubara, W.S. Chow, Populations of photoinactivated photosystem II characterized by Chl fluorescence lifetime in vivo, Proc. Natl. Sci. USA 101 (2004) 18234–18239.
[105] N. D'Ambrosio, C.R. Guadagno, A.V. De Santo, Is qE always the major component of non-photochemical quenching?, in: J.F. Allen, B. Osmond, J.H. Golbeck, E. Gantt (Eds.), Energy from the Sun, Springer, Dordrecht, 2008, pp. 1001–1004.
[106] R.G. Walters, P. Horton, Resolution of non-photochemical chlorophyll fluorescence quenching in barley leaves, Photosynth. Res. 27 (1991) 121–133.
[107] R.G. Walters, P. Horton, Theoretical assessment of alternative mechanisms for non-photochemical quenching of PSII fluorescence in barley leaves, Photosynth. Res. 36 (1993) 119–139.
[108] M. Havaux, R.J. Strasser, H. Greppin, A theoretical and experimental analysis of the qP and qN coefficients of chlorophyll fluorescence quenching and their relation to photochemical and nonphotochemical events, Photosynth. Res. 27 (1991) 41–55.
[109] D.M. Kramer, G. Johnson, O. Kiirats, G.E. Edwards, New fluorescence parameters for the determination of Q_A redox state and excitation energy fluxes, Photosynth. Res. 79 (2004) 209–218.
[110] L. Hendrickson, R.T. Furbank, W.S. Chow, A simple alternative approach to assessing the fate of absorbed light energy using chlorophyll fluorescence, Photosynth. Res. 82 (2004) 73–81.
[111] L. Hendrickson, B. Förster, B.J. Pogson, W.S. Chow, A simple chlorophyll fluorescence parameter that correlates with the rate coefficient of photoinactivation of photosystem II, Photosynth. Res. 84 (2005) 43–49.
[112] E. Weis, D. Lechtenberg, Fluorescence analysis during steady-state photosynthesis, Philos. Trans. Roy. Soc. Lond. B 323 (1989) 253–268.

Please cite this article in press as: A. Stirbet, Govindjee, On the relation between the Kautsky effect (chlorophyll *a* fluorescence induction) and Photosystem II: Basics and applications of the OJIP fluorescence transient, J. Photochem. Photobiol. B: Biol. (2011), doi:10.1016/j.jphotobiol.2010.12.010

[113] B. Demmig-Adams, W. Adams III, D. Barker, B. Logan, D. Bowling, A. Verhoeven, Using chlorophyll fluorescence to assess the fraction of absorbed light allocated to thermal dissipation of excess excitation, Physiol. Plant. 98 (1996) 253–264.
[114] B.J. Strasser, R.J. Strasser, Measuring fast fluorescence transients to address environmental questions: the JIP test, in: P. Mathis (Ed.), Photosynthesis: From Light to Biosphere, vol. 5, Kluwer Academic, The Netherlands, 1995, pp. 977–980.
[115] R.J.Strasser, P. Eggenberg, R. Truan, Diagnostic de la vitalité de l'arbre par mesures de fluorescence, in: J.-L. Sandoz (Ed.), Diagnostic et entretien des Grands Arbres: Proceedings EPFL-IBOIS GS 96, 1996, pp. 1–12.
[116] A. Srivastava, R.J. Strasser, Govindjee, Greening of peas: parallel measurements of 77 K emission spectra, OJIP chlorophyll a fluorescence, period four oscillation of the initial fluorescence level, delayed light emission, and P700, Photosynthetica 37 (1999) 365–392.
[117] M. Tsimilli-Michael, R.J. Strasser, *In vivo* assessment of plants' vitality: applications in detecting and evaluating the impact of mycorrhization on host plants, in: A. Varma (Ed.), Mycorrhiza: State of the Art, Genetics and Molecular Biology, Eco-Function, Biotechnology, Eco-Physiology, Structure and Systematics, 3rd ed., Springer, Dordrecht, The Netherlands, 2008, pp. 679–703.
[118] R. Hill, F. Bendall, Function of the two cytochrome components in chloroplasts: a working hypothesis, Nature 176 (1960) 40–44.
[119] L.N.M. Duysens, J. Amesz, B.M. Kamp, Two photochemical systems in photosynthesis, Nature 190 (1961) 510–511.
[120] Govindjee, J.F. Kern, J. Messinger, J. Whitmarsh, Photosystem II, in: Encyclopedia of Life Sciences (ELS), John Wiley & Sons, Ltd., Chichester, 2010. doi:10.1002/9780470015902.a0000669.pub2.
[121] L. Orr, Govindjee, Photosynthesis online, Photosynth. Res. (2010) 34, doi:10.1007/s11120-010-9570-8.
[122] E. Rabinowitch, Govindjee, Photosynthesis, John Wiley and Sons Inc., NY, 1969, 273pp.
[123] R.E. Blankenship, Molecular Mechanisms of Photosynthesis, Blackwell Science, Oxford, UK, 2002, 321pp.
[124] P.G. Falkowski, J.A. Raven, Aquatic Photosynthesis, 2 nd ed., Princeton University Press, Princeton, NJ, 2007, 484pp.
[125] R.M. Clegg, M. Sener, Govindjee, From Förster resonance energy transfer (FRET) to coherent resonance energy transfer (CRET) and back-A wheen o' mickles mak's a muckle, in: Optical Biopsy VII, R.R. Alfano (Ed.), Proceedings of SPIE, vol. 7561 (SPIE, Bellingham, WA, 2010), pp. 7561–7572 (article CID number: 75610C, 2010, 21pp.).
[126] T. Wydrzynski, K. Satoh (Ed.), Photosystem II: The Light-induced Water-Plastoquinone Oxidoreductase, in: Govindjee (Ed.), Advances in Photosynthesis and Respiration, vol. 22, Springer, Dordrecht, The Netherlands, 2005, p. 756.
[127] J.H. Golbeck (Ed.), Photosystem I: The Light-driven Plastocyanin:Ferredoxin Oxidoreductase, Springer, Dordrecht, The Netherlands, 2006, 713pp.
[128] P. Joliot, J. Lavergne, D. Béal, Plastoquinone compartmentation in chloroplasts: I. Evidence for domains with different rates of photoreduction, Biochim. Biophys. Acta 1101 (1992) 1–12.
[129] J. Lavergne, J.-P. Bouchaud, P. Joliot, Plastoquinone compartmentation in chloroplasts: II. Theoretical aspects, Biochim. Biophys. Acta 1101 (1992) 13–22.
[130] A. Melis, J.S. Brown, Stoichiometry of system I and system II reaction centers and of plastoquinone in different photosynthetic membranes, Proc. Natl. Acad. Sci. USA 77 (1980) 4712–4716.
[131] A.R. Crofts, The Q-cycle-a personal perspective, Photosynth. Res. 80 (2004) 223–243.
[132] W.A. Cramer, H. Zhang, Consequences of the structure of the cytochrome *b6f* complex for its charge transfer pathways, Biochim. Biophys. Acta 1757 (2006) 339–345.
[133] D. Baniulis, E. Yamashita, H. Zhang, S.S. Hasan, W.A. Cramer, Structure-function of the cytochrome *b6f* complex, Photochem. Photobiol. 84 (2008) 1349–1358.
[134] M.A. Schöttler, H. Kirchhoff, E. Weis, The role of plastocyanin in the adjustment of the photosynthetic electron transport to the carbon metabolism in Tobacco, Plant Physiol. 136 (2004) 4265–4274.
[135] H. Böhme, Quantitative determination of ferredoxin, ferredoxin-NADP$^+$ reductase and plastocyanin in spinach chloroplasts, Eur. J. Biochem. 83 (1978) 137–141.
[136] G. Schansker, S.Z. Tóth, R.J. Strasser, Dark recovery of the Chl *a* fluorescence transient (OJIP) after light adaptation: the qT-component of non-photochemical quenching is related to an activated photosystem I acceptor side, Biochim. Biophys. Acta 1757 (2006) 787–797.
[137] K. Asada, The water–water cycle in chloroplasts: scavenging of active oxygens and dissipation of excess photons, Annu. Rev. Plant Physiol. Plant Mol. Biol. 50 (1999) 601–639.
[138] K. Asada, Production and scavenging of reactive oxygen species in chloroplasts and their functions, Plant Physiol. 141 (2006) 391–396.
[139] C. Miyake, Coupled regulation of cyclic electron flow around PSI with photosynthesis-its contribution to non-photochemical quenching evidenced with transplastomic Tobacco plants over-expressing ferredoxin in chloroplasts, in: J.F. Allen, E. Gantt, J.H. Golbeck, B. Osmond (Eds.), Photosynthesis, Energy from the Sun: 14th International Congress on Photosynthesis, Springer, Dordrecht, The Netherlands, 2008, pp. 923–927.
[140] C. Miyake, S. Horiguchi, A. Makino, Y. Shinzaki, H. Yamamoto, K.I. Tomizawa, Effects of light intensity on cyclic electron flow around PSI and its relationship to non-photochemical quenching of Chl fluorescence in tobacco leaves, Plant Cell Physiol. 46 (2005) 1819–1830.
[141] W. Junge, H. Sielaff, S. Engelbrecht, Torque generation and elastic power transmission in the rotary FOF1-ATPase, Nature 459 (2009) 364–370.
[142] P. Mitchell, Coupling of phosphorylation to electron and hydrogen transfer by a chemi-osmotic type of mechanism, Nature 191 (1961) 144–148.
[143] D. Stock, C. Gibbons, I. Arechaga, A.G.W. Leslie, J.E. Walker, The rotary mechanism of ATP synthase, Curr. Opin. Struct. Biol. 10 (2000) 672–679.
[144] A.A. Benson, Following the path of carbon in photosynthesis: a personal story, Photosynth. Res. 73 (2002) 29–49.
[145] J.A. Bassham, Mapping the carbon reduction cycle: a personal retrospective, Photosynth. Res. 76 (2003) 35–52.
[146] P. Schürmann, Redox signaling in the chloroplasts: the ferredoxin/thioredoxin system, Antioxidants Redox Sig. 5 (2003) 69–78.
[147] S. Dai, K. Johansson, H. Eklund, P. Schürmann, Light/dark regulation of chloroplast metabolism, in: R.R. Wise, J.K. Hoober (Eds.), The Structure and Function of Plastids, Chapter 11, in Govindjee (Ser. Ed.), Advances in Photosynthesis and Respiration, vol. 23, Kluwer Academic Press, 2006, pp. 221–236.
[148] M. Lindahl, T. Kieselbach, Disulphide proteomes and interactions with thioredoxin on the track towards understanding redox regulation in chloroplasts and cyanobacteria, J. Proteomics 72 (2009) 416–438.
[149] M. Hall, A. Mata-Cabana, H.E. Akerlund, F.J. Florencio, W.P. Schröder, M. Lindahl, T. Kieselbach, Thioredoxin targets of the plant chloroplast lumen and their implications for plastid function, Proteomics 10 (2010) 987–1001.
[150] B.B. Buchanan, Role of light in the regulation of chloroplast enzymes, Annu. Rev. Plant Physiol. 31 (1980) 341–374.
[151] B.B. Buchanan, Y. Balmer, Redox regulation: a broadening horizon, Annu. Rev. Plant Physiol. 56 (2005) 187–220.
[152] G.H. Krause, P. Jahns, Non-photochemical energy dissipation determined by chlorophyll fluorescence quenching: characterization and function, in: G.C. Papageorgiou, Govindjee (Eds.), Chlorophyll a Fluorescence: A Signature of Photosynthesis, Springer, Dordrecht, The Netherlands, 2004, pp. 463–495.
[153] M. Tsimilli-Michael, G.H.J. Krüger, R.J. Strasser, Suboptimality as driving force for adaptation: a study about the correlation of excitation light intensity and the dynamic fluorescence emission in plants, in: P. Mathis (Ed.), Photosynthesis: From Light to Biosphere, vol. V, Kluwer Academic Publishers, The Netherlands, 1995, pp. 981–984.
[154] A. Srivastava, R.J. Strasser, Stress and stress management of land plants during a regular day, J. Plant Physiol. 148 (1996) 445–455.
[155] G.H.J. Krüger, M. Tsimilli-Michael, R.J. Strasser, Light stress provokes plastic and elastic modifications in structure and function of photosystem II in camellia leaves, Physiol. Plant. 101 (1997) 265–277.
[156] L. van Rensburg, G.H.J. Krüger, P. Eggenberg, R.J. Strasser, Can screening criteria for drought resistance in *Nicotiana tabacum* L. be derived from the polyphasic rise of the chlorophyll *a* fluorescence transient (OJIP)?, S Afr. J. Bot. 62 (1996) 337–341.
[157] G. Ouzounidou, M. Moustakas, R.J. Strasser, Sites of action of copper in the photosynthetic apparatus of maize leaves: kinetic analysis of chlorophyll fluorescence, oxygen evolution, absorption changes and thermal dissipation as monitored by photoacoustic signals, Aust. J. Plant Physiol. 24 (1997) 81–90.
[158] A. Pareek, S.K. Sopory, H.J. Bohnert, Govindjee (Eds.), Abiotic Stress Adaptation in Plants: Physiological, Molecular and Genomic Foundation, Springer, Dordrecht, The Netherlands, 2010, 523pp.
[159] H.J. Bohnert, E. Sheveleva, Plant stress adaptations-making metabolism move, Physiology and metabolism, Curr. Opin. Plant Biol. 1 (1998) 267–274.
[160] R.J. Strasser, M. Tsimilli-Michael, S. Qiang, V. Goltsev, Simultaneous in vivo recording of prompt and delayed fluorescence and 820-nm reflection changes during drying and after rehydration of the resurrection plant *Haberlea rhodopensis*, Biochim. Biophys. Acta 1797 (2010) 1313–1326.
[161] M. Byrdin, I. Rimke, E. Schlodder, D. Stehlik, T.A. Roelofs, Decay kinetics and quantum yields of fluorescence in photosystem I from *Synechococcus elongatus* with P700 in the reduced and oxidized state: are the kinetics of excited state decay trap-limited or transfer-limited?, Biophys J. 79 (2000) 992–1007.
[162] A.A. Gitelson, C. Buschmann, H.K. Lichtenthaler, Leaf chlorophyll fluorescence corrected for reabsorption by means of absorption and reflectance measurements, J. Plant Physiol. 152 (1998) 283–296.
[163] E. Pfündel, Estimating the contribution of photosystem I to total leaf chlorophyll fluorescence, Photosynth. Res. 56 (1998) 185–195.
[164] A.M. Gilmore, S. Itoh, Govindjee, Global spectral kinetic analysis of room temperature chlorophyll a fluorescence from light harvesting antenna mutants of barley, Philos. Trans. Roy. Soc. Lond. B 335 (2000) 1–14.
[165] S. Itoh, K. Sugiura, Fluorescence of photosystem I, in: G.C. Papageorgiou, Govindjee (Eds.), Chlorophyll a Fluorescence: A Signature of Photosynthesis, Springer, Dordrecht, The Netherlands, 2004, pp. 213–250 (reprinted 2010).
[166] B. Genty, J. Wonders, N.R. Baker, Nonphotochemical quenching of F_o in leaves is emission wavelength dependent. Consequences for quenching analysis and its interpretation, Photosynth. Res. 26 (1990) 133–139.
[167] S.Z. Tóth, G. Schansker, R.J. Strasser, In intact leaves, the maximum fluorescence level (F_M) is independent of the redox state of the plastoquinone pool: a DCMU-inhibition study, Biochim. Biophys. Acta 1708 (2005) 275–282.

Please cite this article in press as: A. Stirbet, Govindjee, On the relation between the Kautsky effect (chlorophyll *a* fluorescence induction) and Photosystem II: Basics and applications of the OJIP fluorescence transient, J. Photochem. Photobiol. B: Biol. (2011), doi:10.1016/j.jphotobiol.2010.12.010

[168] L.N.M. Duysens, PhD Thesis: Transfer of Excitation Energy in Photosynthesis, State University, Utrecht, The Netherlands, 1952.
[169] L. Nedbal, V. Brezina, F. Adamec, D. Stys, V. Oja, A. Laisk, Govindjee, Negative feedback regulation is responsible for the non-linear modulation of photosynthetic activity in plants and cyanobacteria exposed to a dynamic light environment, Biochim. Biophys. Acta 1607 (2003) 5–7.
[170] S.Z. Tóth, G. Schansker, G. Garab, R.J. Strasser, Photosynthetic electron transport activity in heat-treated barley leaves: the role of internal alternative electron donors to photosystem II, Biochim. Biophys. Acta 1767 (2007) 295–305.
[171] W.F.J. Vermaas, G. Renger, G. Dohnt, The reduction of the oxygen evolving system in chloroplasts by thylakoid components, Biochim. Biophys. Acta 764 (1984) 194–202.
[172] A. Stirbet, R.J. Strasser, Numerical simulation of the fluorescence induction in plants, Archs. Sci. Genève 48 (1995) 41–60.
[173] S.Z. Tóth, G. Schansker, R.J. Strasser, A non-invasive assay of the plastoquinone pool redox state based on the OJIP-transient, Photosynth. Res. 93 (2007) 193–203.
[174] S. Malkin, B. Kok, Fluorescence induction studies in isolated chloroplasts. I. Number of components involved in the reaction and quantum yields, Biochim. Biophys. Acta 126 (1966) 413–432.
[175] M.A. Yusuf, D.K.R. Rajwanshi, R.J. Strasser, M. Tsimilli-Michael, Govindjee, N.M. Sarin, Overexpression of γ-tocopherol methyl transferase gene in transgenic *Brassica juncea* plants alleviates abiotic stress: physiological and chlorophyll fluorescence measurements, Biochim. Biophys. Acta 1797 (2010) 1428–1438.
[176] B.R. Velthuys, Electron-dependent competition between plastoquinone and inhibitors for binding to photosystem II, FEBS Lett. 126 (1981) 277–281.
[177] C.A. Wraight, Oxidation-reduction physical chemistry of the acceptor quinone complex in bacterial photosynthetic reaction centers: evidence for a new model of herbicide activity, Israel J. Chem. 21 (1981) 348–354.
[178] A. Stirbet, A. Srivastava, R.J. Strasser, The energetic connectivity of PSII centres in higher plants probed *in vivo* by the fast fluorescence rise O–J–I–P and numerical simulations, in: G. Garab (Ed.), Photosynthesis: Mechanisms and Effects, Proceedings of the Xlth International Congress on Photosynthesis, Budapest, Hungary, vol. V, Kluwer Academic Publishers, The Netherlands, 1998, pp. 4317–4320.
[179] R.J. Strasser, A. Stirbet, Estimation of the energetic connectivity of PS II centres in plants using the fluorescence rise O–J–I–P; fitting of experimental data to three different PS II models, Math. Comput. Simul. 56 (2001) 451–461.
[180] G.H. Krause, S. Somersalo, E. Zumbusch, B. Weyers, H. Laasch, On the mechanism of photoinhibition in chloroplasts. Relationship between changes in fluorescence and activity of photosystem II, J. Plant Physiol. 136 (1990) 472–479.
[181] D.E. Goldman, Potential, impedance and rectification in membranes, J. Gen. Physiol. 27 (1943) 37–40.
[182] A.L. Hodgkin, B. Katz, The effect of sodium ions on the electrical activity of the giant axon of the squid, J. Physiol. 108 (1949) 37–77.
[183] B.S. Ripley, S.P. Redfern, J. Dames, Quantification of the photosynthetic performance of phosphorus-deficient *Sorghum* by means of chlorophyll-*a* fluorescence kinetics, S. Afr. J. Sci. 100 (2004) 615–618.
[184] J.F.C. Gonçalves, U.M. Santos Jr., Utilization of the chlorophyll a fluorescence technique as a tool for selecting tolerant species to environments of high irradiance, Braz. J. Physiol. 17 (2005) 307–313.
[185] B. Thach, A. Shapcott, S. Schmidt, C. Critchley, The OJIP fast fluorescence rise characterizes Graptophyllum species and their stress responses, Photosynth. Res. 94 (2007) 423–436.
[186] D. Christen, S. Schönmann, M. Jermini, R.J. Strasser, G. Défago, Characterization and early detection of grapevine (*Vitis vinifera*) stress responses to esca desease by *in situ* chlorophyll fluorescence and comparison with drought stress, Environ. Exp. Bot. 60 (2007) 504–514.
[187] M. Rapacz, A. Woźniczka, A selection tool for freezing tolerance in common wheat using the fast chlorophyll *a* fluorescence transient, Plant Breed. 128 (2009) 227–234.
[188] A. Srivastava, R.J. Strasser, Constructive and destructive actions of light on the photosynthetic apparatus, J. Sci. Ind. Res. 56 (1997) 133–148.
[189] A. Srivastava, F. Jüttner, R.J. Strasser, Action of the allelochemical, fischerellin A, on photosystem II, Biochim. Biophys. Acta 1364 (1998) 326–336.
[190] R.J. Strasser, M. Tsimilli-Michael, Activity and heterogeneity of PSII probed *in vivo* by the chlorophyll *a* fluorescence rise O–(K)–J–I–P, in: G. Garab (Ed.), Photosynthesis: Mechanisms and Effects, Proceedings of the Xlth International Congress on Photosynthesis, Budapest, Hungary, vol. V, Kluwer Academic Publishers, The Netherlands, 1998, pp. 4321–4324.
[191] R.E. Cleland, A. Melis, P.J. Neale, Mechanism of photoinhibition: photochemical reaction center inactivation in system II of chloroplasts, Photosynth. Res. 9 (1986) 79–88.
[192] A. Melis, Functional properties of PSIIβ in spinach chloroplasts, Biochim. Biophys. Acta 808 (1985) 334–342.
[193] J. Cao, Govindjee, Chlorophyll *a* fluorescence transient as an indicator of active and inactive photosystem II in thylakoid membranes, Biochim. Biophys. Acta 1015 (1990) 180–188.
[194] J. Lavergne, J.-M. Briantais, Photosystem II heterogeneity, in: D.R. Ort, C.F. Yocum (Eds.), Oxygenic Photosynthesis: The Light Reactions, Kluwer, Dordrecht, The Netherlands, 1996, pp. 265–287.
[195] R.J. Strasser, A. Stirbet, Heterogeneity of photosystem II probed by the numerically simulated chlorophyll a fluorescence rise (O–J–I–P), Math. Comput. Simul. 48 (1998) 3–9.
[196] R.J. Strasser, P. Eggenberg, K. Pfister, Govindjee, An equilibrium model for electron transfer in photosystem II acceptor complex: an application to *Chlamydomonas reinhardtii* cells of D1 mutants and those treated with formate, Archs. Sci. Genève 45 (1992) 207–224.
[197] R.J. Strasser, G. Schansker, A. Srivastava, Govindjee, Simultaneous measurement of photosystem I and photosystem II probed by modulated transmission at 820 nm and by chlorophyll a fluorescence in the sub ms to second time range. in: C. Critchley (Ed.), Proceedings of the 12th International Congress on Photosynthesis, Brisbane, Australia, CSIRO Publishing, ISBN 0643 06711 6, Melbourne, Australia. <www.publish.csiro/au/ps2001> (S14-003).
[198] P. Tomek, P. Ilik, D. Lazar, M. Stroch, J. Naus, On the determination of Q_B-non-reducing photosystem II centers from chlorophyll a fluorescence induction, Plant Sci. 164 (2003) 665–670.
[199] G. Schansker, R.J. Strasser, Quantification of non-Q_B-reducing centers in leaves using a far-red pre-illumination, Photosynth. Res. 84 (2005) 145–151.
[200] W.J. Vredenberg, Kinetic Analysis and Mathematical Modeling of Primary Photochemical and Photoelectrochemical Processes in Plant Photosystems, BioSystems, Elsevier, 2011. doi:10.1016/j.biosystems.2010.10.016.
[201] B.-D. Hsu, A theoretical study on the fluorescence induction curve of spinach thylakoids in the absence of DCMU, Biochim. Biophys. Acta 1140 (1992) 30–36.
[202] E. Baake, R.J. Strasser, A differential equation model for the description of the fast fluorescence rise (O–I–D–P transient) in leaves, in: M. Baltscheffsky (Ed.), Current Research in Photosynthesis, vol. 1, Kluwer, Dordrecht, The Netherlands, 1990, pp. 567–570.
[203] A. Stirbet, R.J. Strasser, Numerical simulation of the *in vivo* fluorescence in plants, Math. Comput. Simul. 42 (1996) 245–253.
[204] P. Bennoun, The present model for chlororespiration, Photosynth. Res. 73 (2002) 273–277.
[205] P. Joliot, A. Joliot, Cyclic electron transfer in plant leaf, Proc. Natl. Acad. Sci. USA 99 (2002) 10209–10214.
[206] D. Lazár, Modelling of light-induced chlorophyll a fluorescence rise (O–J–I–P transient) and changes in 820 nm-transmittance signal, Photosynthetica 47 (2009) 483–498.
[207] G. Schansker, A. Srivastava, Govindjee, R.J. Strasser, Characterization of the 820-nm transmission signal paralleling the chlorophyll a fluorescence rise (OJIP) in pea leaves, Funct. Plant Biol. 30 (2003) 785–796.
[208] A. Oukarroum, G. Schansker, R.J. Strasser, Drought stress effects on photosystem I content and photosystem II thermotolerance analyzed using Chl *a* fluorescence kinetics in barley varieties differing in their drought tolerance, Physiol. Plant. 137 (2009) 188–199.
[209] R.J. Strasser, M. Tsimilli-Michael, D. Dangre, M. Rai, Biophysical phenomics reveals functional building blocks of plants systems biology: a case study for the evaluation of the impact of mycorrhization with *Piriformospora indica*, in: A. Varma, R. Oelmüler (Eds.), Advanced Techniques in Soil Microbiology, Soil Biology, Berlin, Germany, 2007, pp. 319–341.
[210] F. Bussotti, R.J. Strasser, M. Schaub, Photosynthetic behavior of woody species under high ozone exposure probed with the JIP-test: a review, Environ Pollut. 147 (2007) 430–437.
[211] F. Bussotti, R. Desotgiu, M. Pollastrini, C. Cascio, The JIP test: a tool to screen the capacity of plant adaptation to climate change, Scand. J. Forest Res. 25 (2010) 43–50.
[212] S. Chen, X. Xu, X. Dai, C. Yang, S. Qiang, Identification of tenuazonic acid as a novel type of natural photosystem II inhibitor binding in Q_B-site of *Chlamydomonas reinhardtii*, Biochim. Biophys. Acta 1767 (2007) 306–318.
[213] S. Zubek, K. Turnau, M. Tsimilli-Michael, R.J. Strasser, Response of endangered plant species to inoculation with arbuscular mycorrhizal fungi and soil bacteria, Mycorrhiza 19 (2009) 113–123.
[214] N. Contran, E. Paoletti, W.J. Manning, F. Tagliaferr, Ozone sensitivity and ethylenediurea protection in ash trees assessed by JIP chlorophyll *a* fluorescence transient analysis, Photosynthetica 47 (2009) 68–78.
[215] K. Zeliou, Y. Manetas, Y. Petropoulou, Transient winter leaf reddening in *Cistus creticus* characterizes weak (stress-sensitive) individuals, yet anthocyanins cannot alleviate the adverse effects on photosynthesis, J. Exp. Bot. 60 (2009) 3031–3042.
[216] L.G.R. Pinho, E. Campostrini, P.H. Monnerat, A.T. Neto, A.A. Pires, C.R. Marciano, Y.J.B. Soares, Boron deficiency affects gas exchange and photochemical efficiency (JIP test parameters) in green dwarf coconut, J. Plant Nutr. 33 (2010) 439–451.
[217] Z. Yin, F. Meng, H. Song, X. He, X. Xu, D. Yu, Mapping quantitative trait loci associated with chlorophyll a fluorescence parameters in soybean (*Glycine max* (L.) Merr.), Planta 231 (2010) 875–885.

Please cite this article in press as: A. Stirbet, Govindjee, On the relation between the Kautsky effect (chlorophyll *a* fluorescence induction) and Photosystem II: Basics and applications of the OJIP fluorescence transient, J. Photochem. Photobiol. B: Biol. (2011), doi:10.1016/j.jphotobiol.2010.12.010